Title
Distinct Roles of NF-[kappa]B p50 Homodimer in the Genomic Innate Immune Response

Permalink
https://escholarship.org/uc/item/7km7n2v2

Author
Feldman, Kristyn Elizabeth

Publication Date
2013

Peer reviewed|Thesis/dissertation

UNIVERSITY OF CALIFORNIA, SAN DIEGO

Distinct Roles of NF-κB p50 Homodimer in the Genomic Innate Immune

Response

A dissertation submitted in partial satisfaction of the requirements for the

degree of Doctor of Philosophy

in

Biomedical Sciences

by

Kristyn Elizabeth Feldman

Committee in charge:

      Professor Alexander Hoffmann, Chair
      Professor Partho Ghosh
      Professor Victor Nizet
      Professor Deborah Spector
      Professor Joseph Vinetz

2013

The dissertation of Kristyn Elizabeth Feldman is approved, and it is acceptable

in quality and form for publication on microfilm and electronically:

_____

_____

_____

_____

_____
Chair

University of California, San Diego

2013

DEDICATION

I would like to dedicate this dissertation to everyone who helped me get to graduate school and stay sane during the process: to my parents who didn't strangle me for performing "experiments" in the kitchen as a kid; to my teachers and mentors like Mrs. Rosso during high school Biology and the crew at VaxDesign who practically coerced me into applying for PhD programs; to my UCSD friends who kept me from giving up on the rougher days; to ATB for always being there; and to PML for making it interesting at the end.

EPIGRAPH

"Twenty years from now you will be more disappointed by the things you did not do than by the ones you did do. So throw off the bowlines. Sail away from the safe harbor. Catch the trade winds in your sails. Explore. Dream. Discover." ~Author Unknown

TABLE OF CONTENTS

LIST OF ABBREVIATIONS

AIC - Akaike's information criterion

ATF-2 - c-Jun/activated transcription factor-2

B. melitensis - *Brucella melitensis*

BMDMs - bone marrow derived macrophages

CFU - Colony forming units

ChIP - chromatin immunoprecipitation

CL097 - water-soluble derivative of the imidazoquinoline compound R848

CpG - DNA motif (cytosine and guanine separated by a phosphate)

CRE - c-AMP responsive elements

E. coli - *Escherichia coli*

ELISA - Enzyme-linked immuno sorbent assay

EMCV - encephalomyocarditis virus

EMSA - electrophoretic mobility shift assay

FSL-1 - synthetic lipoprotein derived from *Mycoplasma salivarium*

GAPDH - Glyceraldehyde 3-phosphate dehydrogenase

GFP - green fluorescent protein

GM-CSF - Granulocyte-macrophage colony-stimulating factor

HKBM - heat-killed Brucella melitensis

IFN - interferon

IFNAR - Interferon-α/β receptor

IFNAR/p50ko - Interferon-α/β receptor and nuclear factor-κB1 double knockout

IFNARko - Interferon-α/β receptor knockout

IKK - IκB kinase

IRAK - Interleukin-1 Receptor-associated Kinase

IRE - Interferon response element

IRF - interferon regulatory factor

ISGF3 - Interferon-stimulated gene factor 3

ISRE - IFN-stimulated response element

Jak - Janus kinase

L. lactis - *Lactococcus lactis*

L. monocytogenes - *Listeria monocytogenes*

LDA Linear discriminant analysis

LPS - lipopolysaccharide

MCMV - murine cytomegalovirus

MOI - Multiplicity of infection

MyD88 - Myeloid Differentiation Primary-Response Protein-88

NF-κB - nuclear factor-κB

p50ko - nuclear factor-κB1 knockout

Pam3CSK4 - synthetic triacylated lipoprotein

PAMPs - pathogen-associated molecular patterns

PBMCs - Peripheral blood mononuclear cells

PBS - Phosphate buffered saline

PFU - Plaque forming units

Poly(I:C) - polyinosine-polycytidylic acid

PRRs - pattern-recognition receptors

qPCR - Quantitative real-time PCR

R848 - imidazoquinoline compound

Rev1 - *Brucella melitensis* vaccine strain Rev1

rFLA - recombinant Flagellin

S. pnuemoniae - Streptococcus pneumoniae

Stat - signal transducers and activators of transcription

TBK - TAK1-Binding Protein

Th1 - T helper cells

TIR - Toll–interleukin-1 (IL-1) receptor

TLRs - Toll-like receptors

TNF - tumor necrosis factor

TRIF - Toll–interleukin-1 (IL-1) receptor (TIR) domain–containing adaptor-

inducing Interferon-β

Tyk2 - tyrosine protein kinase

VSV - vesicular stomatitis virus

WT - wild type

LIST OF FIGURES

LIST OF TABLES

ACKNOWLEDGEMENTS

VITA

Education

2007-2013   University of California San Diego, San Diego, CA
Doctor of Philosophy in Biomedical Sciences

2003-2007   University of Central Florida, Orlando, FL
Bachelor of Sciences in Biology with Honors
Bachelor of Sciences in Molecular Biology and Microbiology with Honors

Languages spoken

English (native), Spanish (proficient)

Fellowships

2009-2010   Howard Hughes Medical Institute Med-into-Grad Fellowship.

Publications

Cheng CS, Feldman KE, Lee J, Verma S, Huang DB, Huynh K, Chang M, Ponomarenko JV, Sun SC, Benedict CA, Ghosh G, Hoffmann A. The Specificity of Innate Immune Responses Is Enforced by Repression of Interferon Response Elements by NF-κB p50. Science Signaling. 2011 Feb 22; 4(161):ra11.

Invited Oral Presentations

Feldman KE, Hoffmann A. (2012) *NFκB p50 enforces stimulus-specificity of the type I IFN-dependent innate immune response.* RIKEN Research Center for Allergy and Immunology (RCAI) Summer Program. Yokohama, Japan

Feldman KE, Hoffmann A. (2011) *NFκB p50 enforces stimulus-specificity of the type I IFN-dependent innate immune response.* UCSD Innate Immunity Joint Quarterly meeting

Abstracts at Scientific Meetings

Feldman KE, Hoffmann A. (2012) *NFκB p50 enforces stimulus-specificity of the type I IFN-dependent innate immune response.* RIKEN Research Center for Allergy and Immunology (RCAI) Summer Program. Yokohama, Japan

Feldman KE, Cheng CS, Hoffmann A. (2010) *NFκB p50 is essential for innate immune specificity after PAMP priming.* Keystone Symposia, Innate Immunity: Mechanisms Linking with Adaptive Immunity. Dublin, Ireland

ABSTRACT OF THE DISSERTATION

Distinct Roles of NF-κB p50 Homodimer in the Genomic Innate Immune

Response

by

Kristyn Elizabeth Feldman

Doctor of Philosophy in Biomedical Sciences

University of California, San Diego, 2013

Professor Alexander Hoffmann, Chair

Two signaling systems play major roles in the innate immune response to pathogens. The NF-κB signaling network is primarily associated with the innate immune response to bacterial pathogens, while the network of

interferon response factors (IRFs) is primarily associated with the response to viral pathogens. Some pathogen associated molecular pattern (PAMP) receptors coordinate signaling between both the NF-κB and IRF signaling networks. Although these networks can classically act in a synergistic manner and are capable of crosstalk, I propose that some scenarios provoke antagonistic interactions between the two systems. *I hypothesize that while there is a core innate immune response that is activated in response to disparate pathogens, there is also specificity demonstrated by subsets of innate immune effector genes. Furthermore, I hypothesize that the NF-κB p50 homodimer is binding to and regulating a subset of Interferon Response Elements (IRE) and repressing both IFN-responsive genes and IFN-independent genes.*

To investigate the above hypotheses I undertook experiments to address four primary aims: (1) Determine the role of the NF-κB and IFN signaling systems during macrophage responses to PAMPs and infection by viral and bacterial pathogens; (2) Characterize the aberrant p50ko response to TLR agonists and pathogens by exploring the effect of p50ko in the context of ablated type I IFN signaling; (3) Examine the innate immune specificity in the macrophage expression response to TLR agonists and pathogens using next generation sequencing; (4) Investigate the differences in innate immune activity between acute and relapsing brucellosis in a patient cohort in Lima, Peru by comparing cytokine gene expression and protein secretion in

peripheral blood mononuclear cells in response to TLR ligands and heat-killed *Brucella melitensis*. Taken together, these studies define the role of p50 during macrophage host defense and examine the overall specificity of the innate immune response to pathogens.

Chapter 1: General Introduction

1.1 Significance

Every day healthy individuals are exposed to dozens of microorganisms capable of causing disease and the host's innate immune system is the first line of defense. Generally, many invading organisms can be detected, controlled, and destroyed within minutes to a few hours without ever involving the adaptive, antigen-specific branch of immunity. Only infectious agents capable of subverting or overwhelming the innate immune system ever encounter the adaptive immune system, however, innate mechanisms ensure pathogen progression is delayed enough to allow the adaptive immune system time to activate.

Macrophages play an important role in the innate immune system: these large, phagocytic cells are bone marrow-derived, mononuclear, and can be found in most tissues throughout the body. They have many diverse functions, some of which even span both the innate and adaptive immune systems. Macrophages are effective scavengers and express many pathogen-recognition receptors (PRRs) on their cell surface. Once activated, they can kill many intruding microorganisms and secrete cytokines to recruit and activate other immune cells. While most of these effector functions fall under the innate system, macrophages can also present antigens to cells of the adaptive system.

Two signaling systems play major roles in the innate immune response to pathogens. The nuclear factor-κB (NF-κB) signaling network is primarily associated with the innate immune response to bacterial pathogens, while the network of interferon regulatory factors (IRFs) is primarily associated with the response to viral pathogens. My investigation will predominantly focus on the complex interplay between these pathways in macrophages during either viral or bacterial infections.

1.2 The NF-κB family of transcription factors

When an infectious agent challenges the host, the innate immune system is often first to respond and NF-κB helps regulate many of the ensuing immune processes. The NF-κB family of transcription factors is comprised of five members: p50/p105 (NF-κB1), p52/p100 (NF-κB2), p65 (RelA), RelB and cRel. These five homologous proteins form homo- or heterodimers, which upon activation, translocate from the cytoplasm to the nucleus and regulate transcription [1]. While in the cytoplasm the dimers are in complex with a member of the IκB protein family, which retains the dimer there and inhibits the transcription factor's activity. Once a cell encounters a stimulus, the IκB proteins can be degraded and the NF-κB dimers are released to the nucleus [2].

The five NF-κB polypeptides are able to form 15 distinct transcription factors, each with a different physiological role and transcriptional effect. In

resting macrophages, the most commonly found forms are p50 homodimers and p65:p50 heterodimers. While p65:p50 can be rapidly modified and activated (and acts as a transcriptional activator), both p50 and p52 lack the characteristic transcription activation domain, and are therefore currently thought to act as repressors of gene expression unless associated with other factors [3]. Once in the nucleus, these NF-κB dimers can bind to κB consensus sites (GGR**A**TYYCC, where the bolded A can also be a C or T) in the genome and affect the transcription of a variety of genes, including many immune response genes [4]. Typically, NF-κB activation in response to bacterial pathogens causes the induction of pro-inflammatory cytokines like TNF-α, IL-1α, and IL-6.

1.3 Toll-like receptors

In macrophages, NF-κB can be activated downstream of specific pattern recognition receptors (PRRs) like Toll-like receptors (TLRs). There are 14 known TLRs and they function as both homo- and heterodimers. Each TLR is capable of detecting specific pathogen-associated molecular patterns (PAMPs) found in or on microbial pathogens. Extracellular TLRs are capable of recognizing peptidoglycans, lipoproteins (TLR2/1), lipopolysaccharides, lipoteichoic acids (TLR4), flagellin (TLR5), and flagellin or profilin from bacteria or parasitic microbes (TLR11). Additionally, there are intracellular TLRs capable of recognizing double stranded RNA (TLR3), single stranded RNA

(TLR7/8), and CpG DNA motifs (TLR9) [5]. Once these receptors are activated by an invading pathogen, a complex signaling system is engaged with a large number of signals leading to the activation NF-κB [6].

All of the currently characterized TLRs (except TLR3) recruit the adaptor molecule Myeloid Differentiation Primary-Response Protein-88 (MyD88), which has both a Toll–interleukin-1 (IL-1) receptor (TIR) domain and a death domain [5, 7]. Once activated, MyD88 interacts with the Interleukin-1 Receptor-associated Kinase (IRAK) family of protein kinases. This cascade of reactions culminates in the degradation of IκB and activation of NF-κB (Figure 1.1). While NF-κB can be activated through several other pathways, this MyD88-dependent activation will be the main focus of the investigation.

Alternatively, TIR-domain-containing adapter-inducing interferon-β (TRIF) is an adapter for TLR4 and TLR3 signaling, and signaling through this adaptor results in the activation of IRF3 and the production of type I interferons [8, 9].

1.5 The IRF family of transcription factors

Similar to the NF-κB network, IRFs are activated in response to infectious microbes. The interferon family of cytokines is so named due to their ability to interfere with viral replication, and conveniently the interferon regulatory factors are just as aptly named: when activated, these factors regulate the transcription of both the interferon cytokines and genes affected

by the interferon cytokines [10]. Since the presence of interferon can induce further synthesis of interferon cytokines, feedback and cell priming, or activation from previous inflammation or microbial encounters, are very important to understanding the complex action and physiology of these factors.

As expected, during a viral infection the most prominent group of cytokines produced are the interferons (IFNs). There are two main classes of IFNs: type I IFNs include the multiple IFN-α and single IFN-β family members and type II IFNs include the single IFN-γ [11]. While these cytokines have potent antiviral activity, they also serve many other immunoregulatory functions, and are highly regulated. The type I IFNs are regulated by several key transcription factors capable of binding to positive regulatory domains found within the promoters of these genes: NF-κB can bind to κB sites, IRFs (mainly IRF3, 5, 7, and 9) can bind to the IFN-stimulated response element (ISRE) sites, and c-Jun/activated transcription factor-2 (ATF-2) can form a heterodimer and bind to c-AMP responsive elements (CRE). In macrophages, IRF3 is activated through phosphorylation by TANK-binding kinase 1 (TBK1), a kinase of the TRIF pathway [12].

1.6 The type I interferons

Once secreted, interferons bind to cell surface receptors to initiate signaling: type I interferons bind to the type I IFN receptor, IFNAR (composed

of subunits IFNAR1 and IFNAR2) and activate several members of the Janus family of protein tyrosine kinases (Jak) which can phosphorylate downstream factors. IRF3-driven production of type I IFN results in an autocrine loop that activates a second IRF family member, IFN-α–stimulated gene factor 3 (ISGF3), a heterotrimer composed of signal transducers and activators of transcription (Stat) 1, Stat2 and IRF9 (Figure 1.2). The activated Janus kinases are responsible for phosphorylating Stat1 and 2, which subsequently interact with IRF9, translocate to the nucleus, and bind to ISRE sites [13]. IRF3 and ISGF3 appear to have largely overlapping DNA binding specificities for the IFN response element (IRE) consensus sequence (AANNGAAA) [14].

Complexity and crosstalk arise between the NF-κB and IFN signaling pathways when engagement of TLRs promotes the production of IFN-α/β, leading to subsequent activation of IFN signaling feedback. This network of interactions is important for immune cells, like macrophages, to both control the invading pathogen and recruit other immune cells to amplify the primary innate response. Defects in these signaling pathways (p50 knockouts, IFNAR knockouts) should be able to reveal interesting functional information about exactly which parts of these networks are responsible for the observed biological responses of pivotal cells like the macrophage.

1.7 Brucellosis in Peru

Brucellosis is a disease caused by transmission of bacteria of the *Brucella* genus from infected animals to humans. Four species are typically responsible for human infections, *B. abortus, B. melitensis, B. suis, and B. canis*, and are transmitted from animal reservoirs including infected cows, goats or sheep, pigs, and dogs, respectively. Infection occurs by ingestion of contaminated unpasteurized milk or cheese or through contact with blood or materials from infected animals [15]. *B. melitensis* is recognized as not only the most virulent species, needing only a few organisms (10-100) to establish infection, but is also the predominant species responsible for the brucellosis burden in Peru [16, 17]. While most patients treated with antibiotics will be cured of the infection, between 5-40% of patients experience a relapse of brucellosis. The mechanisms underlying these recurring infections remain poorly understood.

Through a collaborative study in Lima, Peru, I examined the *ex vivo* immune cytokine profiles of peripheral blood mononuclear cells (PBMCs) from patients with a history of acute and relapsing brucellosis. I wanted to determine whether we could detect differences in the gene expression or secretion of innate immune cytokines after stimulating patient PBMCs with a panel of TLR ligand or *Brucella* spp. antigens.

1.8 Objectives of the Dissertation

The objectives of this dissertation are centered on the following hypothesis:

Some pathogen associated molecular pattern (PAMP) receptors coordinate signaling between both the NF-κB and IRF signaling networks. Although these networks can classically act in a synergistic manner and are capable of crosstalk, I propose that some scenarios provoke antagonistic interactions between the two systems. I hypothesize that while there is a core innate immune response that is activated in response to disparate pathogens, there is also specificity demonstrated by subsets of innate immune effector genes. Furthermore, I hypothesize that p50 homodimer is binding to and regulating a subset of Interferon Response Elements (IRE) and repressing both IFN-responsive genes and IFN-independent genes.

To address this hypothesis there are four specific aims, outlined below:

Aim 1: *NF-κB p50 enforces stimulus-specific antiviral responses.*

I wanted to examine the role of the NF-κB and IFN signaling systems during macrophage responses to PAMPs and infection by viral and bacterial pathogens. To do this I tracked the activity of NF-κB dimers and IRF containing complexes following TLR stimulation or infection in wild type (WT), p50 knock out (p50ko), and interferon type-I receptor knock out (IFNARko) bone marrow derived macrophages (BMDMs). Additionally, we examined

gene expression via microarray in WT, p50ko and IFNARko BMDMs in response to TLR ligands.

Aim 2: *NF-κB p50 regulates distinct classes of innate immune response genes.*

I further characterized the aberrant p50ko response to TLR agonists and pathogens by exploring the effect of p50ko in the context of ablated type I IFN signaling. I compared gene expression via microarray of WT, p50ko, IFNARko, and IFNAR/p50dko BMDMs in response to LPS and CpG. Specifically, I wanted to elucidate if removal of the p50 homodimer exerts an effect on the basal IFN response, on the subsequent IFN signaling feedback loop, or on other classes of genes. Additionally, I wanted to investigate the possible mechanisms for the specificity of the p50ko effect in the genes of interest by determining if they share similar promoter regions or motifs and assessing if p50 was physically binding to these promoters.

Aim 3: *Surveying the specificity of innate immune responses.*

I wanted to examine the innate immune specificity in the macrophage response to TLR agonists and pathogens using next generation sequencing. To do this I compared gene expression using RNA-seq in WT BMDMs in response to a panel of TLR ligands and pathogens and determined which innate immunity genes were regulated in a stimulus-specific manner and if

TLR ligands (alone or in combination) can recapitulate macrophage gene expression in response to live pathogens.

Aim 4: *Variability in the innate immune response: the case of Brucella.*

I wished to investigate the differences in innate immune activity between acute and relapsing brucellosis in a patient cohort in Lima, Peru. I compared cytokine gene expression and protein secretion in peripheral blood mononuclear cells in response to TLR ligands and heat-killed *Brucella melitensis*.

The following written document follows the aforementioned order, beginning with Chapter 2, which addresses Aim 1 and the role of p50 homodimer in innate immune specificity. Chapter 3 expands upon this work and addresses Aim 2 and the role of p50 homodimer in the absence of interferon feedback. Chapter 4 addresses Aim 3 and the innate immune transcriptome in response to pathogens or pathogen-derived substances. Chapter 5 addresses Aim 4 and the innate immune cytokine response after brucellosis. Chapter 6 brings this dissertation to a close with a final discussion and future directions for these investigations.
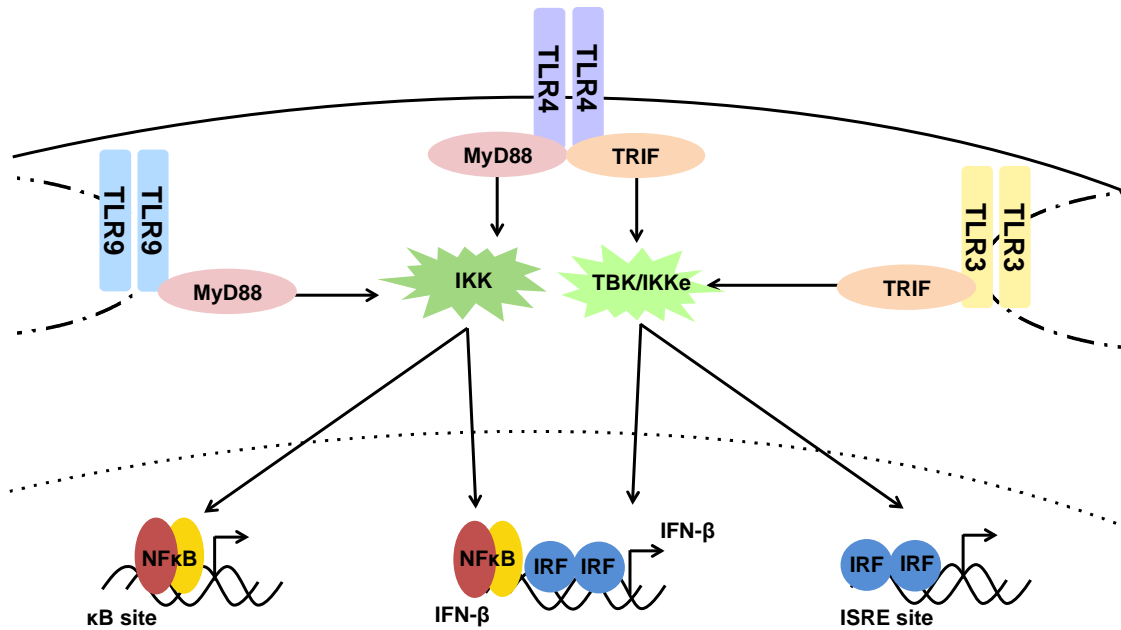
Figure 1.1 TLR activation of NF-κB and IRF. TLR activation of the adaptor protein MyD88 can initiate a signaling cascade culminating in the activation and nuclear translocation of NF-κB. Similarly, signaling through the TRIF adaptor protein leads to activation of the IRF family of transcription factors.
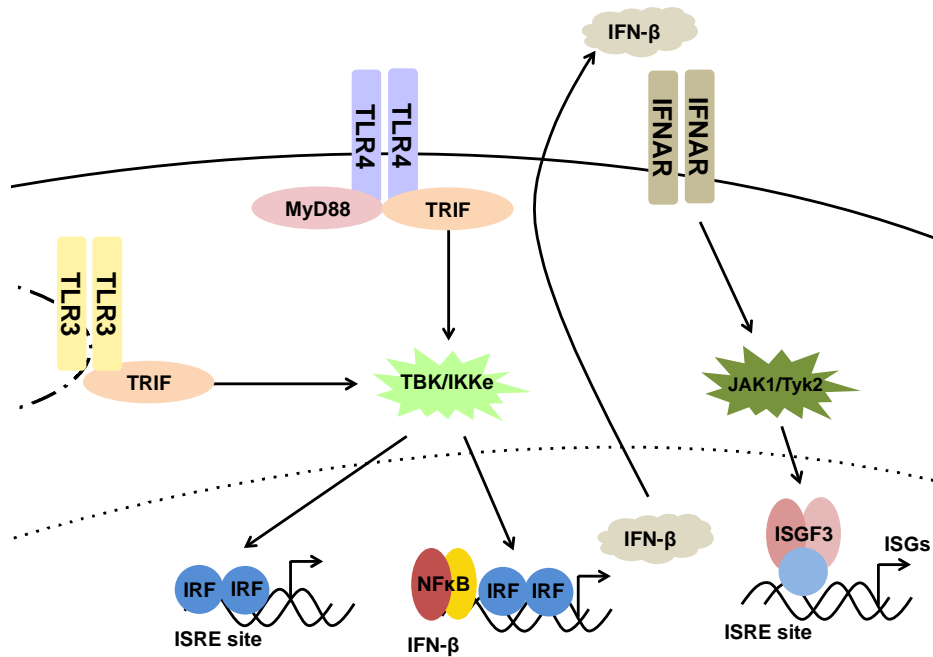
Figure 1.2 Type I interferon signaling. After activation by TLR signaling, coordinated binding of both NF-κB and IRF on the IFN-β promoter leads to gene expression and secretion of the IFN-β protein. Once secreted, IFN-β can act in both an autocrine and paracrine fashion, binding to the IFNAR receptor and initiating a signaling cascade which activates both the transcription factor ISGF3 and other interferon stimulated genes (ISGs).

Chapter 2: NF-κB p50 enforces stimulus-specificity of the type I IFN-dependent innate immune response

2.1 Introduction

Pathogen recognition by macrophages elicits gene expression programs that typically consist of hundreds of genes [18-20], which may be broadly classified as mediating cellular antiviral functions and systemic immune activation through inflammation [21]. Because both types of responses are also potentially detrimental to the organism [22-24], cells are thought to produce pathogen-specific responses, ensuring that unnecessary gene products are not made. Dozens of transcription factors have been implicated in enabling the fine-tuned expression of genes whose products mediate the innate immune response [25, 26]; however, the identities of the critical regulators of pathogen- or stimulus-specific gene expression remain an open question that is of relevance to an understanding of antimicrobial immune responses, chronic inflammatory disease, and the development of relevant therapeutics, including adjuvants for innate and adaptive immune responses.

Two families of transcriptional regulators that play central roles in coordinating the gene expression programs of the cellular innate immune response are the nuclear factor κB (NF-κB) and interferon (IFN) regulatory factor (IRF) families [19, 27-31]. Stimulus-dependent activation of NF-κB and IRFs is determined by signaling adaptors that selectively interact with the

intracellular domains of Toll-like receptors (TLRs) [32]. Myeloid differentiation marker 88 (MyD88) mediates the activation of NF-κB and is associated with most TLRs, including TLR9, which senses bacterial CpG-rich DNA, and TLR4, the sensor for the Gram-negative bacterial cell wall component lipopolysaccharide (LPS). Toll–interleukin-1 (IL-1) receptor (TIR) domain–containing adaptor-inducing IFN-β (TRIF) functions as the primary signaling adaptor for the activation of IRFs and is associated with some TLRs, including TLR4, but not TLR9. Hence, each TLR induces a characteristic combination of transcription factor activities, including those of NF-κB and the IRFs.

NF-κB and the IRFs constitute families of transcription factors that are defined by conserved DNA binding domains. In macrophages, IRF3 is activated through site-specific phosphorylation by TANK-binding kinase 1 (TBK1) [12], an important effector kinase of the TRIF pathway. IRF3-driven production of type I IFN results in an autocrine loop that activates a second IRF family member, IFN-alpha–stimulated gene factor 3 (ISGF3), whose DNA binding component is IRF9. Together with Stat1 and Stat2, this heterotrimer binds to IFN-stimulated response element (ISRE) sites. IRF3 and ISGF3 appear to have largely overlapping DNA binding specificities for the core of the ISRE, the IFN response element (IRE) consensus sequence (AANNGAAA) [14].

Within the NF-κB family, the key transcriptional effectors are the activation domain–bearing RelA (p65) and cRel proteins. These form dimers

with p50 and are responsible for κB-driven gene activation. Overlapping DNA binding specificities for the broad κB consensus sequence [GGRNNN(N)YCC] [33] underlie the fact that there have only been isolated reports of specific cRel or p65 target genes [34, 35].

However, another major NF-κB family member is the p50 homodimer (p50-p50), a presumptive transcriptional repressor of κB sites by virtue of its close sequence and structural homology with other NF-κB family members and its lack of a transcriptional activation domain [36, 37]. Indeed, p50-p50 acts as a competitive repressor of κB-driven transcription in transiently transfected cells and in studies performed in vitro [38, 39] and may repress the expression of the tumor necrosis factor (*tnf*) gene [40-42]; however, the binding specificity and physiological functions of this putative transcriptional repressor remain uncharacterized. Whereas the role of p50 as a dimerization partner for p65 and cRel is compensated for by the *nfkb2* gene product p52 [35], p50-p50 may play unique functions as a repressor within the NF-κB family. Within the innate immune response, during which inappropriate gene expression is potentially detrimental for cellular or organismal health, the role of transcriptional repressors is of pertinent interest.

To characterize the role of p50-p50 in the innate immune response, we investigated its *in vitro* activation, binding activity, and undertook unbiased genome-wide studies to identify its functional targets in response to TLR

stimulation. Furthermore, we determined the effect of its removal during viral infection.

2.2 Materials and Methods

2.2.1 Animals and cell culture

Wild type and genetically deficient C57BL/6 mice were housed in pathogen-free conditions at the University of California, San Diego (UCSD) and all procedures were approved by the Institutional Animal Care and Use Committee. Bone marrow derived macrophages (BMDMs) were isolated from wild type, $nfkb1^{-/-}$, and $ifnar^{-/-}$ femurs. A total of 7×10^6 BM cells were cultured in 15 cm suspension dishes in L929-conditioned media for 7 days at 37°C with 5% CO_2, as described previously [43]. BMDMs were then replated on day 7 in Dulbecco's modified Eagle's medium (DMEM) supplemented with 10% fetal bovine serum and all experiments were performed on day 8. BMDMs were stimulated with 100 ng/ml LPS (Sigma, B5:055), 100 nM Type B CpG ODN 1668 (Invivogen), or 100 units/ml IFN-β (Biogen Inc).

2.2.2 RNA extraction and cDNA synthesis

BMDMs were washed with PBS, homogenized, and total RNA was extracted using the QIAshredder and RNeasy kits per the manufacturer's instructions (Qiagen). RNA was eluted in 30ul of RNase-free water, and 1 μg

was reverse-transcribed into cDNA using the iScript cDNA synthesis kit according to the manufacturer's instruction (Bio-Rad).

2.2.3 qPCR

Quantitative real-time PCR (qPCR) was performed to measure the mRNA expression level of the housekeeping gene GAPDH and several genes of interest. Using a CFX384 Real-Time Detection System (Bio-Rad), each reaction was performed in triplicate in a final reaction volume of 5 µl, including 2.5 µl SsoAdvanced SYBR Green Supermix (Bio-Rad), 1.0 µl cDNA template, and 1.0 µl (100 nM final concentration) of each primer. Primers were designed for each gene using Primer3 (primers are listed in Table 2.1). After amplification, quantification cycle (Cq) values were generated using the Bio-Rad CFX Manager Software 1.6. The fold change of gene expression was calculated using the Δ(ΔCq) method as previously described [44].

2.2.4 Nuclear extraction and gel shift assays

BMDMs were replated with 5 x 10^6 cells per 10 cm plate on day 7. On day 8, BMDMs were left unstimulated or stimulated with LPS (100 ng/ml) or CpG (100nM) for 1, 6 or 24 hours. Cells were collected in CE Buffer (10 mM HEPES pH 7.9, 10 mM KCl, 0.1 mM EGTA, 0.1 mM EDTA, 1 mM dithiothreitol, 0.5 mM phenylmethylsulfonyl fluoride, 10 ug/ml aprotinin and 5 ug/ml leupeptin) in a microcentrifuge tube. To this, 0.5% Nonidet P-40 was

added and the cells were vortexed for lysis. Nuclei were pelleted at 4000 x g and resuspended in 20 µl of high salt buffer (NE Buffer: 20 mM HEPES ph 7.9, 420 mM NaCl, 1.5 mM MgCl2, 0.2 mM EDTA, 25% glycerol, 1 mM dithiothreitol, 0.5 mM phenylmethylsulfonyl fluoride, 10 ug/ml aprotinin and 5 ug/ml leupeptin). Nuclear lysates were cleared by 14,000 x g centrifugation and protein concentrations were determined and normalized by a Bradford assay (Bio-Rad).

Gel-shift assays were performed as previously described [45, 46]. Briefly, nuclear extracts were incubated with 38 bp spanning double-stranded oligonucleotides labeled with phosphorous-32 (P^{32}) containing two consensus κB sites (κB probe) or the 33-bp ISRE site of the ISG15 gene (GATCCTCGGGAAAGGGAAACCTAAACTGAAGCC, the ISRE probe) and left at room temperature for 15 min prior to complex separation on a nondenaturing acrylamide gel. Bands were visualized by autoradiography.

2.2.5 Transcriptome and bioinformatic analysis

RNA from littermate wild type and *nfkb1*$^{-/-}$ BMDMs that were stimulated with LPS (0.1 µg/ml), IFN-β (10 U/ml), or CpG (100 nM) for 1, 3, or 8 hours was hybridized to Illumina mouse RefSeq Sentrix-8 V2 BeadChip arrays. Raw expression data were normalized to several unstimulated control data sets. Probes with ≥$2^{1.2}$-fold (that is, ≥2.97-fold) change in expression at any point of the LPS time course were selected. Fold changes in expression from multiple

probes for a single gene (accession number) were averaged. K-means clustering was performed with wild-type (LPS), p50ko (LPS), wild-type (IFN-β), and *ifnar*$^{-/-}$ (LPS) time course data sets and shown in Figures 2.8 and 2.9. All of the array data shown are available in the NCBI Gene Expression Omnibus database with the accession number GSE27112.

2.2.7 Viral infections

Before infections, BMDMs were seeded into 24-well plates, allowed to adhere, and treated with the indicated stimuli for 24 hours. BMDMs were infected with live murine CMV (MCMV)–GFP and were analyzed for the presence of GFP after 48 hours by flow cytometry.

2.3 Results

2.3.1 p50 homodimer can bind to the ISRE

Wild type (WT) and p50 knockout (p50ko) bone marrow derived macrophages (BMDMs) were isolated and stimulated with various bacterial components or infected with whole bacteria. Time course studies confirmed previous observations that LPS and bacterial stimulation activate both the NF-κB p65-p50 heterodimer and ISGF3 (Figures 2.1 and 2.2). However, we observed the formation of an unexpected complex (indicated with an arrow) on the ISRE probe (Figure 2.1). Not only did this complex have the same mobility as that of p50-p50 on the κB probe, but it was also absent from p50-deficient

BMDMs. Further investigation showed this complex was activated as early as 12 hours after LPS stimulation or *E.* coli infection and persisted for at least 48 hours (Figure 2.2). Antibody supershifts using an antibody against p50 completely shifted the complex and indicated that this complex contained p50 but not p65 (Figure 2.3).

Additionally, the p50-p50 homodimer was induced and found on both the κB and ISRE probe after infection with live, but not heat-killed, MCMV (Figure 2.4).

2.3.2 CpG promotes aberrant ISGF3 activity

We characterized the IFN-β, LPS, and CpG-induced profiles of ISGF3 activation in both WT and p50ko BMDMs. We found similar activation of ISGF3 after IFN-β or LPS stimulation, however we observed inappropriate elevated induction of ISGF3 in response to CpG in p50ko macrophages (Figure 2.5). These findings suggest that in WT macrophages, CpG does not activate IFNAR-dependent ISGF3 but that in the absence of p50, type I interferon is produced and ISGF3 is subsequently induced.

2.3.3 CpG pretreatment protects p50ko BMDMs from viral infection

We established a viral infection assay in which the priming of macrophages by IFN-β inhibited the infectivity of a green fluorescent protein (GFP)–expressing CMV [47] whereas macrophages defective in IFN signaling

(IFNARko) were more susceptible than WT cells to infection (Figure 2.6). Exposing macrophages to LPS rendered them more resistant than untreated cells to infection by CMV, whereas exposure to CpG did not (Figure 2.7, A and B), which reflected the stimulus-specific production of IFN-β. Such stimulus specificity in the mounting of resistance to viral infection was severely compromised in p50ko macrophages because CpG also resulted in increased antiviral resistance in these cells (Figure 2.7, A and B). Our results may relate to the resistance of p50ko mice to encephalomyocarditis virus (EMCV) [40] and to that of a p50ko immortalized fibroblast cell line to influenza [48].

2.3.4 p50 represses LPS-inducible IFN-responsive genes

To identify functional targets of p50-p50 during the cellular response to pathogens in an unbiased manner, we profiled gene expression induced by LPS after 1, 3 or 8 hours in p50ko cells by microarray analysis. BMDMs revealed a p50-mediated repressive effect on many genes in response to LPS (Figure 2.8, clusters B, C, and E). Many of the genes that demonstrated hyperexpression in the p50ko were IFN-β-inducible (Figure 2.8, clusters C, and E). The known function of p50 as a binding partner for the transcriptional activator p65 was apparent in only a small reduction in the extent of expression of some NF-κB–regulated genes (Figure 2.8, clusters D and F), indicating redundancy with p52 or the presence of p65 homodimers, or that

the repressive functions of p50-p50 masked the stimulatory effects of p50-p65 [35].

2.3.5 CpG promotes aberrant gene expression in p50ko BMDMs by microarray analysis

To assess gene induction by CpG in p50ko cells, we stimulated BMDMs for 1, 3, or 8 hours and profiled expression by microarray analysis. Like LPS, CpG stimulation also revealed a p50-mediated repressive effect on many genes (Figure 2.9). To determine the role of IFN signaling on these genes, genes that were hyperexpressed in p50ko BMDMs were profiled in both WT and IFNARko BMDMs after LPS stimulation, and many of these CpG-inducible p50-repressed genes were indeed IFNAR-dependent (Figure 2.9 clusters B, E, and F). These findings support that CpG stimulation in p50ko cells can induce aberrant IFN response genes.

2.3.6 CpG promotes aberrant antiviral gene expression in p50ko BMDMs by qPCR

To confirm trends observed via microarray, gene expression of IFN-β and IFN responsive genes were assessed by qPCR. Indeed, our experimental analysis revealed that whereas WT cells did not exhibit expression of IFN-β in response to CpG, p50ko cells showed substantial misexpression (Figure 2.10). Furthermore, in p50ko macrophages, CpG induced the expression of

known antiviral genes and IFN response genes that were revealed by microarray studies (Figure 2.10).

2.4 Discussion

Our findings have revealed unexpected cross-regulation between two primary transcription factor families that coordinate innate immune responses. Whereas the NF-κB and IRF activators bind to their respective cognate sites (κB and ISRE, respectively), we report that the NF-κB p50-p50 repressor is able to bind to and regulate a previously unrecognized NF-κB binding site, the ISRE. By using both *in vitro* biochemical assays and unbiased gene expression phenotyping studies, we showed that p50 homodimers are highly induced and can bind to a subset of ISREs after bacterial or viral PAMP stimulation (Figures 2.2 and 2.4), and that many of these genes are also IFN responsive (Figures 2.8 and 2.9). Furthermore, we confirmed that many genes that are hyperexpressed in response to these stimuli in the absence of p50 do indeed contain the core IRE binding site in their promoters.

Since several of the hyperexpressed genes revealed via microarray were indicated to have antiviral activity, we assessed the ability of p50ko BMDMs to mount a response to *in vitro* viral infections. While resting p50ko BMDMs were not resistant to viral infection, after priming with CpG p50ko cells demonstrated increased resistance to CMV-GFP, confirming the aberrant IFN and IFN response phenotype observed biochemically. This stimulus-specific

protection of p50ko cells indicates an important role for p50 in antiviral immunity, and taken together with the observed gene expression phenotype, suggests p50 is a novel and key regulator of IFN and ISG expression.

While we also observed p50, but not p65, was capable of competing with ISGF3 *in vitro* [49], expression phenotypes observed in p50ko cells were apparent at early time points after LPS exposure (Figure 2.8). These findings suggest p50 may be competing with other transcription factors, namely IRF3, that bind to ISRE sites with earlier activation kinetics: IRF3 is activated 30 minutes to 2 hours after LPS exposure [49], while ISGF3 activity peaks at 2 to 6 hours. Further studies are necessary to determine the extent to which p50 is competing *in vivo* with IRF3 and ISGF3 and to demonstrate that the p50-repressed genes identified via microarray are directly controlled by p50 *in vivo* and are not a consequence of increased IFN signaling.

2.5 Acknowledgements

Table 2.1 Primers used for qPCR

Gene	Accession Number	Name	Sequence
Gapdh	NM_008084.2	rt.Gapdh.f	AACTTTGGCATTGTGGAAGG
		rt.Gapdh.r	GGATGCAGGGATGATGTTCT
Gbp1	NM_010259	rt.Gbp1.f	CGGAAAGAGTTAATGGCAGAGC
		rt.Gbp1.r	GTTGCAAGCTCTCATTCTGG
Gbp3	NM_018734	rt.Gbp3.f	GATGGAGAGAGAGCCATAGCA
		rt.Gbp3.r	CCTTCTGTCTCTGCCTCAGC
Ifit3	NM_010501	rt.Ifit3.f	CCAGCAGCACAGAAACAGAT
		rt.Ifit3.r	GAAATGGCACTTCAGCTGTG
Ifnb	NM_010510.1	rt.IFNb.f	GGTCCGAGCAGAGATCTTCA
		rt.IFNb.r	CTGAGGCATCAACTGACAGG
Mx1	NM_010846	rt.Mx1.f	GACCCTGAAGGGGATAGGAC
		rt.Mx1.r	CTTGCCTTCAGCACCTCTGT
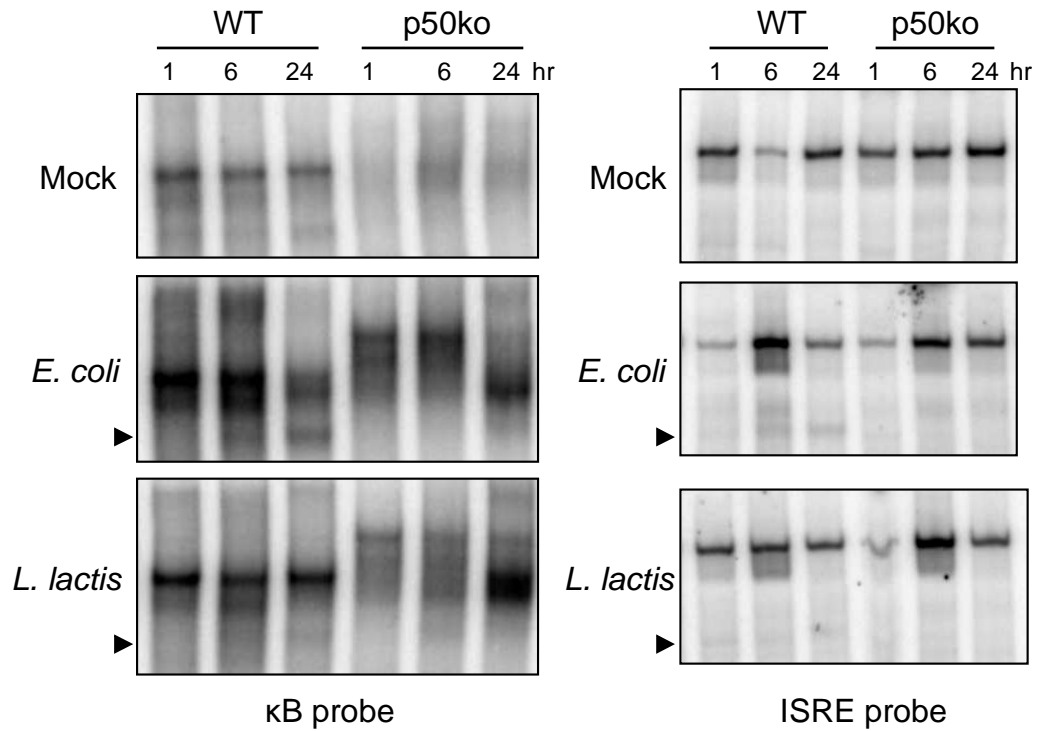
Figure 2.1 NF-κB and ISGF3 activity in WT and p50ko BMDMs after bacterial stimulation. WT and p50ko BMDMs were stimulated with *E. coli* or *L. lactis* for the indicated times and transcription factor activity was assessed by EMSA. In WT cells, the p50 homodimer (marked with an arrow) is visible binding to both the κB and ISRE probe.
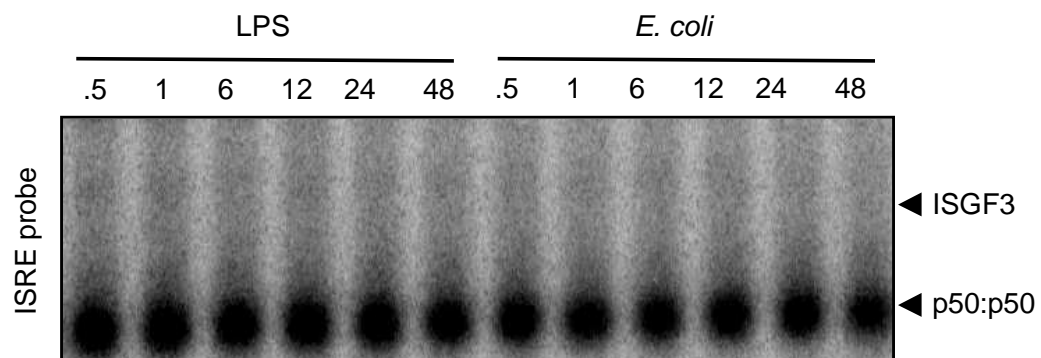
Figure 2.2 ISGF3 and NF-κB activity after LPS or bacterial stimulation.
BMDMs were stimulated with LPS (100 ng/ml) or *E. coli* for the indicated times and transcription factor activity was assessed by EMSA. As expected, ISGF3 was activated after LPS and bacterial stimulation, however, p50 homodimer also bound to the ISRE.
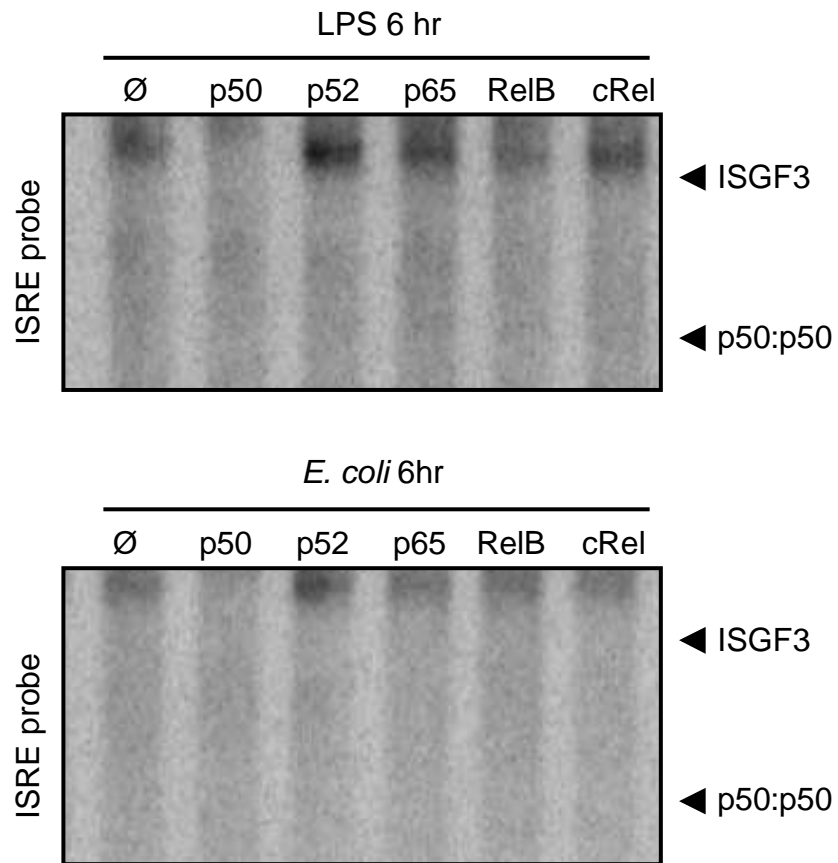
Figure 2.3 NF-κB p50-p50 binding to ISRE after bacterial stimulation. BMDMs were stimulated with LPS (100 ng/ml) or *E. coli* for the indicated times and transcription factor activity was assessed by supershift EMSA. Nuclear lysates were incubated with PBS or antibodies against p50, p52, p65, RelB or cRel. Only NF-κB p50 shifted the lower band, indicating p50 homodimer binding to the ISRE.
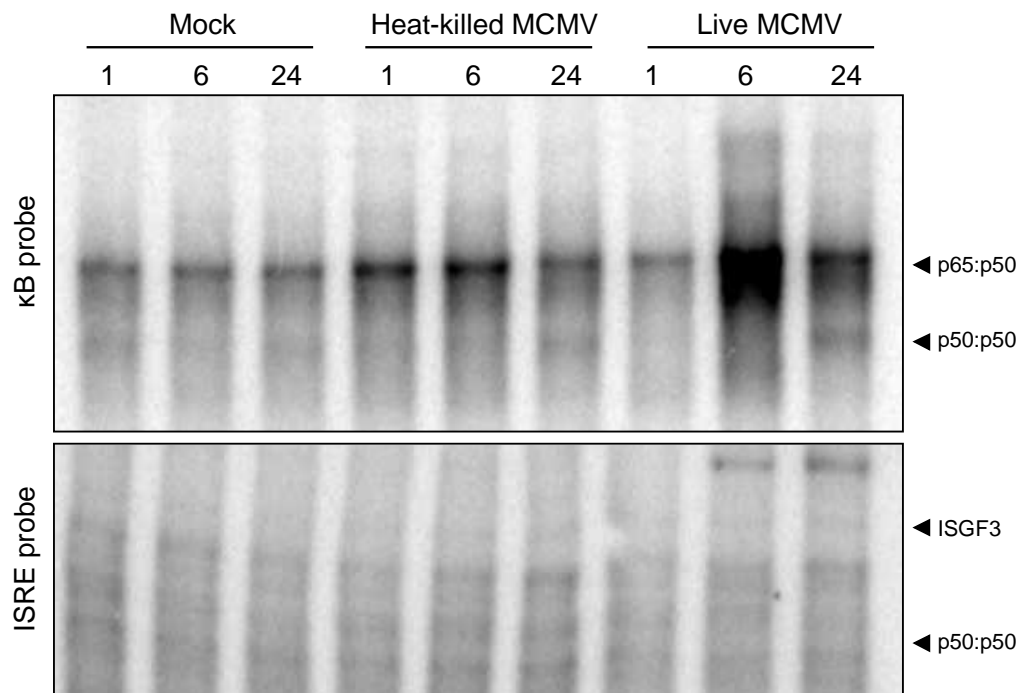
Figure 2.4 NF-κB and ISGF3 activity after viral infection. BMDMs were exposed to heat-killed or live MCMV for the indicated times and transcription factor activity was assessed by EMSA. Live MCMV induced p50 homodimer binding to both κB and ISRE sites.
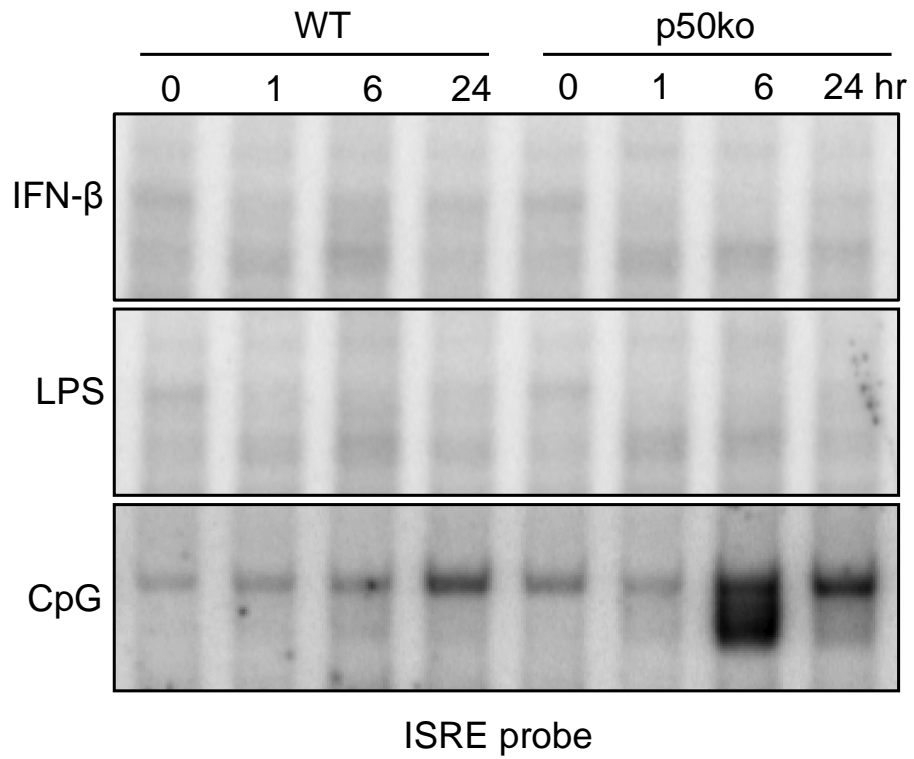
Figure 2.5 CpG stimulation promotes aberrant ISGF3 activity in p50ko BMDMs. BMDMs were stimulated with IFN-β, LPS, or CpG for the indicated times and transcription factor activity was assessed by EMSA. After CpG stimulation, ISGF3 activity is highly induced in p50ko, but not WT, BMDMs.
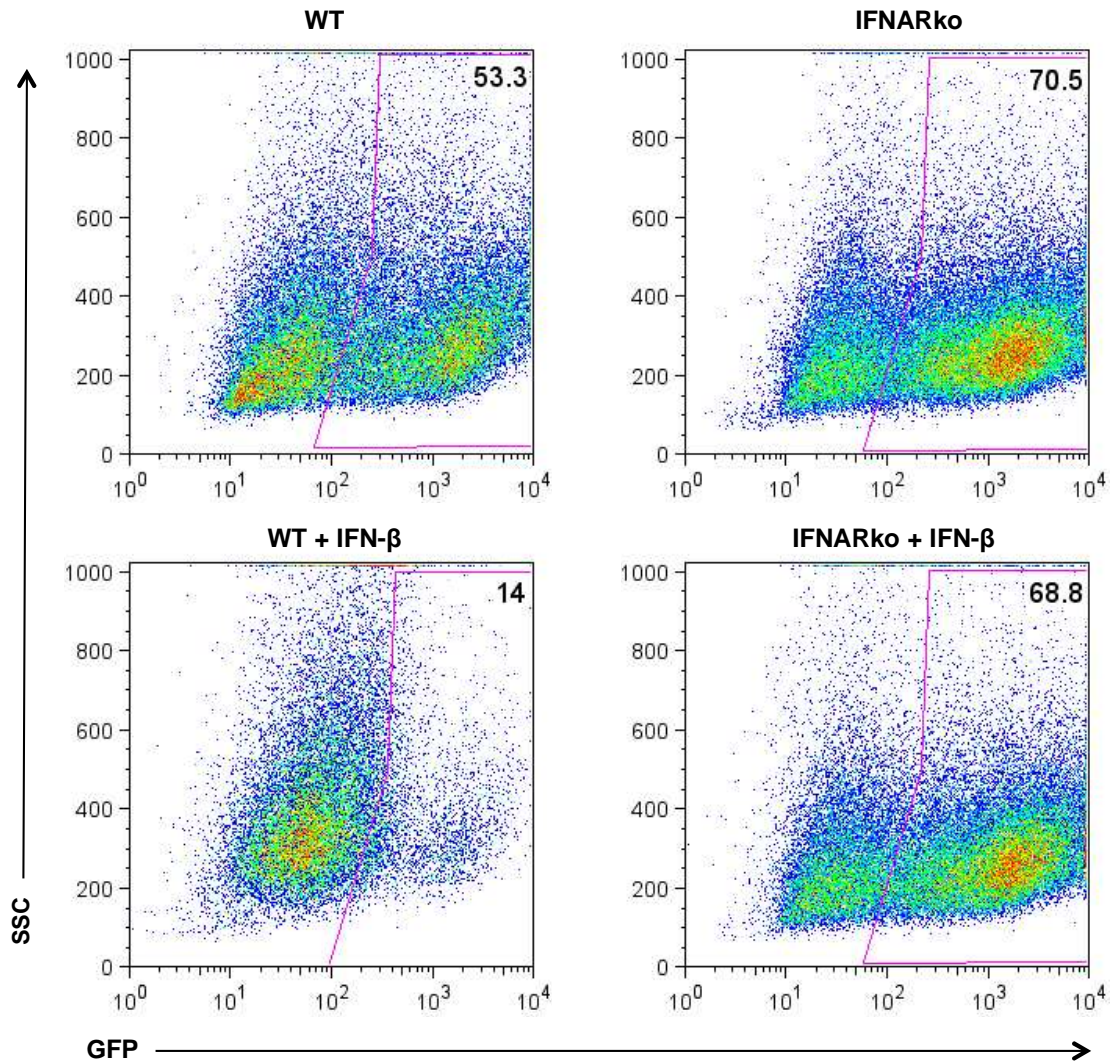
Figure 2.6 IFN-β treatment protects WT BMDMs from MCMV infection. After a 24-hour treatment with IFN-β, WT and IFNARko BMDMs were infected with MCMV-GFP. Forty-eight hours later, productively infected cells expressing GFP were quantified (pink gate) by flow cytometry (side scatter versus GFP). The data are representative of three independent experiments.

A.

Mock **LPS** **CpG**

WT
61.4   3.84   47.9

p50ko
64.6   1.35   10.2

SSC

GFP

B.

☐ WT   ■ p50ko

% infected with MCMV

No   LPS   CpG
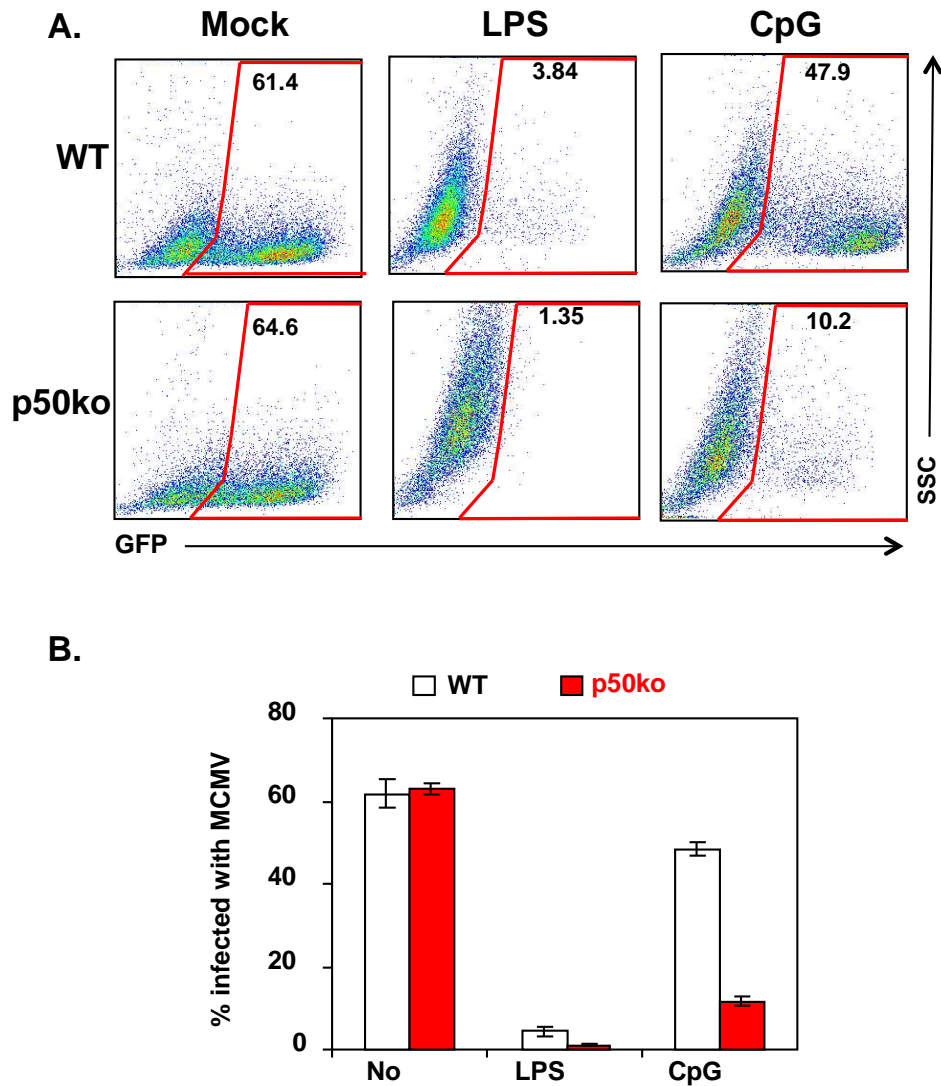
Figure 2.7 CpG treatment protects p50ko BMDMs from MCMV infection.
Induction of antiviral resistance after priming treatments. (A) After a 24-hour treatment with PBS (mock), LPS, or CpG, WT and p50ko BMDMs were infected with MCMV-GFP. Forty-eight hours later, productively infected cells expressing GFP were quantified (red gate) by flow cytometry (side scatter versus GFP). (B) The percentage of infected WT or p50ko BMDMs expressing GFP in (A) were plotted as averages from triplicate determinations. The data are representative of three independent experiments.
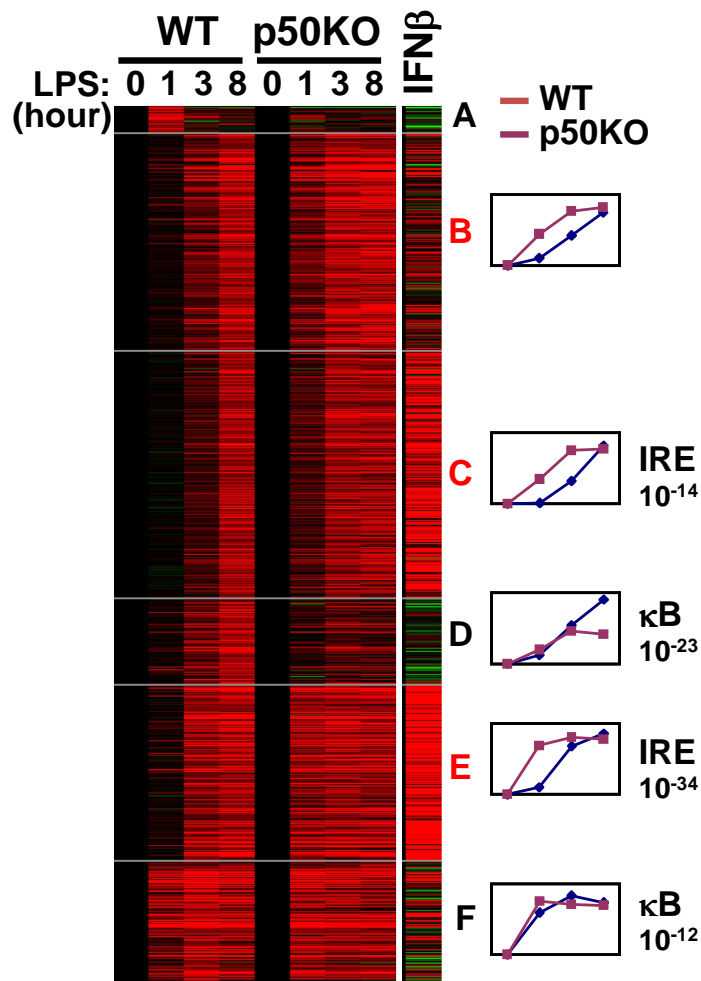
Figure 2.8 NF-κB p50 represses IFN response genes. Microarray mRNA expression data from WT and p50ko BMDMs stimulated with LPS and IFN-β were analyzed by K-means clustering. Red represents stimulus-responsive gene induction, whereas green represents repression. Cluster identifiers are indicated on the right, with red symbols indicating clusters with increased expression in the p50ko cells compared to that in WT cells. The average fold induction (log2) of each cluster in WT (blue) and p50ko (purple) cells was graphed at 0, 1, 3, and 8 hours. The most highly enriched motifs identified *de novo* within –1.0 to +0.3 kb of the transcriptional start sites are shown in each cluster, with P values to indicate statistical significance for each motif. Figure was prepared by Christine Cheng.
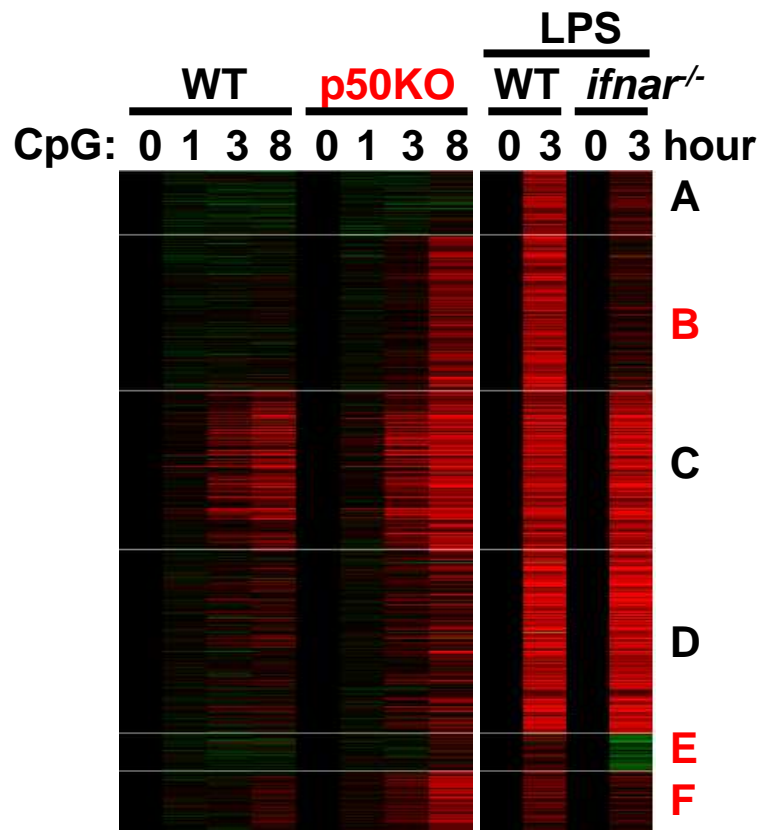
Figure 2.9 CpG promotes aberrant gene expression in p50ko macrophages. Microarray gene expression profiles of WT and p50ko BMDMs that were left unstimulated or were stimulated with CpG for 3, 8, or 24 hours, together with microarray expression profile of WT and IFNARko BMDMs that were left unstimulated or were stimulated with LPS for 3 hours, were analyzed by K-means clustering. Cluster identifiers are indicated on the right. Red indicates IFN-β and IFNAR-dependent clusters. Figure was prepared by Christine Cheng.
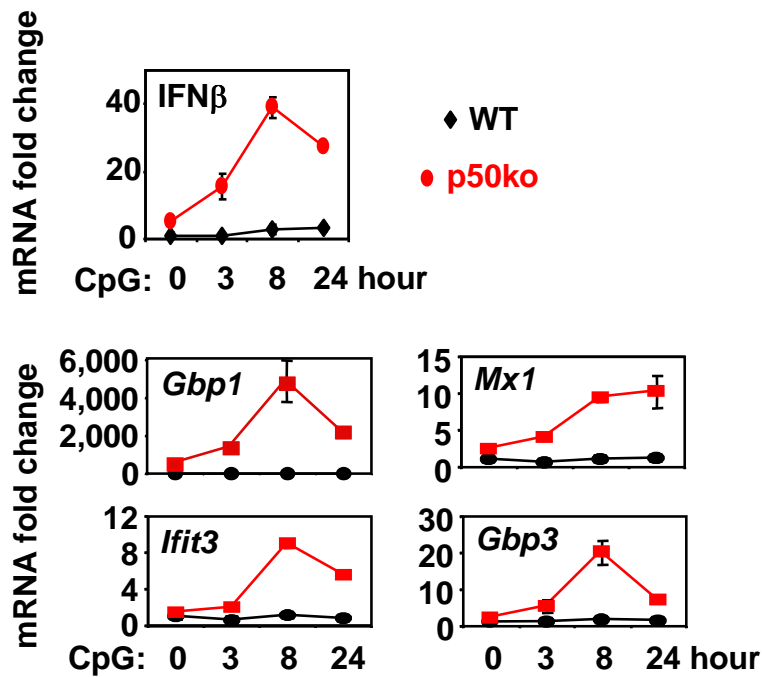
Figure 2.10 CpG promotes aberrant antiviral gene expression in p50ko macrophages. qPCR determination of the fold change in the abundance of IFN-β mRNA or IFN-β-inducible genes in WT (black) BMDMs compared to that in p50ko BMDMs (red) following stimulation with CpG for the indicated times. Data are from, or representative of, at least three experiments. Figure was prepared by Christine Cheng.

Chapter 3: NF-κB p50 regulates distinct classes of innate immune response genes

3.1 Introduction

In Chapter 2 we established that the p50-p50 homodimer can repress the expression of a large number of genes, many of which are IFN responsive [49]. This previous study supported two possible mechanisms of p50-repression: 1) we showed that p50-p50 is able to enforce the stimulus-specific repression of target genes, with a deficiency of p50 leading specifically to the inappropriate induction of IFN-β after stimulation with the TLR9 agonist, CpG and 2) we found that p50-p50 is capable of binding to ISRE sites and controlling expression of many ISGs. To expand this work, we sought to investigate the role of p50 in gene expression in the absence of the type I IFN receptor (IFNAR) and assess the extent of the direct control of p50 on the promoters of target genes we identified previously.

In the literature, p50 is commonly recognized as a transcriptional repressor and mechanisms have been proposed to explain how p50 achieves its repressive effects. Classically, p50 is considered a repressor because unlike p65, RelB, and cRel, it lacks a transcriptional activation domain. Therefore, when p50 forms a homodimer and binds to κB sites it can subsequently block or prevent the access of other activating NF-κB dimers like

36

p65-p50 [50]. Notably, this competitive action of the p50 homodimer was described to have a role in the mechanism of repression of the TNF-α gene during tolerance to LPS [42]. After extended stimulation with LPS, p50 production is highly increased leading to large amounts of p50 homodimer in the nucleus, which is then able to bind to specific κB sites on the TNF-α promoter and repress transcriptional activation by p65-p50 [51]. This mechanism of competitive repression has also been confirmed in transiently transfected cells and *in vitro* studies [38, 39, 52].

Previous studies indicating that p50ko mice were resistant to infection by encephalomyocarditis virus (EMCV) [40] were confirmed and expanded by infecting both p50ko and IFNAR/p50ko mice with EMCV [55]. Even in the absence of type I IFN signaling, IFNAR/p50ko mice showed increased resistance to EMCV infection compared to both WT and IFNARko mice, however the exact mechanism of this resistance remains poorly understood. These preliminary reports suggest that the viral resistance observed both *in vitro* and *in vivo* in p50ko mice may be directly mediated by the transcriptional effects of p50 and not merely a consequence of increased type I IFNs.

Other groups have also reported that p50-containing NF-κB dimers can control a subset of IFN response genes [48, 56], however the direct effect of p50 on these ISGs still remains poorly characterized. Since we showed that p50-deficiency severely affects the production of type I IFNs, and altered IFN production may be able to affect ISGs by a variety of mechanisms, we

proposed to examine the effect of p50 deficiency on gene expression in the absence of IFNAR, thus eliminating the confounding downstream signaling. We used three approaches to explore the effects of p50: gene expression microarrays, ChIP and ChIP-seq, and *in vivo* pathogen infections in WT, p50ko, IFNARko, and IFNAR/p50ko BMDMs and mice. By combining unbiased, genome-wide expression studies in the absence of both IFNAR and p50 and p50 binding studies, we hoped to delineate the subsets of genes which are directly controlled by p50 binding and the subset of genes which were predominantly affected by misexpression of type I IFN.

3.2 Materials and Methods

3.2.1 Animals and cell culture

Wild type and genetically deficient C57BL/6 mice were housed in pathogen-free conditions at the University of California, San Diego (UCSD) and all procedures were approved by the Institutional Animal Care and Use Committee. Bone marrow derived macrophages (BMDMs) were isolated from wild type, *nfkb1*^{-/-}, *ifnar*^{-/-}, and *ifnar*^{-/-}*nfkb1*^{-/-} femurs. A total of 7×10^6 BM cells were cultured in 15 cm suspension dishes in L929-conditioned media for 7 days at 37°C with 5% CO_2, as described previously [43]. BMDMs were then replated on day 7 in Dulbecco's modified Eagle's medium (DMEM) supplemented with 10% fetal bovine serum and all experiments were performed on day 8. BMDMs were stimulated with 100 ng/ml LPS (Sigma,

B5:055) or 100 nM Type B CpG ODN 1668 (Invivogen).

3.2.2 RNA extraction and cDNA synthesis

BMDMs were washed with PBS, homogenized, and total RNA was extracted using the QIAshredder and RNeasy kits per the manufacturer's instructions (Qiagen). RNA was eluted in 30ul of RNase-free water, and 1 µg was reverse-transcribed into cDNA using the iScript cDNA synthesis kit according to the manufacturer's instruction (Bio-Rad).

3.2.3 qPCR

Quantitative real-time PCR (qPCR) was performed to measure the mRNA expression level of the housekeeping gene GAPDH and several genes of interest. Using a CFX384 Real-Time Detection System (Bio-Rad), each reaction was performed in triplicate in a final reaction volume of 5 µl, including 2.5 µl SsoAdvanced SYBR Green Supermix (Bio-Rad), 1.0 µl cDNA template, and 1.0 µl (100 nM final concentration) of each primer. Primers were designed for each gene using Primer3 (primers are listed in Table 3.1). After amplification, quantification cycle (Cq) values were generated using the Bio-Rad CFX Manager Software 1.6. The fold change of gene expression was calculated using the $\Delta(\Delta Cq)$ method as previously described [44].

3.2.4 Nuclear extraction and gel shift assays

BMDMs were replated with 5 x 10^6 cells per 10 cm plate on day 7. On day 8, BMDMs were left unstimulated or stimulated with LPS (100 ng/ml) or CpG (100nM) for 1, 6 or 24 hours. Cells were collected in CE Buffer (10 mM HEPES pH 7.9, 10 mM KCl, 0.1 mM EGTA, 0.1 mM EDTA, 1 mM dithiothreitol, 0.5 mM phenylmethylsulfonyl fluoride, 10 ug/ml aprotinin and 5 ug/ml leupeptin) in a microcentrifuge tube. To this, 0.5% Nonidet P-40 was added and the cells were vortexed for lysis. Nuclei were pelleted at 4000 x g and resuspended in 20 µl of high salt buffer (NE Buffer: 20 mM HEPES ph 7.9, 420 mM NaCl, 1.5 mM MgCl2, 0.2 mM EDTA, 25% glycerol, 1 mM dithiothreitol, 0.5 mM phenylmethylsulfonyl fluoride, 10 ug/ml aprotinin and 5 ug/ml leupeptin). Nuclear lysates were cleared by 14,000 x g centrifugation and protein concentrations were determined and normalized by a Bradford assay (Bio-Rad).

Gel-shift assays were performed as previously described [45, 46]. Briefly, nuclear extracts were incubated with 38 bp spanning double-stranded oligonucleotides labeled with phosphorous-32 (P^{32}) containing two consensus κB sites (κB probe) or the 33-bp ISRE site of the ISG15 gene (GATCCTCGGGAAAGGGAAACCTAAACTGAAGCC, the ISRE probe) and left at room temperature for 15 min prior to complex separation on a nondenaturing acrylamide gel. Bands were visualized by autoradiography.

3.2.5 Western blotting

For western blot analysis, whole-cell extracts were prepared after stimulation using RIPA buffer supplemented with PMSF, DTT, and phosphatase inhibitors, or cytoplasmic and nuclear fractions were extracted as described above. Samples were normalized for equal amounts of proteins using a Bradford assay. Antibodies to IRF3 (D83B9, #4302) and phosph-IRF3 (4D4G, #4947) were from Cell Signaling. Antibodies to α-tubulin (sc-5286) were from Santa Cruz Biotechnology.

3.2.6 Microarray analysis

BMDMs from wild type, *nfkb1*$^{-/-}$, *ifnar*$^{-/-}$, and *ifnar*$^{-/-}$*nfkb1*$^{-/-}$ mice were replated with 1.5 x 10^6 cells per 6 cm plate on day 7. On day 8, BMDMs were left unstimulated or stimulated with LPS (100 ng/mL) or CpG (100nM) for 1, 3 or 8 hours. RNA was extracted and hybridized to Illumina Mouse RefSeq Sentrix-8 V2 BeadChips microarrays at the University of California, San Diego Biogem facility. Probes with ≥2-fold hyperexpression in *nfkb1*$^{-/-}$ (p50ko) compared to wild type (WT) or ≥2-fold hyperexpression in *ifnar*$^{-/-}$*nfkb1*$^{-/-}$ (IFNAR/p50ko) compared to *ifnar*$^{-/-}$ (IFNARko) were selected for analysis.

K-means clustering was performed for both p50ko compared to WT datasets and IFNAR/p50ko compared to IFNARko datasets. Transcription factor *de novo* motif searches were performed with the promoter sequences 400 bp upstream and 100 bp downstream of the transcription start site with the

motif search program Homer, developed by C. Benner [57]. An in-depth description of this software suite can be found at http://biowhat.ucsd.edu/homer/.

3.2.7 In vivo bacterial challenge

WT, p50ko, IFNARko, and IFNAR/p50ko mice were challenged with an intraperitoneal injection of 50 CFU of *S. pneumoniae* or 20,000 CFU of *L. monocytogenes* and survival was monitored at daily intervals. 4-5 mice were infected for each group.

3.3 Results

3.3.1 IFN-β and antiviral gene expression is misregulated in both p50ko and IFNAR/p50ko BMDMs

To determine if the previously observed p50ko gene expression phenotype persists in the absence of IFNAR-signaling, BMDMs were isolated from WT, p50ko, IFNARko, and IFNAR/p50ko mice. After stimulation for 1, 3, 8 or 24 hours with LPS or CpG, we confirmed that IFN-β expression (Figure 3.1 A) and many ISGs were elevated in p50ko compared to WT cells (Figure 3.2 A and B); in addition, IFNAR/p50ko cells also demonstrated increased IFN-β expression and antiviral gene expression compared to IFNARko BMDMs (Figure 3.3 A and B). Gbp3 and Gbp5 have demonstrated anti-influenza and inflammasome activating activity, respectively [58, 59]; Ifit2 (or

ISG54) is known to have anti-VSV activity [60], while Oasl2 has antiviral dsRNA enzymatic activity [61], and Rsad2 (or Viperin) has broad anti-viral effects [62]. Hyperexpression of these genes in the IFNAR/p50ko may suggest the p50-mediated effect on the transcriptional control of these genes is not merely a consequence of increased type I IFN signaling, as the IFNAR receptor is absent.

3.3.2 NF-κB and IRF activity in IFNARko and IFNAR/p50ko BMDMs after TLR or pathogen stimulation

IFNARko and IFNAR/p50ko BMDMs were stimulated with LPS, CpG, or vesicular stomatitis virus (VSV) and NF-κB activity was measured by EMSA. As expected, IFNAR/p50ko BMDMs exhibited attenuated but inducible NF-κB activity after viral infection (Figure 3.4 B). Like in p50ko BMDMs, without the preferred binding partner, p65 formed homodimers or was found in complex with p52 (Figure 3.4 A). We confirmed comparable levels of ISGF3 were observed in both WT and p50ko cells.

Additionally, BMDMs were stimulated with LPS and phosphorylated IRF3 (p-IRF3) was measured by western blotting analysis. Similar levels of p-IRF3 were observed in WT and all knockout BMDMs (Figure 3.5). IFNARko and IFNAR/p50ko BMDMs were also stimulated with LPS, CpG, and VSV, and nuclear p-IRF3 was measured by western blotting analysis. Again, similar levels of p-IRF3 were observed (Figure 3.6). While p65:p50 activity is

attenuated in p50ko mice, we show that p65 is still activated in knockout cells and that IRF3 and ISGF3 activity is not significantly diminished.

3.3.3 p50 represses distinct classes of genes in response to LPS and CpG

WT and p50ko BMDMs were left unstimulated or stimulated with LPS or CpG for 1, 3, or 8 hours and gene expression was assessed by microarray analysis. 151 unique genes were ≥2-fold hyperexpressed in the p50ko compared to WT after LPS and 192 unique genes were ≥2-fold hyperexpressed in the p50ko compared to WT after CpG stimulation. K-means clustering was performed and DNA binding motif enrichment was determined for all hyperexpressed genes and for each individual cluster (Figures 3.7-3.10).

LPS-responsive p50-repressed genes were enriched for both *de novo* p65 and ISRE or IRF binding sites (Figure 3.8). CpG-responsive p50-repressed genes were also enriched for both *de novo* p65 and ISRE binding sites, however, a much larger percentage of CpG-responsive genes (26.04% versus 6% of LPS-responsive) were enriched for the p65 binding motif after CpG stimulation (Figures 3.8 and 3.10).

3.3.4 p50 represses distinct classes of genes in response to LPS and CpG in the absence of IFNAR signaling

IFNARko and IFNAR/p50ko BMDMs were left unstimulated or stimulated with LPS or CpG for 1, 3, or 8 hours and gene expression was assessed by microarray analysis. 115 unique genes were ≥2-fold hyperexpressed in the IFNAR/p50ko compared to IFNARko after LPS and 194 unique genes were ≥2-fold hyperexpressed in the IFNAR/p50ko compared to IFNARko after CpG stimulation. K-means clustering was performed and DNA binding motif enrichment was determined for all hyperexpressed genes and for each individual cluster (Figures 3.11-3.14).

In the absence of IFNAR, LPS-responsive p50-repressed genes overall did not show significant *de novo* motif enrichment, however, individual clusters were enriched for p65 and ISRE/IRF binding sites. CpG-responsive p50-repressed genes were enriched for *de novo* p65 binding motifs. The loss of motif enrichment for these ISRE sites in the absence of IFNAR suggests p50-repression of ISRE containing genes may be predominantly a consequence of IFNAR-signaling feedback.

3.3.7 p50-repressed genes are primarily IFNAR-dependent

Genes which were identified as p50-repressed in WT compared to p50ko BMDMs were examined in IFNAR/p50ko BMDMs (Figure 3.15 and 3.16). While there were 151 LPS-responsive, p50-repressed genes, only 48 of these genes retained the phenotype in the absence of IFNAR (Figure 3.16 A). Additionally, while there were 192 CpG-responsive, p50-repressed genes, only

39 of these genes retained the phenotype in the absence of IFNAR (Figure 3.16 C). This loss of phenotype can been seen when the LPS-responsive, p50-repressed genes are analyzed in the IFNAR and IFNAR/p50ko (Figure 3.15 A) and also with the CpG-responsive, p50-repressed genes (Figure 3.15 B). Additionally, many of the genes which retain the p50-repressed phenotype in the absence of IFNAR demonstrated later (8 hour) induction (Figures 3.16 B and D).

3.3.8 p50 is directly binding to the promoters of inflammatory genes

WT and p50ko BMDMs were left unstimulated or stimulated with LPS for 1 or 24 hours and analyzed by chromatin immunoprecipitation (ChIP) followed by qPCR. Several p50-repressed genes previously identified by microarray analysis were assessed for their ability to recruit p65, p50, or IRF3 to their promoters. Ccl5 (RANTES), cathepsin C (Ctsc), Gbp2, Gbp3, Gbp5 and IFN-β were found to be both hyperexpressed in the p50ko and reduced in IFNAR/IRF3ko BMDMs (data not shown), suggesting both p50 and IRF3 may play a role in their control. IκBα was examined as a positive control for NF-κB target genes and a negative control for IRF3.

Notably, Ccl5, Gbp3, and IFN-β showed increased recruitment of both p65 and IRF3 in p50ko BMDMs compared to WT after 1 hour of LPS stimulation (Figure 3.17). Gbp3, which was found to be hyperexpressed in both p50ko and IFNAR/p50ko cells (Figures 3.2 and 3.3), displayed

recruitment of all three factors after 1 hour of stimulation (Figure 3.18). As expected, detailed analysis of the Gbp3 promoter (from -400 to +100 bp of the transcriptional start site) revealed both potential κB and ISRE sites. These preliminary results suggest genome wide ChIP-seq studies will provide further valuable insight into the promoter occupancy of IRF3 and NF-κB p50 regulated genes.

3.3.9 p50 mice display no clear phenotype after in vivo bacterial infection

WT, p50ko, IFNARko, and IFNAR/p50ko mice were challenged with an intraperitoneal injection of 50 CFU of *S. pneumoniae* or 20,000 CFU of *L. monocytogenes* and survival was monitored at daily intervals. While it was expected that p50ko mice would show increased susceptibility to *S. pneumoniae* [40], both p50ko and IFNAR/p50ko mice showed greater survival than WT and IFNAR mice, respectively (Figure 3.20). Furthermore, p50ko mice were expected to show increased susceptibility to *L. monocytogenes* compared to WT mice, however all but one WT mouse succumbed to infection (data not shown). These preliminary studies were not preformed with littermate mice, and future studies would be required to determine if the results we observed were due to genetic variations of the mice, bacterial strain variation from previously published studies, or infection dosage dependent.

3.4 Discussion

Here we report that NF-κB p50-p50 is controlling several distinct classes of genes, even in the absence of type I IFN signaling. While we previously observed that p50 was capable of binding to and controlling a number of genes containing ISRE sites, many of which were also IFN- β inducible [49], we wanted to investigate the effects of p50 without the effects of downstream IFNAR activation and signaling.

To this end, we generated IFNAR/p50ko mice, which lack both the nfkb1 gene and the type I IFN receptor. We observed that while BMDMs from these mice have slightly attenuated NF-κB activation (Figure 3.4), they have comparable levels of p-IRF3 (Figures 3.5 and 3.6) and show hyperexpression of a number of inflammatory genes previously identified to be hyperexpressed in p50ko BMDMs (Figure 3.3).

Using genome wide expression analysis, we show that LPS- and CpG-responsive p50-repressed genes are enriched for ISRE and p65 binding motifs, which suggests that p50-p50 may be competing with these transcription factors and repressing transcription in WT mice. Furthermore, we show that while a number of these p50-repressed genes are still hyperexpressed in IFNAR/p50ko BMDMs, the vast majority of the expression phenotype is lost in the absence if type I IFN signaling (Figures 3.15 and 3.16).

Recently described additional repressive mechanisms of the p50 homodimer include the p50-mediated recruitment of the transcriptional repressor histone deacetylase (HDAC)-1 [53], and the interaction of p50 with the euchromatic histone H3 lysine 9 (H3K9) methyltransferase-1 (EHMT1) [54]. These studies describe co-repressor complexes that allow p50 to recruit other factors to inflammatory or antiviral genes and regulate their transcription; these support our findings by confirming many of the genes we identified as p50 targets and demonstrating that a subset of these genes may be regulated these p50-mediated mechanisms.

Although we previously reported that p50-p50 was able to compete with ISGF3 in *in vitro* binding assays [48], gene expression studies indicated that p50-repression was affecting genes with earlier activation kinetics (as early as 1 hour after stimulation) than genes which may be controlled by ISGF3 whose activation peaks at 2 hours or later. To determine if p50 was competing with transcription factors with earlier activation kinetics, namely IRF3, ChIP assays were performed. Indeed, we found that both p50 and IRF3 were binding to several genes simultaneously. Interestingly, IRF3 binding was observed to be higher in the absence of p50.

These ChIP results suggest genome wide ChIP-seq studies will provide further valuable insight into the promoter occupancy of IRF3 and NF-κB p50 regulated genes. WT and p50ko BMDMs stimulated with LPS have been collected and submitted for next generation sequencing. Future directions for

this study include analyzing this ChIP-seq dataset to determine the genome wide binding of p50, IRF3, and p65.

3.5 Acknowledgements

Chapter 3 is original work performed under the guidance of A. Hoffmann. The dissertation author was the primary investigator and author of this material.

Table 3.1 Primers used for qPCR

Gene	Accession Number	Name	Sequence
Fam26f	NM_175449.4	rt.Fam26f.f	GGCTCCCTGCAACAAGCAGAA
		rt.Fam26f.r	AATCCAACCGAACACCTGAGACTG
Gapdh	NM_008084.2	rt.Gapdh.f	AACTTTGGCATTGTGGAAGG
		rt.Gapdh.r	GGATGCAGGGATGATGTTCT
Gbp3	NM_018734	rt.Gbp3.f	GATGGAGAGAGAGCCATAGCA
		rt.Gbp3.r	CCTTCTGTCTCTGCCTCAGC
Gbp5	NM_153564.2	rt.Gbp5.f	CAGGAGGCCACAAGCTCTTCC
		rt.Gbp5.r	AGCACTTCCTCAGCCTGTGTTC
Ifit2	NM_008332.3	rt.Ifit2.f	CGCTTTGACACAGCAGACAG
		rt.Ifit2.r	GTCGCAGATTGCTCTCCAGT
Ifnb	NM_010510.1	rt.IFNb.f	GGTCCGAGCAGAGATCTTCA
		rt.IFNb.r	CTGAGGCATCAACTGACAGG
IκBa	NM_010907.2	rt.ikba.f	AGACTCGTTCCTGCACTTG
		rt.ikba.r	AGTCTGCTGCAGGTTGTTC
Il15	NM_001254747.1	rt.IL15.f	CGTGCTCTACCTTGCAAACA
		rt.IL15.r	TCTCCTCCAGCTCCTCACAT
Oasl1	NM_145209.3	rt.Oasl1.f	CCTGGAGACCGTGCAGACAG
		rt.Oasl1.r	AGCAGCCTACCTTGAGTACCTTGA
Oasl2	NM_011854.2	rt.Oasl2.f	TGGAATGTACAGCGAGCGAGG
		rt.Oasl2.r	GGGGCTGTAGGGGTTTGTCC
Rantes	NM_013653.3	rt.Ccl5.f	GCTGCTTTGCCTACCTCTCCC
		rt.Ccl5.r	TCCTTCGAGTGACAAACACGAC
Rgs1	NM_015811.2	rt.Rgs1.f	CCTTGCCAACCAGACAGGTCAA
		rt.Rgs1.r	AGTCCTCACAAGCCAACCAG
Rsad2	NM_021384.4	rt.Rsad2.f	TGGTTCAAGGACTATGGGGAGT
		rt.Rsad2.r	GACCACGGCCAATCAGAGCA
Tyki	NM_020557	rt.Tyki.f	AGACAGGTACTGGCATAGCACA
		rt.Tyki.r	ACTGTAGGCCTCCACTCACC

Table 3.2 Primers used for ChIP

Gene	Accession Number	Name	Sequence
IκBα	NM_010907.2	chip.IκBα.f	GCTTCTCAGTGGAGGACGAG
		chip.IκBα.r	CTGGCAGGGGATTTCTCAG
Ccl5	NM_013653.3	chip.ccl5.f	GAGTTTCCACAAAAGACACCA
		chip.ccl5.r	GAGGCAGAGTCATACTTCCAA
Ctsc	NM_009982.4	chip.ctsc.f	AACTAACTTCCTCAGGCCAC
		chip.ctsc.r	GTTACAGGGTGGTGAGAACA
Gbp2	NM_010260	chip.Gbp2.f	AGCTAGCTGATTTCCCAGCA
		chip.Gbp2.r	GGAAGGAGGGAGGAAGAAAA
Gbp3	NM_018734	chip.Gbp3.f	CAAAGCTGGTTCATGTCAGG
		chip.Gbp3.r	AAGCCCTTTCTCCTCCCTTT
Gbp5	NM_153564.2	chip.gbp5.f	GCAACGAGTTTGTCCTCTTG
		chip.gbp5.r	AAGAAAAACTGAAGAGCGGG
Ifnb	NM_010510.1	chip.ifnb.f	
		chip.ifnb.r	
Gbp3	NM_018734	chip.Gbp3.f1	TTTGAGACATCCCCAGAAAGACA
		chip.Gbp3.r1	TCTGTCAGTAGAGCTAACAACTC
Gbp3	NM_018734	chip.Gbp3.f2	CTGAATCATGCATTGTTCTTGC
		chip.Gbp3.r2	CAGCTCCCTGTTAGAGTCTTTA
Gbp3	NM_018734	chip.Gbp3.f3	ACTTTAAGGAAACTGGGGACTT
		chip.Gbp3.r3	AGGGAGTCAAAGATGATTGCTC
Gbp3	NM_018734	chip.Gbp3.f4	CAAAGCTGGTTCATGTCAGG
		chip.Gbp3.r4	AAGCCCTTTCTCCTCCCTTT
Gbp3	NM_018734	chip.Gbp3.f5	TTCTGCTGGGGGGAAGTCC
		chip.Gbp3.r5	TGCAGCAGGAGAAAATAGCA

A. CpG stimulated
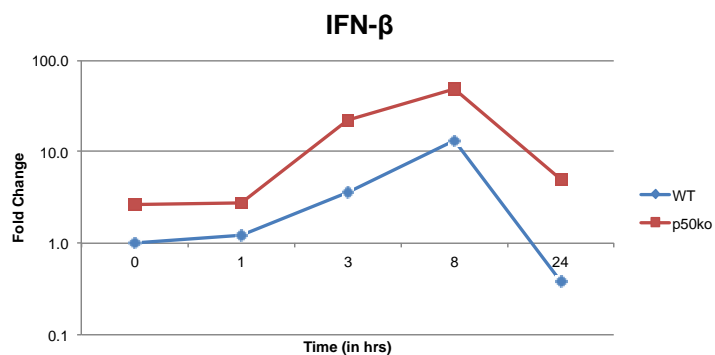
B. LPS stimulated
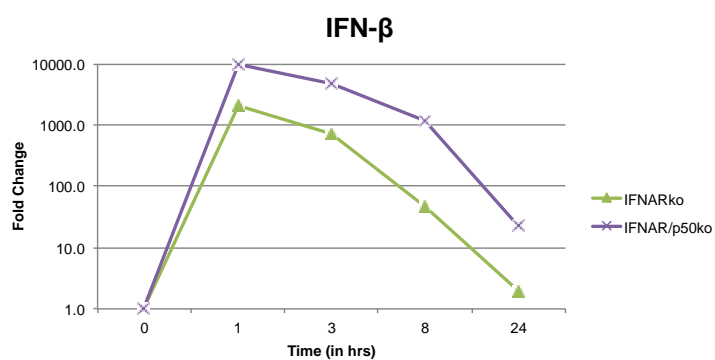
C. CpG stimulated
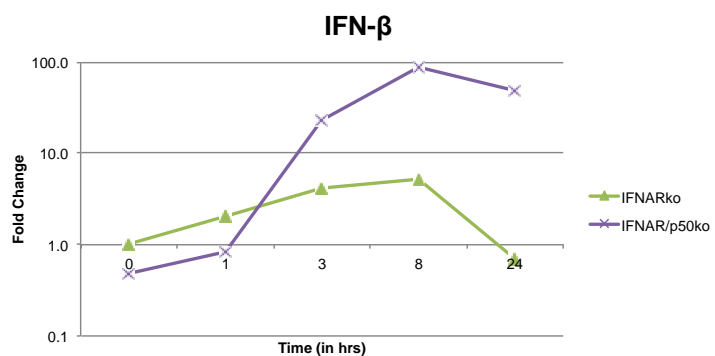
Figure 3.1 Hyperexpression of IFN-β in p50ko and IFNAR/p50ko. qPCR determination of the fold change in the abundance of IFN-β mRNA in (A) p50ko BMDMs (red) compared to that in WT (blue) BMDMs following stimulation with LPS or (B) IFNAR/p50ko BMDMs (purple) compared to that in IFNARko (green) BMDMs following stimulation with LPS or (C) CpG for 0, 1, 3, or 8 hours.
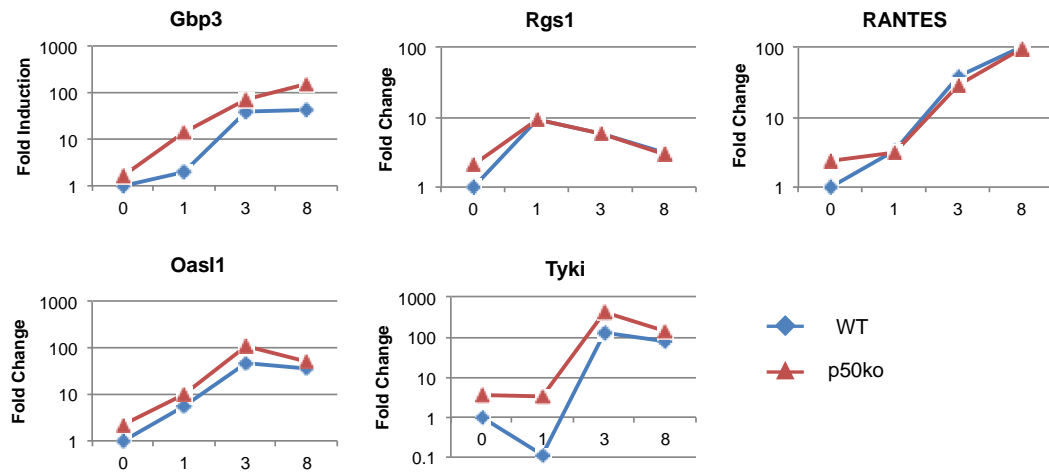
A. LPS stimulated
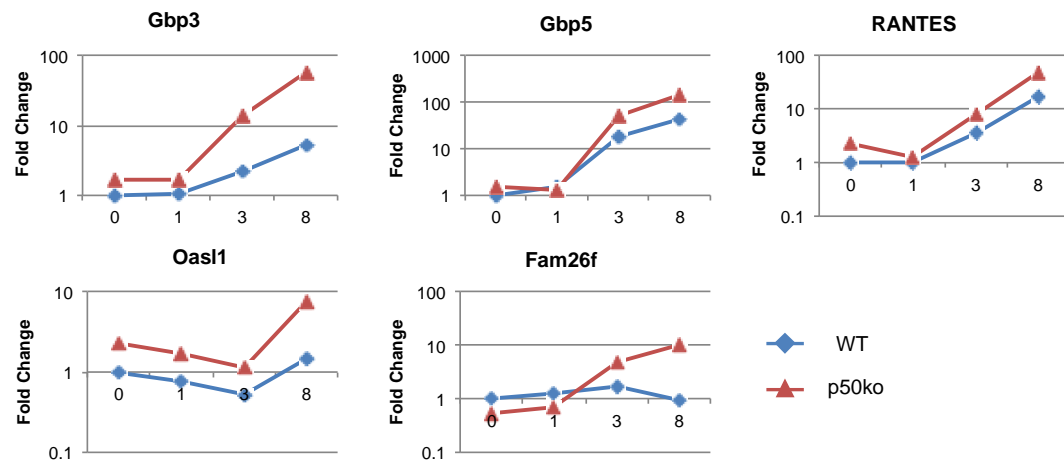
B. CpG stimulated

Figure 3.2 Hyperexpression of inflammatory genes in p50ko. qPCR determination of the fold change in the abundance of inflammatory gene mRNA in p50ko BMDMs (red) compared to that in WT (blue) BMDMs following stimulation with (A) LPS or (B) CpG for 0, 1, 3 or 8 hours.
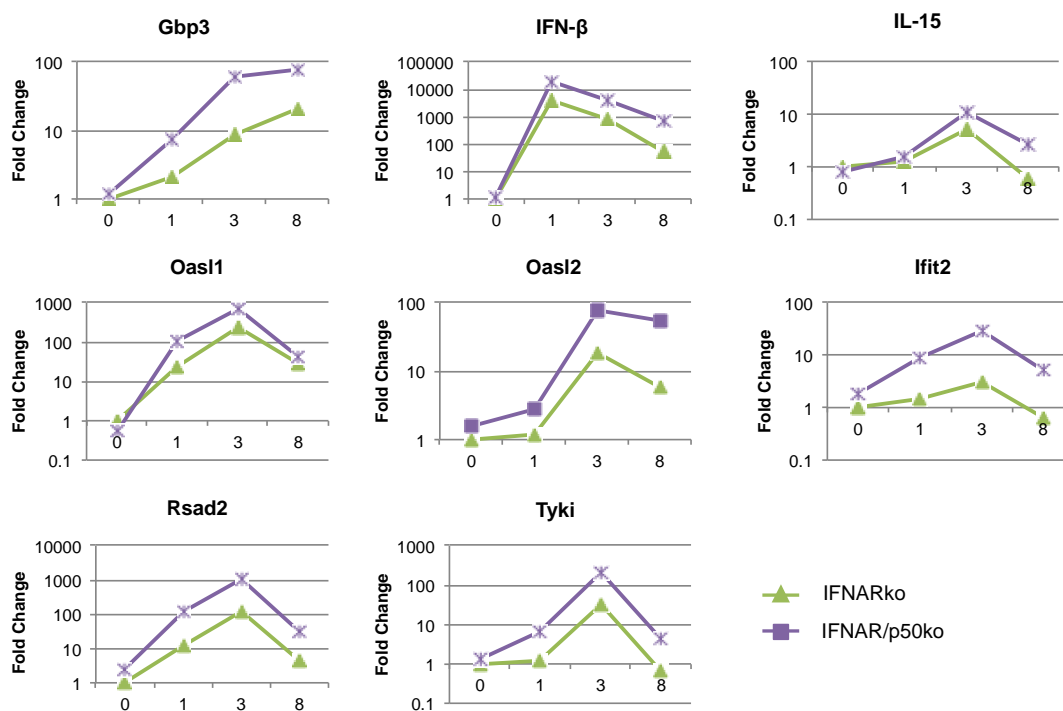
A. LPS stimulated

B. CpG stimulated
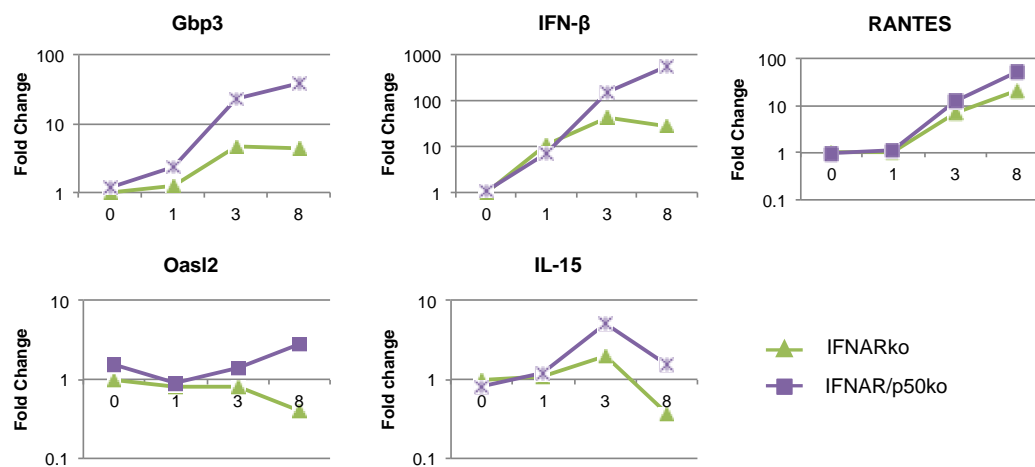
Figure 3.3 Hyperexpression of inflammatory genes in IFNAR/p50ko. qPCR determination of the fold change in the abundance of inflammatory gene mRNA in IFNAR/p50ko BMDMs (purple) compared to that in IFNARko (green) BMDMs following stimulation with (A) LPS or (B) CpG for 0, 1, 3 or 8 hours.
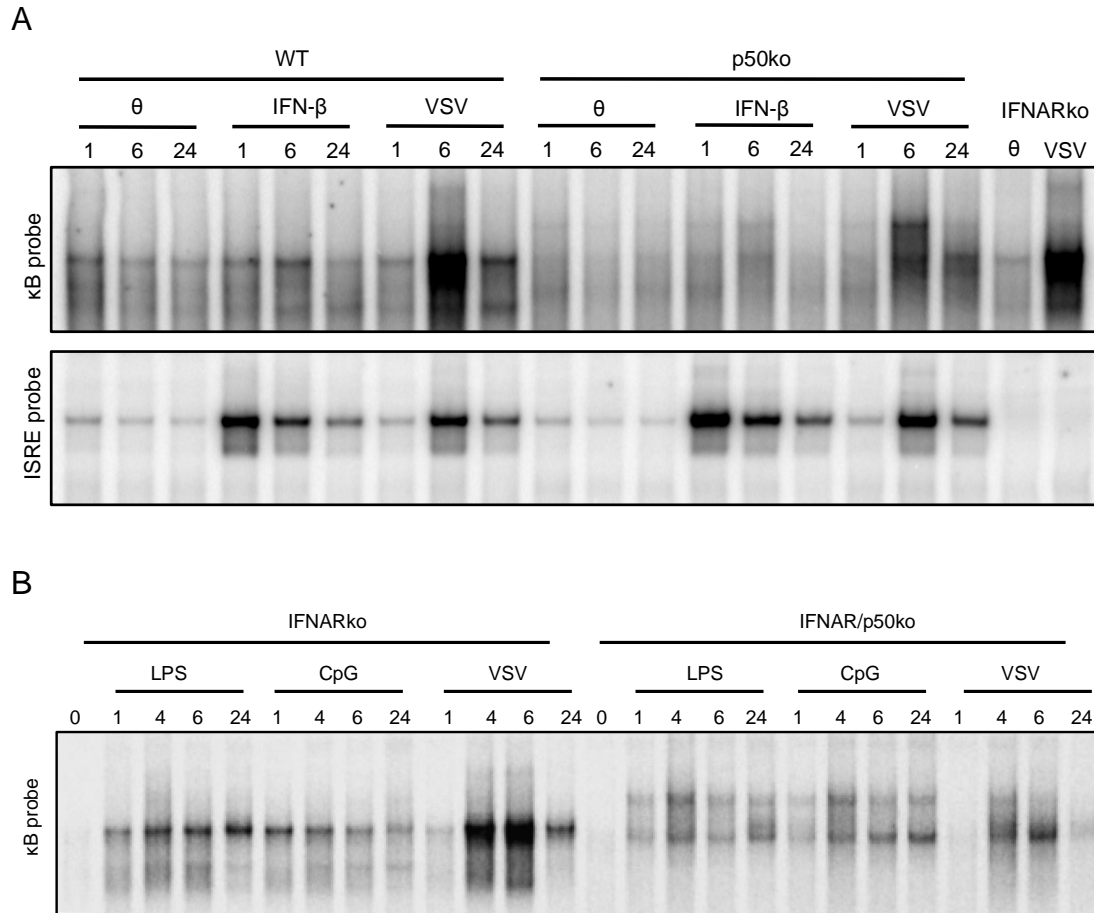
Figure 3.4 NF-κB and ISGF3 activity in WT, p50ko, IFNARko, and IFNAR/p50ko BMDMs after stimulation. (A) WT and p50ko BMDMs were left unstimulated or stimulated with IFN-β or VSV for the indicated times and transcription factor activity was assessed by EMSA. ISGF3 activation levels are comparable in both WT and p50ko cells, while IFNARko show no activity. (B) IFNARko and IFNAR/p50ko BMDMs were left unstimulated or stimulated with LPS, CpG, or VSV for the indicated times and NF-κB activity was assessed by EMSA. IFNARko cells show strong p65-p50 (upper band) and p50-p50 (lower band) activation after viral infection, while the loss of p50 attenuates NF-κB activity in IFNAR/p50ko BMDMs.
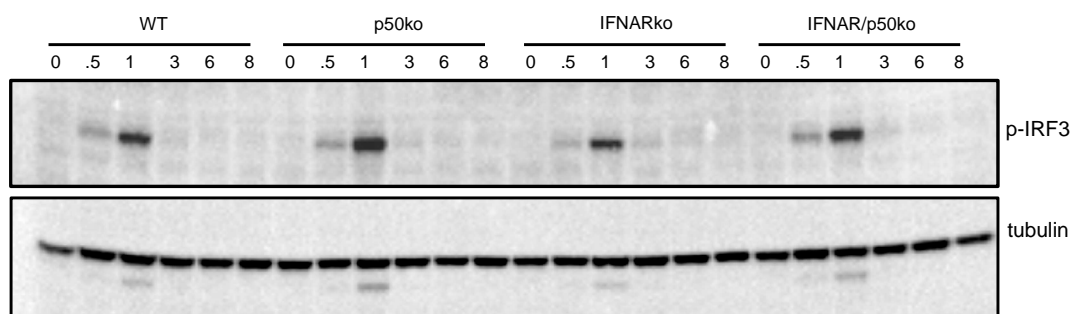
Figure 3.5 Phosphorylated IRF3 activity in WT, p50ko, IFNARko, and IFNAR/p50ko BMDMs after LPS stimulation. BMDMs were left unstimulated or stimulated with LPS for the indicated times and phosphorylated IRF3 was assessed by western blotting analysis. Whole cell extracts indicated comparable levels of p-IRF3 after 1 hour of stimulation, with slightly higher activity in the absence of p50.
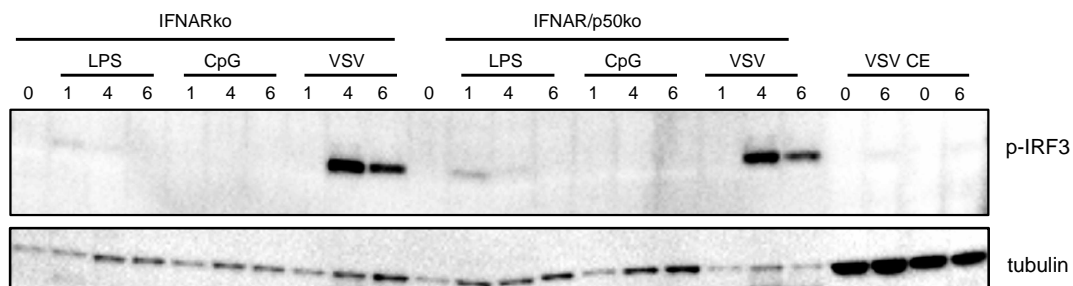
Figure 3.6 Phosphorylated IRF3 activity in IFNARko and IFNAR/p50ko BMDMs after stimulation. BMDMs were left unstimulated or stimulated with LPS, CpG or VSV for the indicated times and phosphorylated IRF3 was assessed by western blotting analysis. Nuclear extracts indicated comparable levels of nuclear p-IRF3 after 4 or 6 hour of stimulation with VSV.
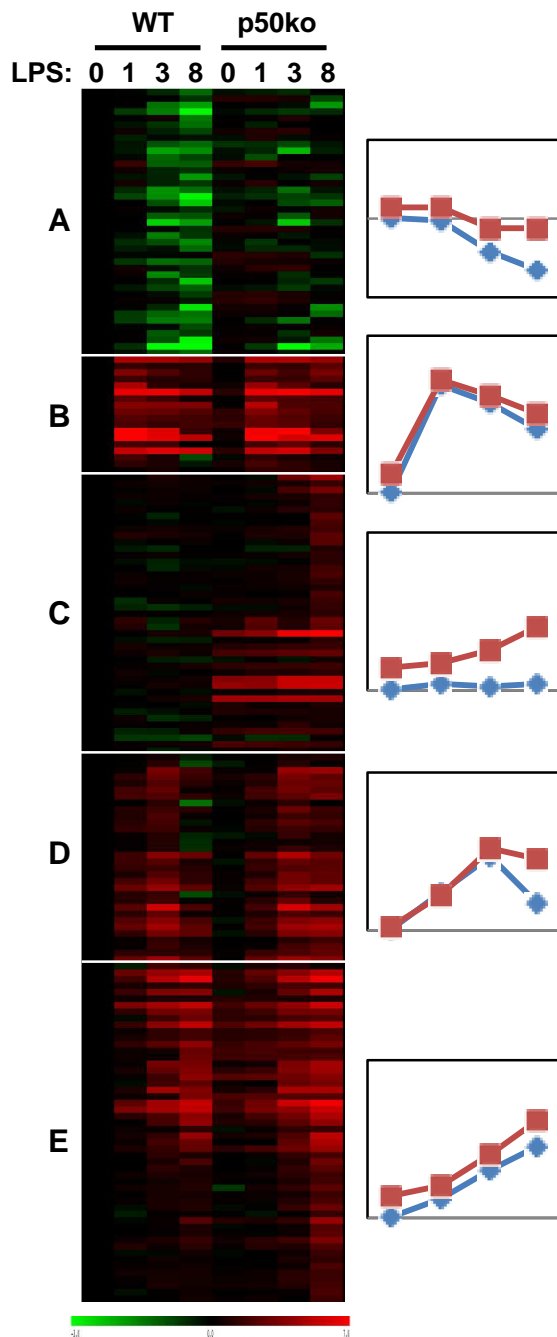
Figure 3.7 WT and p50ko gene expression after LPS stimulation. WT and p50ko BMDMs were left unstimulated or stimulated with LPS for 1, 3, or 8 hours and gene expression was analyzed via microarray. 151 genes were 2-fold hyperexpressed in p50ko compared to WT cells. K-means clustering was performed and the average fold induction ($\log_2$) of each cluster for WT (blue) or p50ko (red) was graphed.

A

Cluster	Motif name	# genes	% enrich	p-value	Motif
A	p65	7/33	21.2% (.77%)	1^{-8}	
B	p65*	2/16	12.5% (.71%)	1^{-2}	
C	IRF	4/34	11.8% (.0%)	1^{-11}	

B

Motif name	# genes	% enrich	p-value	Motif
IRF	7/151	4.64% (.04%)	1^{-11}	
ISRE	11/151	7.28% (.34%)	1^{-10}	
p65	9/151	5.96% (.42%)	1^{-7}	

Figure 3.8 De novo motif enrichment for genes hyperexpressed in p50ko BMDMs after LPS stimulation. WT and p50ko BMDMs were left unstimulated or stimulated with LPS for 1, 3, or 8 hours and gene expression was analyzed via microarray. 151 genes were 2-fold hyperexpressed in p50ko compared to WT cells. K-means clustering was performed and the most highly enriched motifs identified *de novo* are shown in (A) for each cluster from Figure 3.7 (asterisk indicates known, not *de novo,* motifs). The most highly enriched motifs identified *de novo* for all 151 unique genes are shown in (B). In the first column, the motif name is listed. In the next, the number of genes (over the number of genes analyzed) is shown. Next, the percent enrichment is indicated, with the percent enrichment in the background sequences in parentheses, followed by the p-value. In the last column, the upper motif pictured in each row is the *de novo* motif, while the lower motif is the known motif which most closely matched with the *de novo* motif.

Figure 3.9 WT and p50ko gene expression after CpG stimulation. WT and p50ko BMDMs were left unstimulated or stimulated with CpG for 1, 3, or 8 hours and gene expression was analyzed via microarray. 192 genes were 2-fold hyperexpressed in p50ko compared to WT cells. K-means clustering was performed and the average fold induction ($\log_2$) of each cluster for WT (blue) or p50ko (red) was graphed. The most highly enriched motifs identified *de novo* are shown (asterisk indicates known, not *de novo,* motifs).

A

Cluster	Motif name	# genes	% enrich	p-value	Motif
B	p65	12/25	48.0% (4.8%)	1^{-9}	
C	p65	10/20	50.0% (2.9%)	1^{-10}	
D	p65	17/59	28.8% (4.8%)	1^{-8}	
D	ISRE*	4/59	6.78% (.74%)	1^{-2}	
E	IRF	9/57	15.8% (.68%)	1^{-9}	
E	ISRE*	7/57	12.3% (.97%)	1^{-2}	

B

Motif name	# genes	% enrich	p-value	Motif
p65	50/192	26.04% (6.91%)	1^{-15}	
ISRE	17/192	8.85% (0.7%)	1^{-12}	

Figure 3.10 De novo motif enrichment for genes hyperexpressed in p50ko BMDMs after CpG stimulation. WT and p50ko BMDMs were left unstimulated or stimulated with CpG for 1, 3, or 8 hours and gene expression was analyzed via microarray. 192 genes were 2-fold hyperexpressed in p50ko compared to WT cells. K-means clustering was performed and the most highly enriched motifs identified *de novo* are shown in (A) for each cluster from Figure 3.9 (asterisk indicates known, not *de novo,* motifs). The most highly enriched motifs identified *de novo* for all 192 unique genes are shown in (B). In the first column, the motif name is listed. In the next, the number of genes (over the number of genes analyzed) is shown. Next, the percent enrichment is indicated, with the percent enrichment in the background sequences in parentheses, followed by the p-value. In the last column, the upper motif pictured in each row is the *de novo* motif, while the lower motif is the known motif which most closely matched with the *de novo* motif.
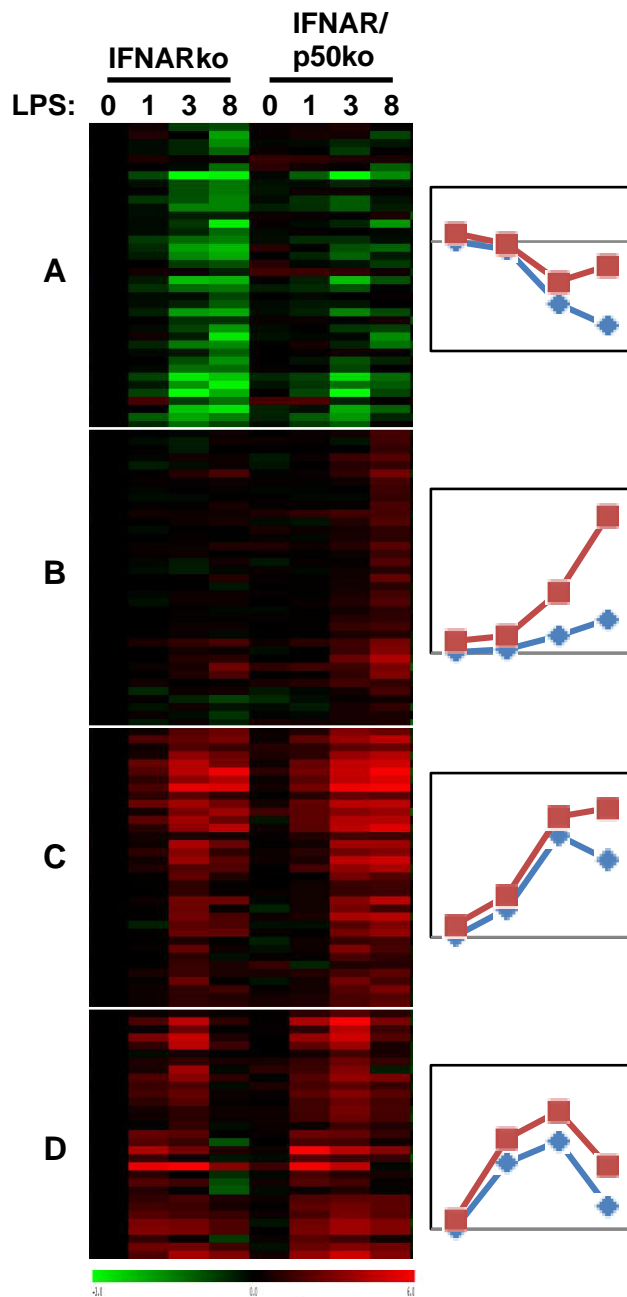
Figure 3.11 IFNARko and IFNAR/p50ko gene expression after LPS stimulation. IFNARko and IFNAR/p50ko BMDMs were left unstimulated or stimulated with LPS for 1, 3, or 8 hours and gene expression was analyzed via microarray. 115 genes were ≥2-fold hyperexpressed in IFNAR/p50ko compared to IFNARko cells. K-means clustering was performed and the average fold induction (log_2) of each cluster for IFNARko (blue) or IFNAR/p50ko (red) was graphed. The most highly enriched motifs identified *de novo* are shown (asterisk indicates known, not *de novo,* motifs).

A

Cluster	Motif name	# genes	% enrich	p-value	Motif
A	IRF3	6/33	18.2% (.48%)	1^{-7}	
A	IRF(6/4)	7/33	21.2% (.88%)	1^{-7}	
B	p65	3/30	10.0% (.15%)	1^{-4}	
C	ISRE	7/28	25.0% (.69%)	1^{-9}	
C	REL	8/28	28.6% (4.6%)	1^{-4}	

B

Motif name	# genes	% enrich	p-value	Motif
ISRE*	4/115	3.48% (.65%)	1^{-2}	

Figure 3.12 De novo motif enrichment for genes hyperexpressed IFNAR/p50ko BMDMs after LPS stimulation. IFNARko and IFNAR/p50ko BMDMs were left unstimulated or stimulated with LPS for 1, 3, or 8 hours and gene expression was analyzed via microarray. 115 genes were 2-fold hyperexpressed in IFNAR/p50ko compared to IFNARko cells. K-means clustering was performed and the most highly enriched motifs identified *de novo* are shown in (A) for each cluster from Figure 3.11 (asterisk indicates known, not *de novo,* motifs). The most highly enriched motifs identified *de novo* for all 115 unique genes are shown in (B). In the first column, the motif name is listed. In the next, the number of genes (over the number of genes analyzed) is shown. Next, the percent enrichment is indicated, with the percent enrichment in the background sequences in parentheses, followed by the p-value. In the last column, the upper motif pictured in each row is the *de novo* motif, while the lower motif is the known motif which most closely matched with the *de novo* motif.
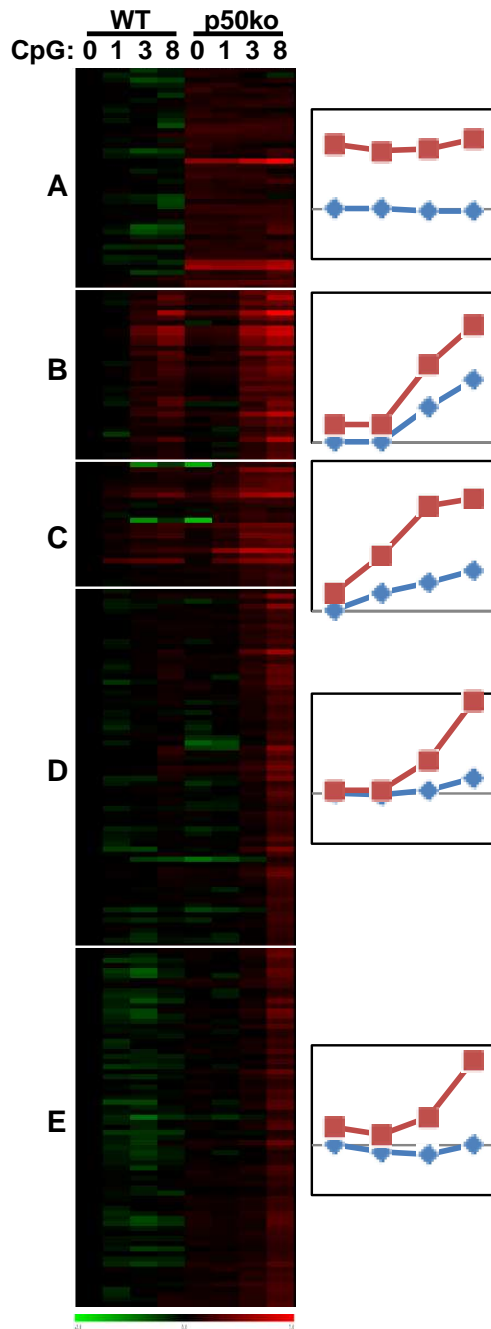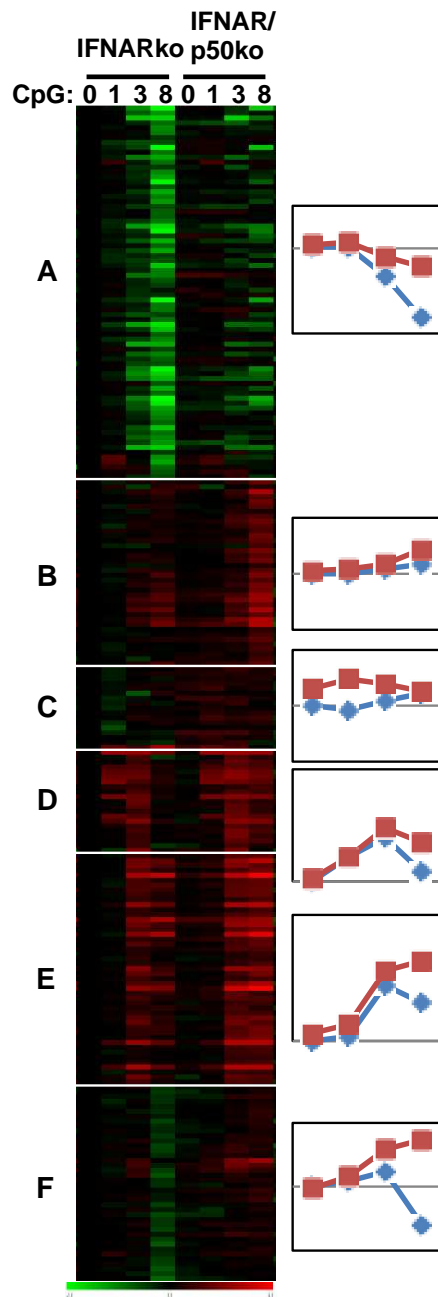
Figure 3.13 IFNARko and IFNAR/p50ko gene expression after CpG stimulation. IFNARko and IFNAR/p50ko BMDMs were left unstimulated or stimulated with CpG for 1, 3, or 8 hours and gene expression was analyzed via microarray. 194 genes were ≥2-fold hyperexpressed in IFNAR/p50ko compared to IFNARko cells. K-means clustering was performed and the average fold induction ($\log_2$) of each cluster for IFNARko (blue) or IFNAR/p50ko (red) was graphed. The most highly enriched motifs identified *de novo* are shown (asterisk indicates known, not *de novo,* motifs).

A

Cluster	Motif name	# genes	% enrich	p-value	Motif
B	p65	4/34	11.8% (.13%)	1⁻⁶	
C	REL	4/13	30.8% (.55%)	1⁻⁶	
D	REL	3/15	20.0% (.0%)	1⁻⁹	

B

Motif name	# genes	% enrich	p-value	Motif
p65	13/194	6.70% (.88%)	1⁻⁷	

Figure 3.14 De novo motif enrichment for genes hyperexpressed IFNAR/p50ko BMDMs after LPS stimulation. IFNARko and IFNAR/p50ko BMDMs were left unstimulated or stimulated with CpG for 1, 3, or 8 hours and gene expression was analyzed via microarray. 194 genes were 2-fold hyperexpressed in IFNAR/p50ko compared to IFNARko cells. K-means clustering was performed and the most highly enriched motifs identified *de novo* are shown in (A) for each cluster from Figure 3.13 (asterisk indicates known, not *de novo,* motifs). The most highly enriched motifs identified *de novo* for all 194 unique genes are shown in (B). In the first column, the motif name is listed. In the next, the number of genes (over the number of genes analyzed) is shown. Next, the percent enrichment is indicated, with the percent enrichment in the background sequences in parentheses, followed by the p-value. In the last column, the upper motif pictured in each row is the *de novo* motif, while the lower motif is the known motif which most closely matched with the *de novo* motif.
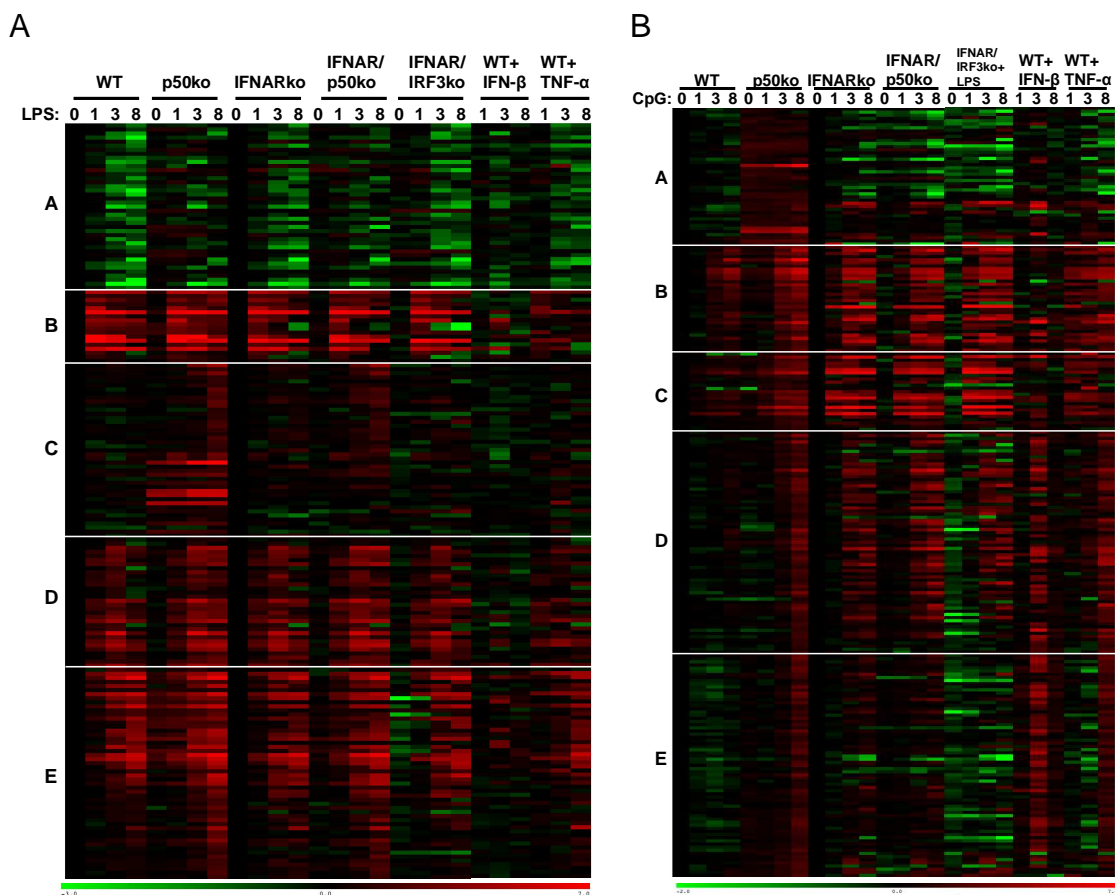
Figure 3.15 LPS- or CpG-responsive p50-repressed genes in the absence of IFNAR. WT, p50ko, IFNARko, and IFNAR/p50ko BMDMs were left unstimulated or stimulated with (A) LPS or (B) CpG for 1, 3, or 8 hours and gene expression was analyzed via microarray. Genes displayed here were ≥2-fold hyperexpressed in p50ko compared to WT cells. K-means clustering was performed with respect to WT and p50ko, and gene expression for IFNARko, IFNAR/p50ko and IFNAR/IRF3ko for each cluster is also shown.
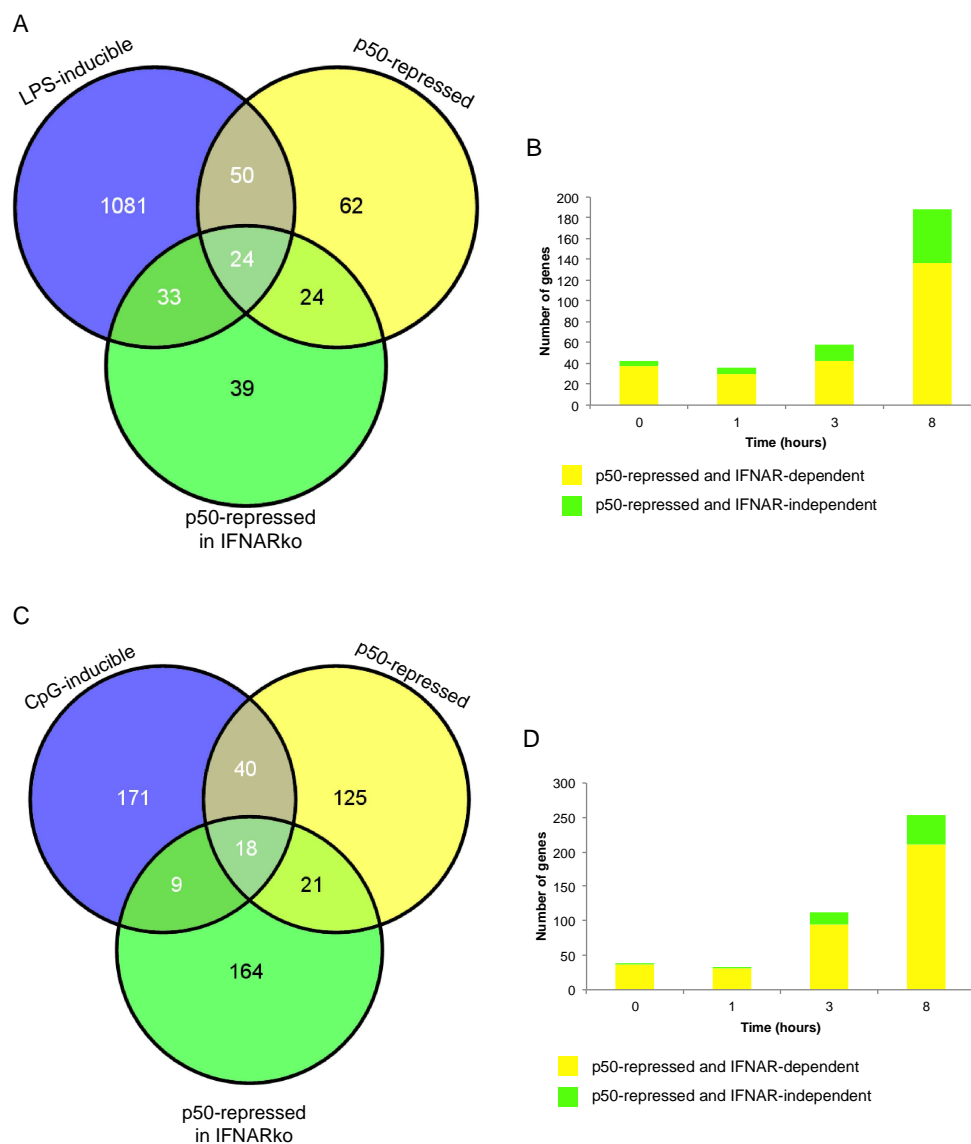
Figure 3.16 p50-repressed genes are largely IFNAR-dependent. WT, p50ko, IFNARko, and IFNAR/p50ko BMDMs were left unstimulated or stimulated with (A-B) LPS or (C-D) CpG for 1, 3, or 8 hours and gene expression was analyzed via microarray. (A) LPS-responsive genes that were ≥2-fold induced in WT cells (blue) or ≥2-fold hyperexpressed in p50ko (yellow) or ≥2-fold hyperexpressed in IFNAR/p50ko (green). (B) Number of LPS-responsive genes ≥2-fold hyperexpressed p50ko (yellow) that were also ≥2-fold hyperexpressed in IFNAR/p50ko (green) at each time point. (C) CpG-responsive genes that were ≥2-fold induced in WT cells (blue) or ≥2-fold hyperexpressed p50ko (yellow) or ≥2-fold hyperexpressed in IFNAR/p50ko (green). (D) Number of CpG-responsive genes ≥2-fold hyperexpressed p50ko (yellow) that were also ≥2-fold hyperexpressed in IFNAR/p50ko (green) at each time point.
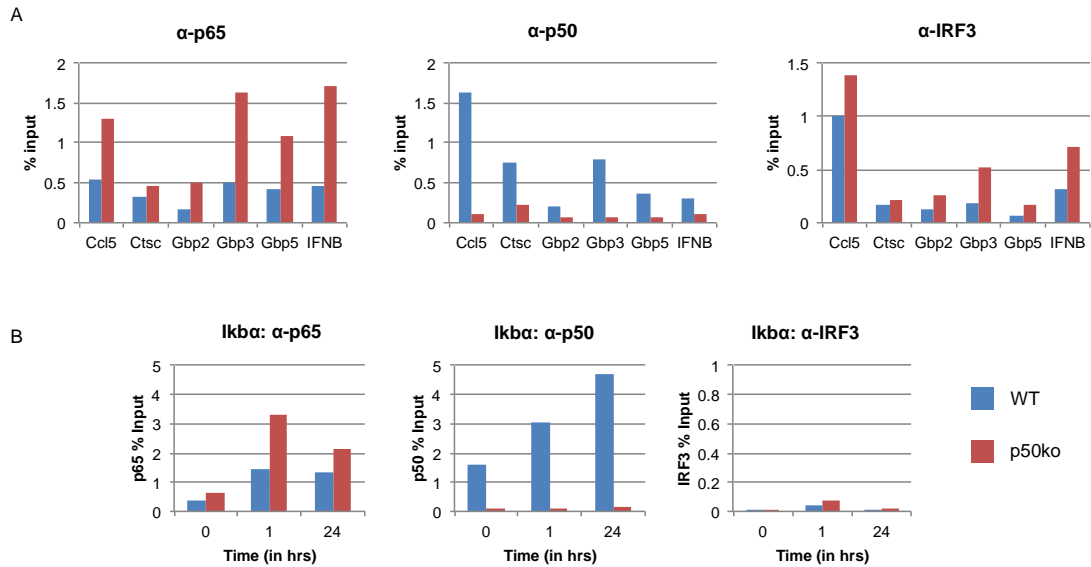
Figure 3.17 Chromatin immunoprecipitation of p65, p50 and IRF3 after LPS stimulation. BMDMs were left unstimulated or stimulated with LPS for 1 or 24 hours then analyzed by ChIP followed by qPCR. p50-repressed genes identified by microarray analysis were assessed for their recruitment of p65, p50 or IRF3. (A) Notably, Ccl5 (RANTES) and IFN-β showed increased recruitment of both p65 and IRF3 in p50ko BMDMs compared to WT after 1 hour of LPS stimulation. (B) IκBα was a positive control for NF-κB target genes.
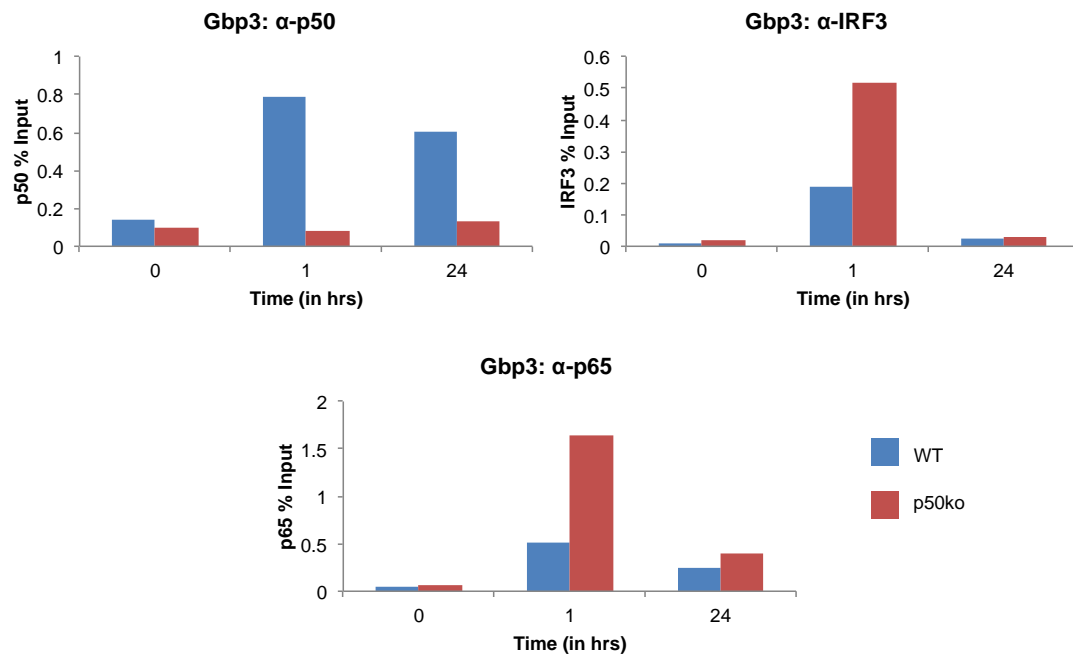
Figure 3.18 Chromatin immunoprecipitation of p65, p50 and IRF3 on the Gbp3 promoter after LPS stimulation. BMDMs were left unstimulated or stimulated with LPS for 1 or 24 hours then analyzed by ChIP followed by qPCR. Gbp3, a p50-repressed genes identified by microarray analysis, was assessed for the recruitment of p65, p50 or IRF3 to its promoter. Gbp3 showed increased recruitment of both p65 and IRF3 in p50ko BMDMs compared to WT, with both IRF3 and p50 occupying the promoter simultaneously in WT cells.
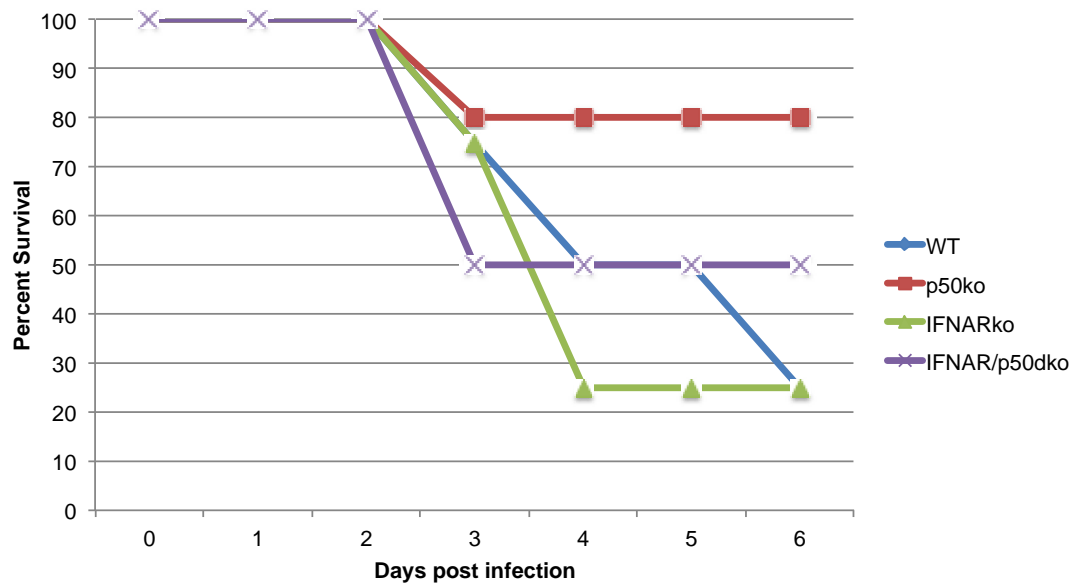
Figure 3.19 Survival curves of mice after S. pneumoniae infection. WT, p50ko, IFNARko, and IFNAR/p50ko mice were challenged with an intraperitoneal injection of 50 CFU of *S. pneumoniae* and survival was monitored at daily intervals.

Chapter 4: Surveying the specificity of innate immune responses

4.1 Introduction

Macrophages are resident in every tissue and are integral as potent inducers of the inflammatory reactions against invading pathogens. To mediate host defense, macrophages are capable of recognizing a broad range of PAMPs allowing them to detect, engulf, and kill a diverse number of microorganisms [63]. Once a macrophage senses a pathogen, elaborate and extensive signaling cascades are activated which allow the cell to perform its effector functions like chemotaxis, secretion of cytokines, or phagocytosis.

Purified microbial components capable of activating individual TLRs have commonly been used to study the gene activation programs of macrophages, for example, using LPS to study gene expression after TLR4 activation [3, 18]. However, during live microbe challenges immune cells are confronted by complex intact bacteria and viruses that may be able to activate multiple receptors simultaneously.

While a limited number of studies have attempted to investigate and compare the gene expression profiles of macrophages after challenge with whole bacteria [64], these studies neglected to examine gene expression after viral challenge and were previously performed using microarray analysis. RNA sequencing (RNA-seq) can also be used to interrogate the transcriptome, and its use and findings are now challenging earlier gene expression studies.

Many have found that RNA-seq provides better transcript quantity and quality, offers a larger dynamic range, and even allows for the detection of alternative splicing events [65-67].

In this study, we compared cytokine or TLR ligand stimulation to whole bacterial and viral challenge and assess subsequent macrophage gene expression via RNA-seq. By using both purified microbial components and live microorganisms, we were able to investigate whether responses to bacteria or virus are dominated by individual TLR signals or if whole organisms provoke cumulative activation through multiple TLRs.

4.2 Materials and Methods

4.2.1 Animals and cell culture

Wild type C57BL/6 mice were housed in pathogen-free conditions at the University of California, San Diego (UCSD) and all procedures were approved by the Institutional Animal Care and Use Committee. Bone marrow derived macrophages (BMDMs) were isolated from wild type femurs. A total of 7×10^6 BM cells were cultured in 15 cm suspension dishes in L929-conditioned media for 7 days at 37°C with 5% CO_2, as described previously [43]. BMDMs were then replated on day 7 at of 2×10^6 cells per 6 cm plate in Dulbecco's modified Eagle's medium (DMEM) supplemented with 10% fetal bovine serum and all experiments were performed on day 8.

4.2.2 Stimuli

BMDMs were stimulated on day 8 with various TLR ligands (or PAMPs) from Invivogen: a TLR2/1 agonist, the synthetic triacylated lipoprotein Pam3CSK4 (3 μg/ml), a TLR2/6 agonist, a synthetic lipoprotein derived from *Mycoplasma salivarium*, FSL-1 (50 ng/ml), a TLR3 agonist, low molecular weight polyinosine-polycytidylic acid (Poly(I:C), 50 μg/ml), a TLR4 agonist, lipopolysaccharide B5:055 from *Escherichia coli* (LPS, 100 ng/ml, Sigma), a TLR5 agonist, recombinant flagellin from *Salmonella typhimurium* (30 ng/ml), a TLR7/8 agonist, the imidazoquinoline compound R848 (5 μg/ml), a TLR9 agonist, the synthetic CpG ODN 1668 (CpG, 100 mM), or IFN-β (100 U/ml), TNF-α (10 ng/ml), live *S. pneumoniae* (MOI 1.0), live *L. monocytogenes* (MOI 1.0), murine cytomegalovirus (MCMV, MOI 5.0), or vesicular stomatitis virus (VSV, MOI 1.0) as listed in Table 4.1. Additionally, BMDMs were transfected with Poly(I:C) using the Lipofectamine 2000 kit per the manufacturer's instructions (Poly(I:C) 50 μg/ml, Life Technologies).

4.2.3 Nuclear extraction and gel shift assays

BMDMs were replated with 5×10^6 cells per 10 cm plate on day 7. On day 8, BMDMs were left unstimulated or stimulated with LPS (100 ng/ml) or CpG (100nM) for 1, 6 or 24 hours. Cells were collected in CE Buffer (10 mM HEPES pH 7.9, 10 mM KCl, 0.1 mM EGTA, 0.1 mM EDTA, 1 mM dithiothreitol, 0.5 mM phenylmethylsulfonyl fluoride, 10 ug/ml aprotinin and 5

ug/ml leupeptin) in a microcentrifuge tube. To this, 0.5% Nonidet P-40 was added and the cells were vortexed for lysis. Nuclei were pelleted at 4000 x g and resuspended in 20 µl of high salt buffer (NE Buffer: 20 mM HEPES ph 7.9, 420 mM NaCl, 1.5 mM MgCl2, 0.2 mM EDTA, 25% glycerol, 1 mM dithiothreitol, 0.5 mM phenylmethylsulfonyl fluoride, 10 ug/ml aprotinin and 5 ug/ml leupeptin). Nuclear lysates were cleared by 14,000 x g centrifugation and protein concentrations were determined and normalized by a Bradford assay (Bio-Rad).

Gel-shift assays were performed as previously described [45, 46]. Briefly, nuclear extracts were incubated 38 bp spanning double-stranded oligonucleotides labeled with 32P containing two consensus κB sites (κB probe) and left at room temperature for 15 min prior to complex separation on a nondenaturing acrylamide gel. Bands were visualized by autoradiography.

4.2.4 RNA extraction and cDNA synthesis

BMDMs were washed with PBS, homogenized, and total RNA was extracted using the QIAshredder and RNeasy kits per the manufacturer's instructions (Qiagen). RNA was eluted in 30ul of RNase-free water. For subsequent qPCR analysis, 1 µg of RNA was reverse-transcribed into cDNA using the iScript cDNA synthesis kit according to the manufacturer's instruction (Bio-Rad).

4.2.5 qPCR

Quantitative real-time PCR (qPCR) was performed to measure the mRNA expression level of the housekeeping gene GAPDH and several genes of interest. Using a CFX384 Real-Time Detection System (Bio-Rad), each reaction was performed in triplicate in a final reaction volume of 5 µl, including 2.5 µl SsoAdvanced SYBR Green Supermix (Bio-Rad), 1.0 µl cDNA template, and 1.0 µl (100 nM final concentration) of each primer. Primers were designed for each gene using Primer3 (primers are listed in Table 4.2). After amplification, quantification cycle (Cq) values were generated using the Bio-Rad CFX Manager Software 1.6. The fold change of gene expression was calculated using the Δ(ΔCq) method as previously described [44].

4.2.6 RNA-seq

RNA sequencing was performed as previously described [68, 69]. In brief, mRNA was extracted from 2 µg total RNA using oligo(dT) magnetic beads and fragmented at high temperature using divalent cations. Next a cDNA library was generated using the Illumina TruSeq kits and quantitation was performed using the Roche Light Cycler 480. Sequencing was performed on Illumina's HiSeq 2000, according to the manufacturer's recommendations by the University of California, San Diego Biogem facility. Paired-end 100 bp reads were aligned to the mouse mm10 genome and RefSeq genes (PMID 12045153, PMID 12466850) with Tophat (PMID 19289445). Cufflinks was

used to ascertain differential expression of genes. Gene differential FPKMs were obtained with Cuffdiff, and analyzed with the CummeRbund package [70]. In R, we took the log base 2 of the FPKM values and used the wild type zero hour to normalize.

The subset of genes that showed ≥2-fold induction or repression in 2 consecutive time points or showed ≥4-fold induction or repression in one time point in pathogen infected BMDMs compared to PAMP stimulated BMDMs were considered significant. Using R's gplots package heat maps were created and significant genes were clustered hierarchically.

4.3 Results

4.3.1 Optimal TLR agonist concentration and microbial MOI for transcription factor activation

To optimize stimuli concentrations which allow for robust and similar levels of NF-κB activation, BMDMs were left unstimulated or stimulated with cytokines, PAMPs, or pathogens for up to 24 hours. Nuclear extracts were collected at the time points indicated. We tested serial dilutions of stimuli and pathogens to determine comparable levels of transcription factor activity across multiple conditions. Previous studies indicated small but detectable gene program induction differences when different MOIs of *E. coli* were used to stimulate macrophages [18].

We found that after stimulation with PAMPs, strong NF-κB activation was observed at most concentrations (Figures 4.1 and 4.2). Concentrations which demonstrated similar level of NF-κB activation (100 ng.ml FSL-1, 1 µg/ml Pam3CSK4, 1 µg/ml R848, and 10^7 CFU/ml heat-killed *L. monocytogenes*) were reconfirmed and directly compared in Figure 4.3. Additionally, NF-κB and ISGF3 activity after MCMV infection was assessed and an MOI of 5 demonstrated robust transcription factor activation as early as 1 hour after virus addition.

4.3.2 Optimal TLR agonist concentration and microbial MOI for gene expression

As with transcription factor activity, we wished to optimize stimuli concentrations which allow for robust and similar levels of inflammatory gene activation. To achieve this, BMDMs were left unstimulated or stimulated with cytokines, TLR agonists, or pathogens for 1, 3, 8, or 24 hours and RNA was extracted for analysis by qPCR. We tested serial dilutions of stimuli and pathogens to determine comparable levels of gene expression of inflammatory genes across several conditions. Fold induction of A20 (tnfaip3), Gbp3, IFN-β, IκBα, and TNF-α were compared for serial dilutions of each stimulus (data not shown for all dilutions). While some stimuli induced significantly higher gene expression than others for specific genes (for example, Poly(I:C) and LPS induce high levels of IFN-β compared to other stimuli, Figure 4.5), we

determined optimal concentration for each stimulus considering both transcription factor activation and gene expression, with optimal stimulus gene expression displayed in Figures 4.5 and 4.6 (see Methods for final concentrations chosen for RNA-seq analysis).

4.3.3 RNA-seq

To assess genome-wide gene expression, BMDMs were left unstimulated or stimulated with cytokines, TLR agonists, or pathogens for 1, 3, 8, or 24 hours and RNA was extracted for analysis by RNA-seq. Overall, we found that 4,664 genes were significantly induced or repressed after stimulation compared to unstimulated BMDMs (Figure 4.7). Significant genes were clustered hierarchically, and though many stimuli did demonstrate a core innate gene activation program, stimulus-specific gene activation clusters were still apparent. These stimulus-specific clusters were examined in more detail below by determining the genes which demonstrated viral- or bacterial-specific induction or repression (Figures 4.8 and 4.9).

4.3.4 Viral pathogens compared to PAMPs

In order to compare gene expression after TLR agonists or cytokines to live viral infection, BMDMs were exposed to virally related stimuli (Poly(I:C), transfected Poly(I:C), CpG DNA, R848 or IFN-β) or MCMV or VSV for 1, 3, 8 or 24 hours and gene expression was analyzed via RNA-seq. We examined

genes with either ≥2-fold repression in 2 consecutive time points (or ≥4-fold repression in one time point) in virally infected BMDMs compared to PAMP stimulated BMDMs, or genes with ≥2-fold induction in 2 consecutive time points (or ≥4-fold induction in one time point) in virally infected BMDMs compared to PAMP stimulated BMDMs. We observed 17 genes which were significantly repressed and 22 genes which were significantly induced after MCMV infection compared to PAMPs (Figure 4.8 A and B); we also observed 39 genes which were significantly repressed and 64 genes which were significantly induced after VSV infection compared to PAMPs (Figure 4.9 A and B). Genes which are differentially expressed after live viral infection but not PAMP stimulation represent possible virus-targeted genes which may be manipulated by the live virus to enhance infection. Further studies would be necessary to determine if these observed expression effects were directly controlled by the virus and what effect they have on infection outcome.

4.5.5 Bacterial pathogens compared to PAMPs

In order to compare gene expression after TLR agonists or cytokines to live bacterial infection, BMDMs were exposed to bacteria-derived stimuli (Pam3SCK4, LPS, rFlagellin, FSL-1, or CpG) or *L. monocytogenes* or *S. pneumoniae* for 1, 3, 8 or 24 hours and gene expression was analyzed via RNA-seq. We examined genes with either ≥2-fold repression in 2 consecutive time points (or ≥4-fold repression in one time point) in bacteria-infected

BMDMs compared to PAMP stimulated BMDMs, or genes with ≥2-fold induction in 2 consecutive time points (or ≥4-fold induction in one time point) in bacteria-infected BMDMs compared to PAMP stimulated BMDMs. We observed 40 genes which were significantly repressed and 146 genes which were significantly induced after *S. pneumoniae* infection compared to PAMPs (Figure 4.10 A and B); we also observed 43 genes which were significantly repressed and 93 genes which were significantly induced after *L. monocytogenes* infection compared to PAMPs (Figure 4.11 A and B). Like with viral infection, genes which are differentially expressed after live bacterial infection but not PAMP stimulation represent possible bacteria-targeted genes which may be manipulated by the live bacteria to enhance infection. Further studies would be necessary to determine if these observed expression effects were directly controlled by the bacteria and what effect they have on infection outcome

4.4 Discussion

Although a handful of studies have endeavored to investigate the gene expression profiles of macrophages after challenge with live pathogens [64], many neglected to examine gene expression after viral challenge and all were previously performed using microarray analysis. Here we used unbiased next-generation RNA-sequencing to interrogate the transcriptome of BMDMs which were stimulated with an extensive panel of cytokines, PAMPs, or live

pathogens. While many stimuli did display a core innate immune gene activation program, stimulus-specific activation clusters were still apparent.

To illustrate this, we determined which genes were uniquely induced or repressed after MCMV, VSV, *L. monocytogenes* or *S. pneumoniae* infection compared to PAMP stimulation. Genes which are differentially expressed after live viral or bacterial infection but not PAMP stimulation represent possible pathogen-targeted genes which may be manipulated by the live microbes to enhance infection. Further studies would be necessary to determine if these observed expression effects were directly controlled by the pathogens and what effect they have on infection outcome. These subsets of genes represent putative virulence factors, although additional characterization and analysis would be needed to confirm this.

Our results indicate the early innate immune gene expression is capable of stimulus-specific responsiveness. Future directions for this study include GO analysis on stimulus-specific or differentially expressed gene clusters and splice variant analysis.

4.5 Acknowledgements

Chapter 4 is original work performed under the guidance of A. Hoffmann. The dissertation author was the primary investigator and author of this material.

Table 4.1 Stimuli concentrations for RNA-seq. This table lists the various TLR agonists, pathogens, and cytokines used to stimulate BMDMs. These concentrations were determined to give robust and comparable levels of transcription factor activation and gene expression.

Pathway	Ligand/Pathogen	Conc/Titers
TLR2/1	Pam3CSK4	3.0 ug/ml
TLR3	Poly(I:C)	50 ug/ml
RIG-I	Transfected Poly(I:C)	50 ug/ml
TLR4	LPS	100 ng/ml
TLR5	rFlagellin	30 ng/ml
TLR2/6	FSL-1	50 ng/ml
TLR7/8	R848	5.0 ug/ml
TLR9	CpG DNA	100 nM
Type I IFN	IFN-β	100 U/ml
TNFR	TNF-α	10ng/ml
DNA virus	MCMV	MOI 5.0
RNA virus	VSV	MOI 1.0
Gram+	S. pneumoniae	MOI 1.0
Gram+	L. monocytogenes	MOI 1.0

Table 4.2 Primers used for qPCR

Gene	Accession Number	Name	Sequence
Ifnb	NM_010510.1	IFNb.f	GGTCCGAGCAGAGATCTTCA
		IFNb.r	CTGAGGCATCAACTGACAGG
Gapdh	NM_008084.2	Gapdh.f	AACTTTGGCATTGTGGAAGG
		Gapdh.r	GGATGCAGGGATGATGTTCT
A20	NM_001166402.1	Tnfaip3.f	GCACACTCGGAAGCACCATG
		Tnfaip3.r	ATGCTGGCTTGATCTCAGCTG
IκBa	NM_010907.2	ikba.f	AGACTCGTTCCTGCACTTG
		ikba.r	AGTCTGCTGCAGGTTGTTC
TNFa	NM_013693.2	Tnf.f	CACCACGCTCTTCTGTCTAC
		Tnf.r	AGAAGATGATCTGAGTGTGAGG
Gbp3	NM_018734	Gbp3.f	GATGGAGAGAGAGCCATAGCA
		Gbp3.r	CCTTCTGTCTCTGCCTCAGC
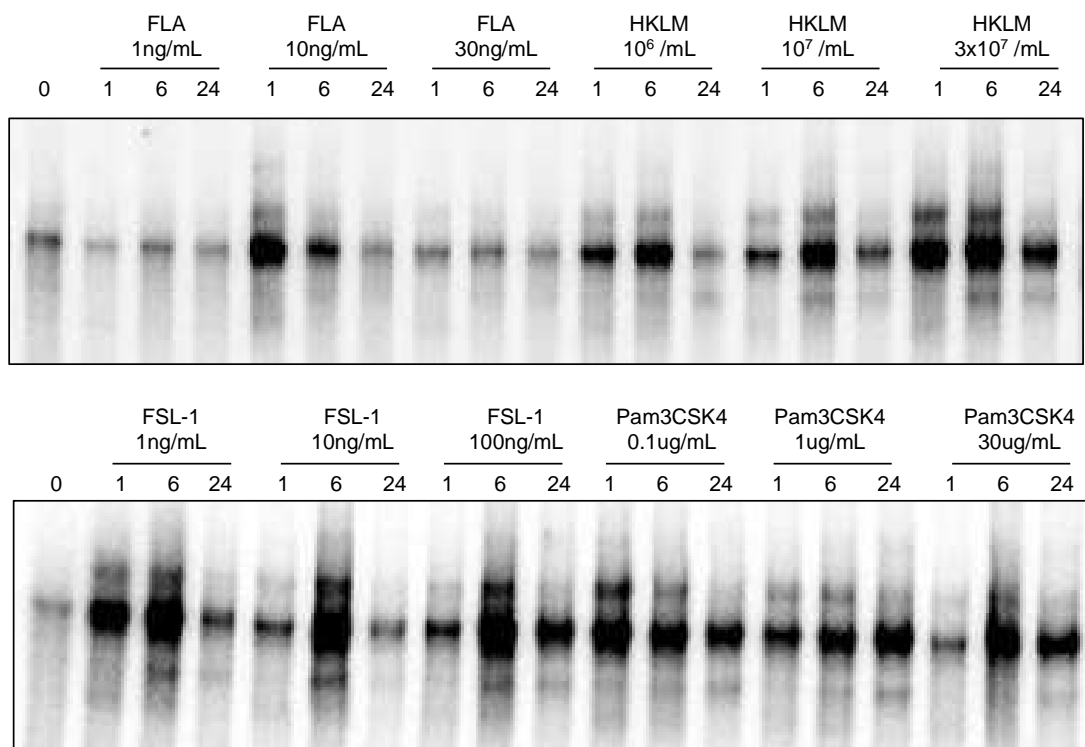
Figure 4.1 NF-κB activity after various TLR stimuli. BMDMs were left unstimulated or were stimulated with various TLR ligands for the times and concentrations indicated. NF-κB activity was assessed by EMSA.
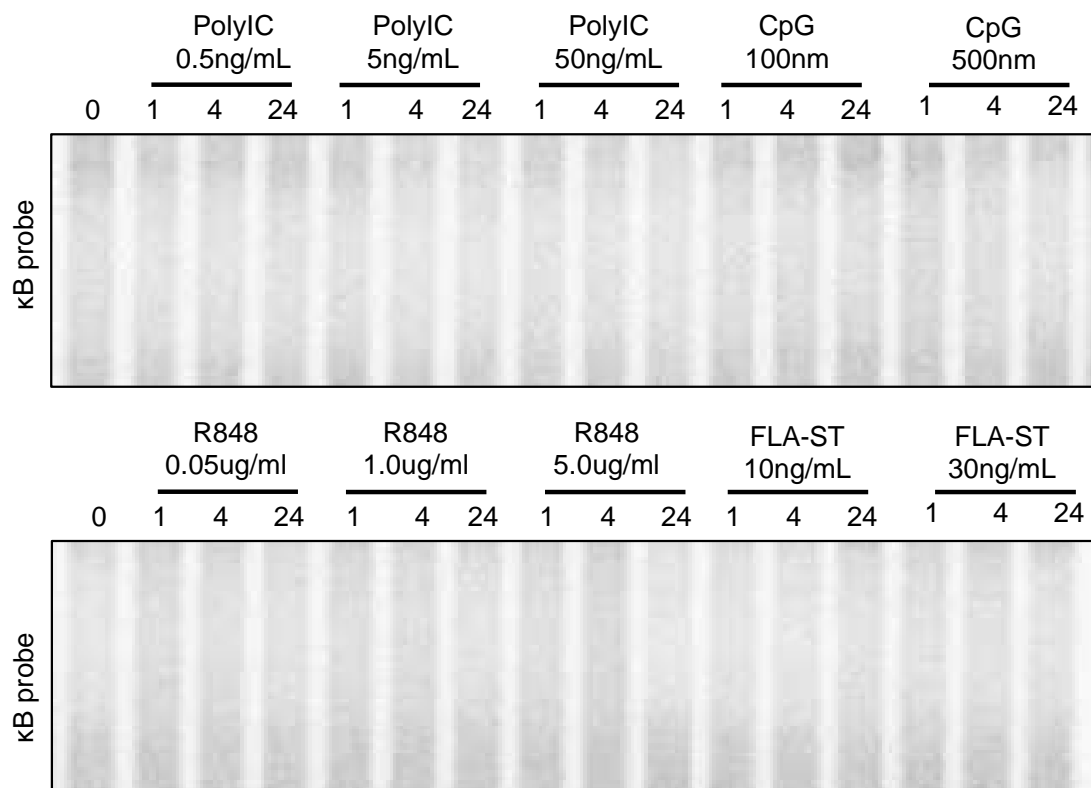
Figure 4.2 NF-κB activity after various TLR stimuli. BMDMs were left unstimulated or were stimulated with various TLR ligands for the times and concentrations indicated. NF-κB activity was assessed by EMSA.
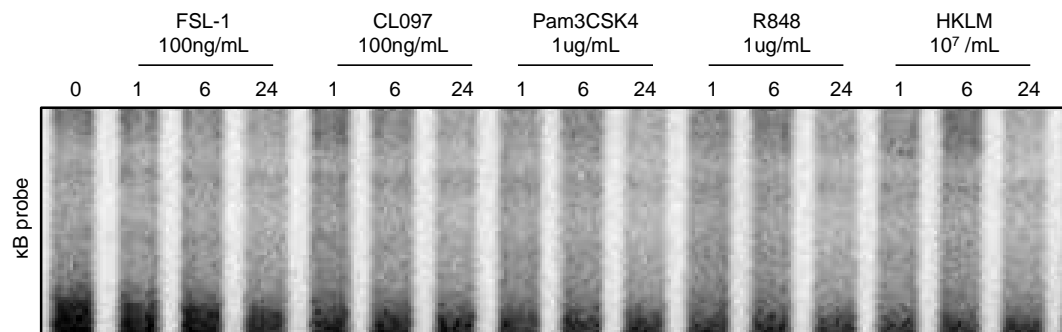
Figure 4.3 NF-κB activity after various TLR stimuli. BMDMs were left unstimulated or were stimulated with various TLR ligands for the times and concentrations indicated. NF-κB activity was assessed by EMSA.
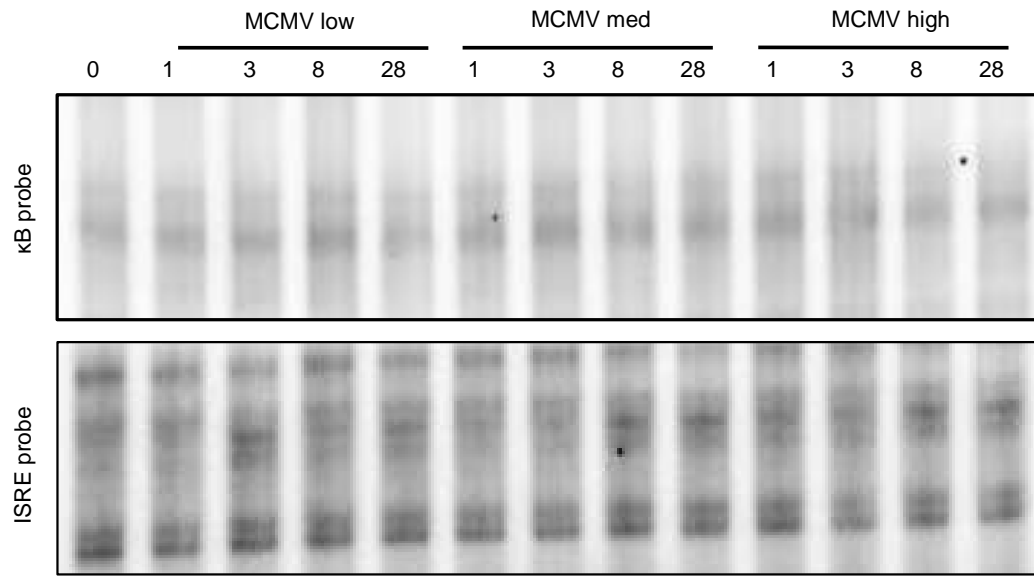
Figure 4.4 Transcription factor activity after MCMV infection. BMDMs were infected with MCMV (MOI 0.1, 1.0, or 5.0). NF-κB activity and ISGF3 activity were assessed after the timepoints (in hours) indicated. Robust transcription factor activity was observed with an MOI of 5.0.
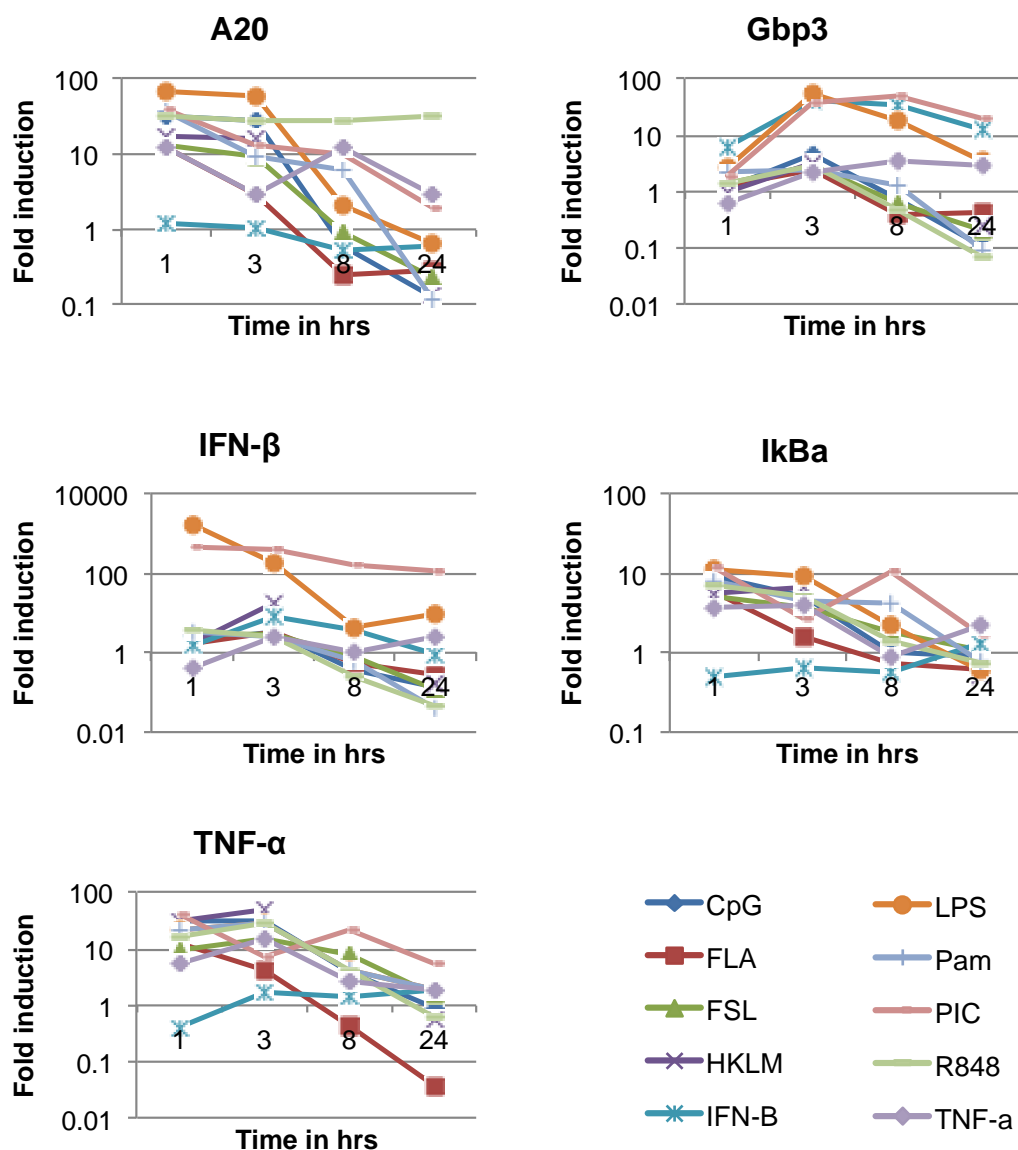
Figure 4.5 Gene expression after stimulus. BMDMs were stimulated with the 10 PAMPs, pathogens or cytokines indicated and several inflammatory and control genes of interest were assessed by qPCR to determine if comparable levels of gene expression were observed. Concentrations were as follows: Pam3CSK4, 3.0 ug/ml; Poly(I:C), 50 ug/ml; LPS, 100 ng/ml; rFlagellin, 30 ng/ml; FSL-1, 50 ng/ml; R848, 5.0 ug/ml; CpG, 100 nM; IFN-β, 100 U/ml; TNF-α, 10ng/ml; heat-killed L. monocytogenes, MOI 1.0.
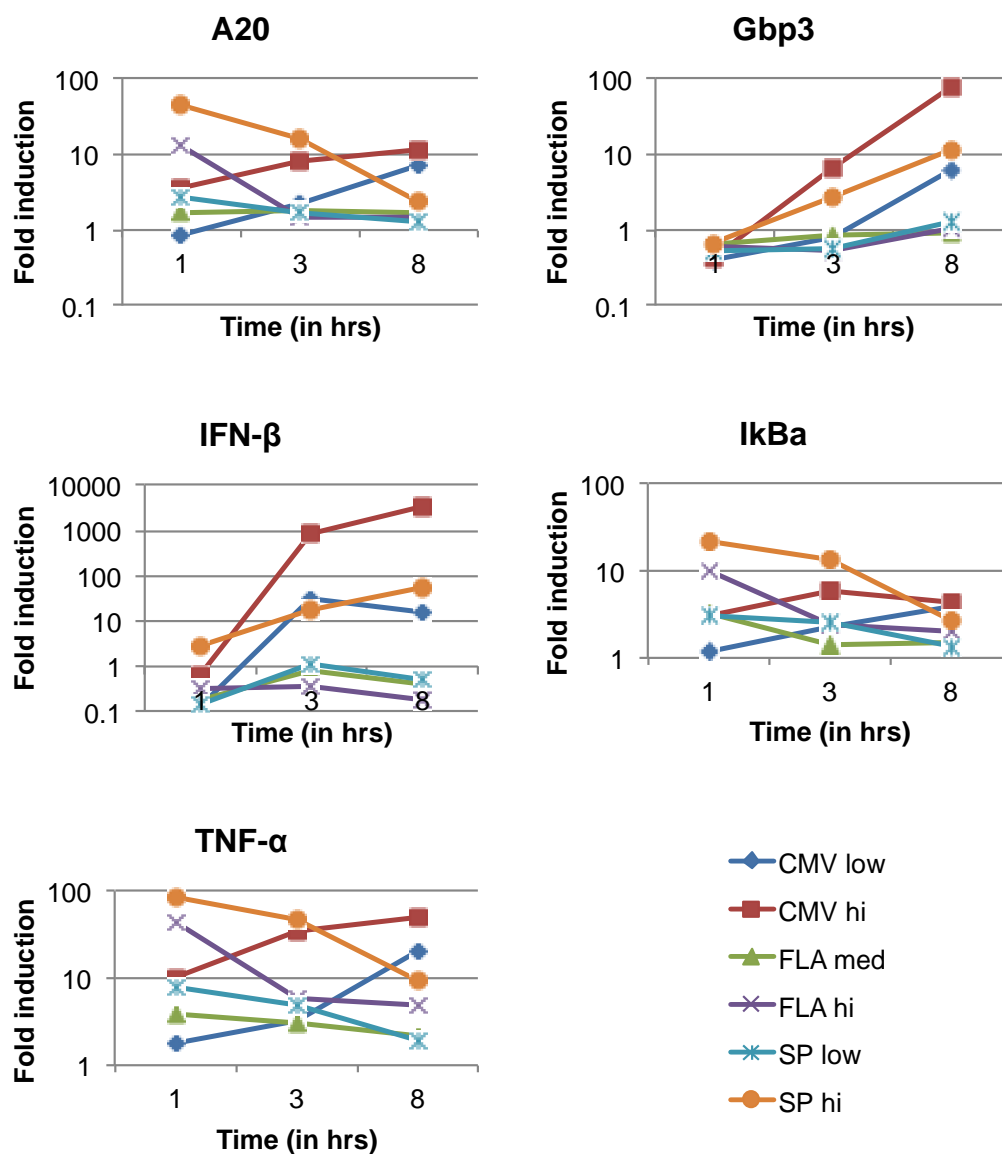
Figure 4.6 Gene expression after infection or stimulus. BMDMs were stimulated with the 10 PAMPs, pathogens or cytokines indicated and several inflammatory and control genes of interest were assessed by qPCR to determine if comparable levels of gene expression were observed Concentrations were as follows: MCMV, MOI 0.5 and 5.0; rFlagellin, 3 ng/ml or 30 ng/ml; or *S. pneumoniae,* MOI 0.1 or 1.0.
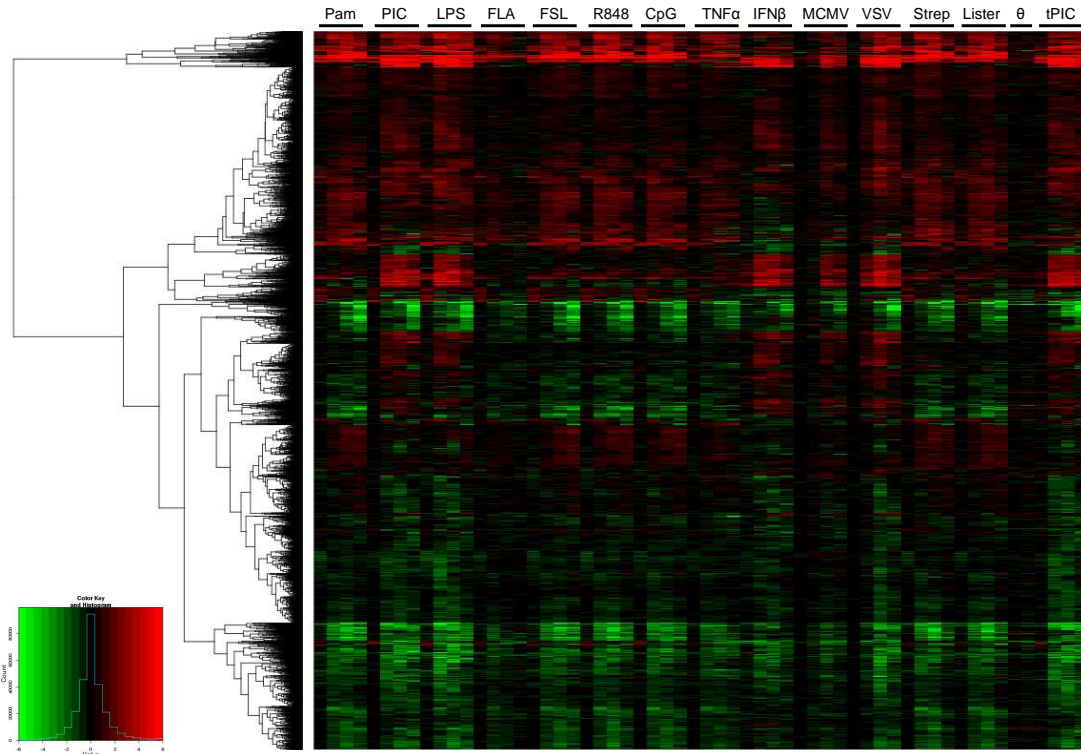
Figure 4.7 Gene expression or repression after TLR stimulation or pathogen infection in BMDMs. BMDMs were exposed to stimuli or pathogens for 1, 3, 8 or 24 hours and gene expression was analyzed via RNA-seq. Genes with ≥4-fold induction or repression in 2 consecutive time points were clustered hierarchically and are shown here. See Table 4.1 for stimuli and pathogen concentrations.
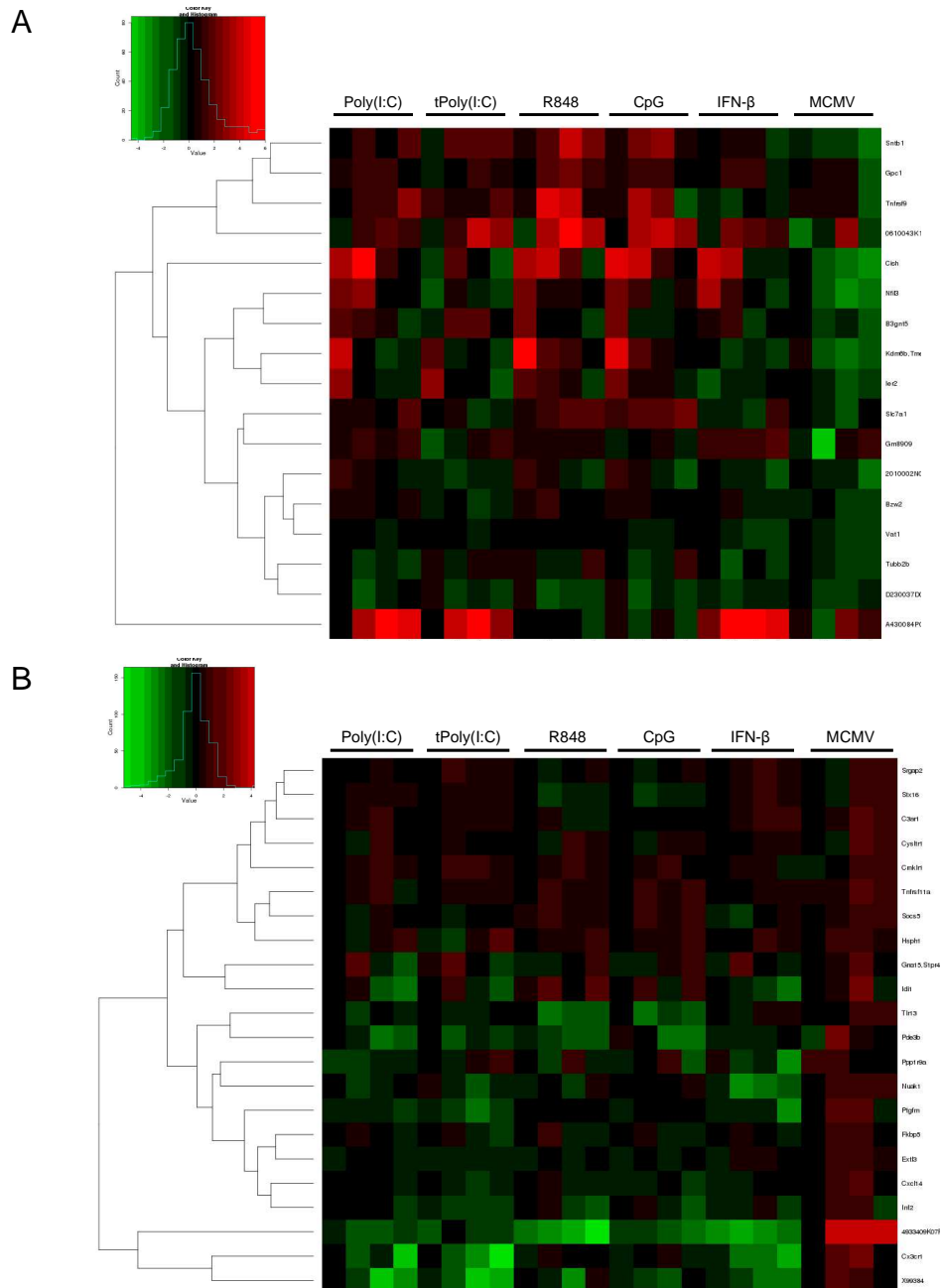
Figure 4.8 Gene expression or repression after TLR stimulation or MCMV infection in BMDMs. BMDMs were exposed to stimuli or MCMV for 1, 3, 8 or 24 hours and gene expression was analyzed via RNA-seq. (A) Genes with ≥2-fold repression in 2 consecutive time points or ≥4-fold repression in MCMV infected BMDMs compared to PAMP stimulated BMDMs are shown. (B) Genes with ≥2-fold induction in 2 consecutive time points or ≥4-fold induction in MCMV infected BMDMs compared to PAMP stimulated BMDMs are shown.
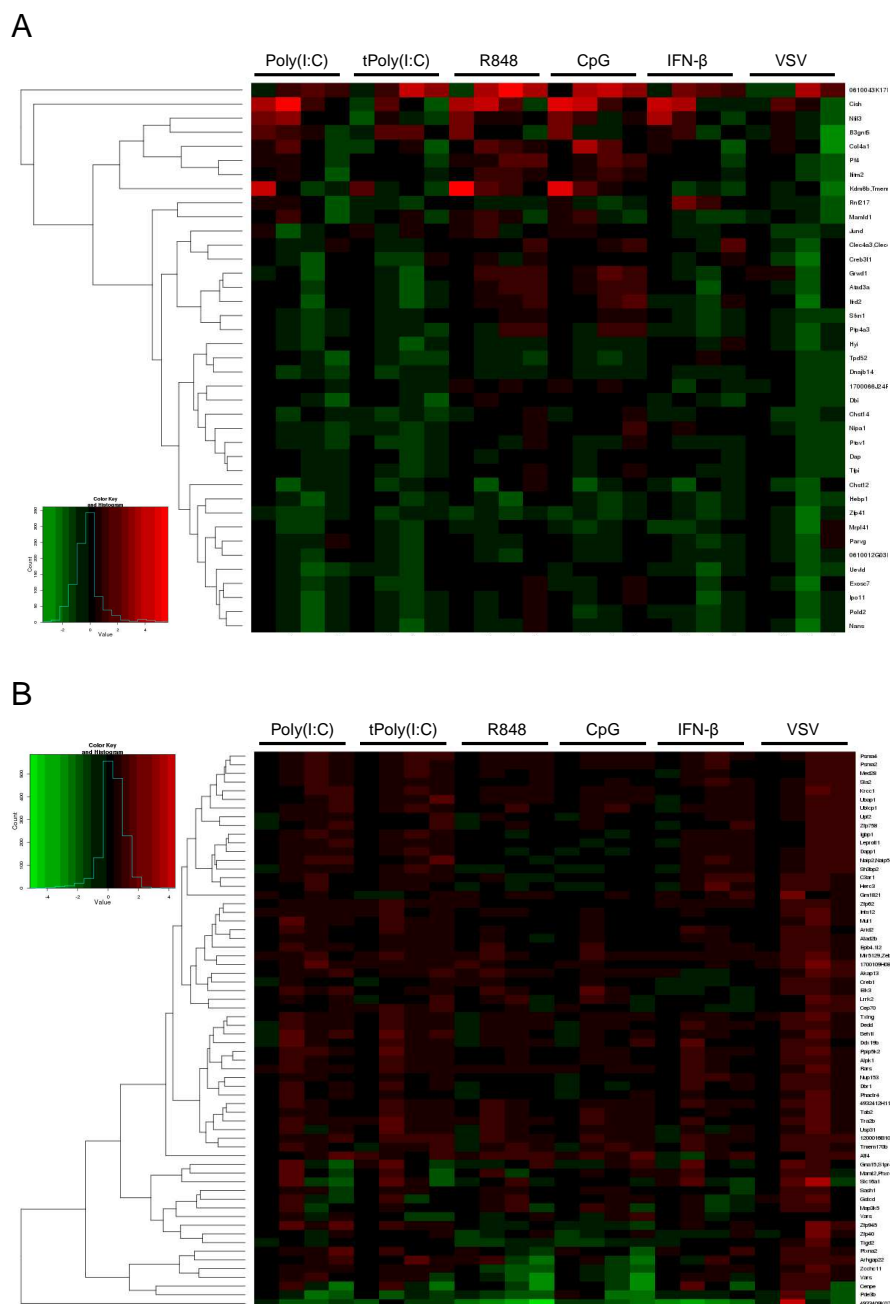
Figure 4.9 Gene expression or repression after TLR stimulation or VSV infection in BMDMs. BMDMs were exposed to stimuli or VSV for 1, 3, 8 or 24 hours and gene expression was analyzed via RNA-seq. (A) Genes with ≥2-fold repression in 2 consecutive time points or ≥4-fold repression in MCMV infected BMDMs compared to PAMP stimulated BMDMs are shown. (B) Genes with ≥2-fold induction in 2 consecutive time points or ≥4-fold induction in VSV infected BMDMs compared to PAMP stimulated BMDMs are shown.
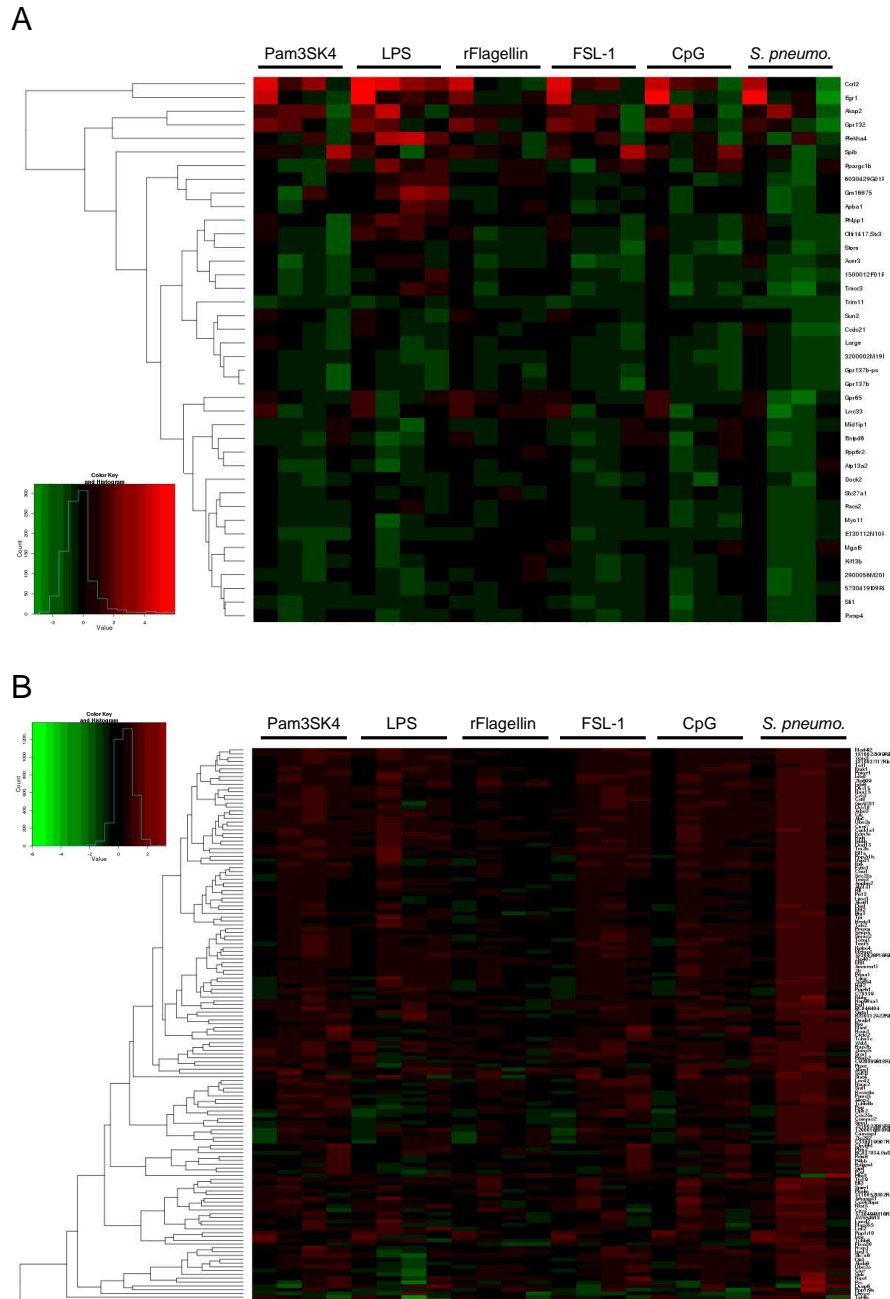
Figure 4.10 Gene expression or repression after TLR stimulation or S. pneumoniae infection in BMDMs. BMDMs were exposed to stimuli or VSV for 1, 3, 8 or 24 hours and gene expression was analyzed via RNA-seq. (A) Genes with ≥2-fold repression in 2 consecutive time points or ≥4-fold repression in *S. pneumoniae* infected BMDMs compared to PAMP stimulated BMDMs are shown. (B) Genes with ≥2-fold induction in 2 consecutive time points or ≥4-fold induction in *S. pneumoniae* infected BMDMs compared to PAMP stimulated BMDMs are shown.

A

B
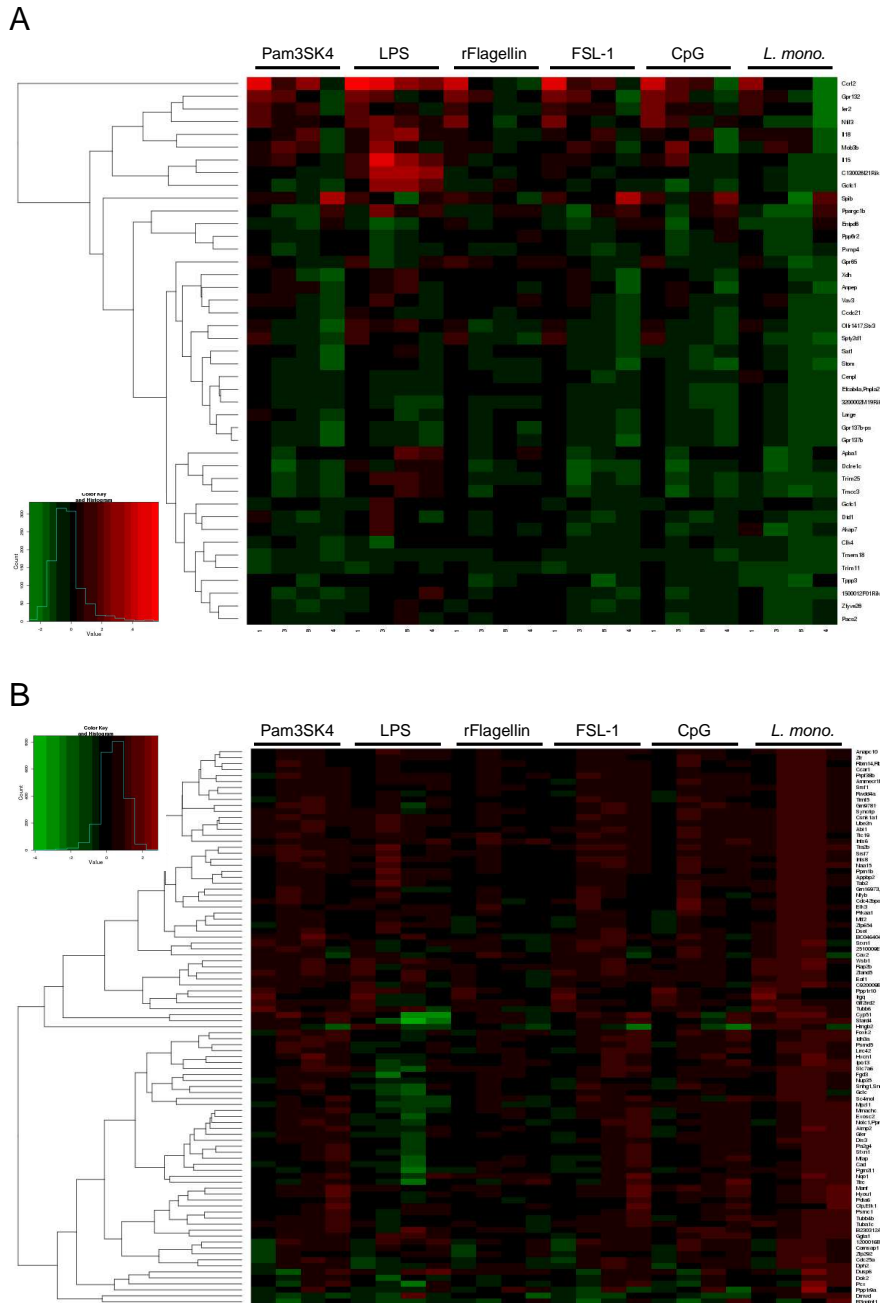
Figure 4.11 Gene expression or repression after TLR stimulation or L. monocytogenes infection in BMDMs. BMDMs were exposed to stimuli or VSV for 1, 3, 8 or 24 hours and gene expression was analyzed via RNA-seq. (A) Genes with ≥2-fold repression in 2 consecutive time points or ≥4-fold repression in *L. monocytogenes* infected BMDMs compared to PAMP stimulated BMDMs are shown. (B) Genes with ≥2-fold induction in 2 consecutive time points or ≥4-fold induction in *L. monocytogenes* infected BMDMs compared to PAMP stimulated BMDMs are shown.

Chapter 5: *Ex Vivo* Innate Immune Cytokine Signature of Enhanced Risk of Relapsing Brucellosis

5.1 Introduction

Brucellosis in humans is a zoonotic infection caused by Gram-negative facultative intracellular bacteria of the *Brucella* genus. Four species are typically responsible for human infections, *B. abortus, B. melitensis, B. suis, and B. canis*, and are transmitted from animal reservoirs including infected cows, goats or sheep, pigs, and dogs, respectively. Infection occurs by ingestion of contaminated unpasteurized milk or cheese or through contact with blood or materials from infected animals [15]. *B. melitensis* is recognized as not only the most virulent species, needing only a few organisms (10-100) to establish infection, but also the predominant species responsible for the brucellosis burden in Perú [71, 72]. *Brucella* spp. are of particular interest because they are easily aerosolized, which is underscored by the designation of brucellosis as the most common laboratory-acquired infection [73] and *Brucella* spp. as a category B agent on the Centers for Disease Control bioterrorism hazard list.

Approximately 5-40% of patients treated for brucellosis suffer a relapse, with the wide variation in risk historically being attributed to the duration and combination of antibiotic treatment [74]. However, few investigations have focused on the variation of the innate immune reaction to *Brucella* spp. and its

impact on the rate of relapse. While studies have examined the association of genetic polymorphisms in cytokines and other immunity-related genes with brucellosis susceptibility [75, 76], less emphasis has been placed on the overall functional cytokine reaction of patients who demonstrate brucellosis susceptibility or relapse.

Brucella spp. are able to survive and replicate within macrophages, and effective control of brucellosis requires a potent Th1 response to activate cellular mediated immunity which is driven by the production of IFN-γ, IL-2, and TNF-α [77-81]. A Th2 response, driven by IL-4 and IL-10, is detrimental to combating brucellosis as it promotes humoral immunity and suppresses macrophage activation [82, 83].

In this study, we examined the *ex vivo* cytokine profiles of patients with a history of brucellosis in the absence of stimuli and after toll-like receptor (TLR) and heat-killed *Brucella melitensis* (HKBM) stimulation. This approach is unique because we assessed human cytokine expression and secretion in fully recovered patient blood cells to determine if there is a brucellosis cytokine signature. While previous studies employ animal models, cell lines, or look at post-treatment serum cytokine levels [84], we assessed the *ex vivo* immune reaction of primary cells from human patients. We found that several cytokines showed altered expression and secretion in both unstimulated and stimulated conditions. Patients with a history of acute or relapsing brucellosis can be accurately identified by a robust inflammatory cytokine signature, months and

even years after successful treatment. This signature consists of increased secretion of TNF-α and IL-2 in response to HKBM and LPS, IL-1β in response to Rev1 and LPS, IFN-γ in response to HKBM, and basal IL-6.

In summary, this work demonstrates that cytokine variations in brucellosis patients can be detected using an *ex vivo* assay system and can be used to distinguish between relapse and acute patients. Targeted diagnosis of this signature may allow for improved treatment of brucellosis by identifying patients at risk for relapse.

5.2 Materials and Methods

5.2.1 Ethics

Human blood was obtained from patients enrolled in a clinical study of brucellosis in Lima, Peru in 2010. The study was approved by the Human Research Protection Program of the University of California, San Diego, and the Comité de Ética of Universidad Peruana Cayetano Heredia (UPCH), Lima, Peru. All patients provided written informed consent prior to enrollment in the study, and signed consent forms have been stored in locked files in study offices at UPCH.

5.2.2 Patients and healthy volunteers

Sixteen patients with a previously confirmed history of acute brucellosis (6 males and 10 females; 44.8 ± 12.5 years, "acute") and 6 patients previously

diagnosed with relapsing brucellosis (2 male and 5 females; 39 ± 15.2 years, "relapse") were enrolled in the study. Brucellosis was confirmed by serology, positive culture, or both methods (Table 5.1). At the time of sample collection all patients were 18 years of age or older, had completed treatment and were asymptomatic for brucellosis for 6 months or more, had a normal physical examination, and showed no signs or symptoms of other illness. 11 healthy volunteers with no history of brucellosis were also enrolled as negative controls (5 males and 6 females; 30.8 ± 7.3 years, "control").

Volunteers provided 120 ml of venous blood or underwent leukapheresis. Peripheral blood mononuclear cells (PBMCs) were isolated using Ficoll Paque (GE Healthcare) as previously described [85].

5.2.3 Ex vivo cell culture

Isolated PBMCs were cultured in RPMI-1640 (Sigma) with 10% fetal bovine serum at a density of 2.5×10^6 cells per well of a 24-well plate at 37°C with 5% CO_2. After isolation, cells were allowed to rest for 4 hours and were then stimulated with either PBS (resting, basal), a TLR4 agonist, lipopolysaccharide B5:055 from *Escherichia coli* (LPS, 1 µg/ml, Sigma), a TLR2/1 agonist, the synthetic triacylated lipoprotein Pam3CSK4 (1 µg/ml), a TLR3 agonist, low molecular weight polyinosine-polycytidylic acid (Poly(I:C), 10 µg/ml), a TLR7/8 agonist, the imidazoquinoline compound R848 (3 µg/ml), a TLR9 agonist, the synthetic CpG ODN 1668 (CpG, 5 mM), heat-killed

Brucella melitensis vaccine strain Rev1 (Rev1, 65 CFU/ml) or a heat-killed, virulent *B. melitensis* patient isolate (HKBM, 65 CFU/ml). After 18 hours of stimulation, the supernatant was removed and preserved at -80℃ and the cells were washed with PBS and frozen for subsequent RNA isolation.

5.2.4 RNA Extraction and cDNA synthesis

After the culture supernatant was removed, PBMCs were washed in PBS, centrifuged, and the cell pellets were frozen at -80℃. Cells were thawed, lysed, homogenized, and total RNA was extracted using the QIAshredder and RNeasy kits per the manufacturer's instructions (Qiagen). RNA was eluted in 30 μl of RNase-free water, and 1 μg was reverse-transcribed into cDNA using the iScript cDNA synthesis kit according to the manufacturer's instruction (Bio-Rad).

5.2.5 Quantitative real-time PCR and gene expression

Quantitative real-time PCR (qPCR) was performed to measure the mRNA expression level of the housekeeping gene GAPDH, and several inflammatory cytokines (GM-CSF, IFN-γ, IL-1β, IL-10 and TNF-α). Using a CFX384 Real-Time Detection System (Bio-Rad), each reaction was performed in triplicate in a final reaction volume of 5 μl, including 2.5 μl SsoAdvanced SYBR Green Supermix (Bio-Rad), 1.0 μl cDNA template, and 1.0 μl (100 nM final concentration) of each primer. Primers were designed for each gene

using Primer3 (Table 5.2). After amplification, threshold cycle (C_T) values were generated using the Bio-Rad CFX Manager Software 1.6. The fold change of gene expression was calculated as previously described [44].

5.2.6 Cytokine protein secretion levels

A multiplex bead-based immunoassay was used to quantify cytokine levels secreted into the culture supernatant after stimulation. Using the Human Cytokine 10-Plex Panel for the Luminex® platform, the following cytokines were measured according to the manufacturer's instruction: GM-CSF, IFN-γ, IL-1β, IL-2, IL-4, IL-5, IL-6, IL-8, IL-10 and TNF-α (Invitrogen). Briefly, either recombinant protein standards or 50 μl of each culture supernatant sample were first incubated, in duplicate, with antibody-conjugated fluorophore beads, and then with protein-specific biotinylated antibodies. Finally, following the addition of Streptavidin-RPE, samples were analyzed using the Bio-Plex 200 system (Bio-Rad). Data analysis was performed using the manufacturer provided software and the included recombinant proteins were used to generate standard curves to determine the sensitivity of the assay.

5.2.7 Statistical analysis

Significance values were calculated using the R software environment for statistical computing. For each pairwise comparison, Welch's t-test was used to estimate the probability that the two samples have equal mean.

Probabilities less than 0.05 suggest significant differences between the two samples and are indicated by an asterisk.

5.2.8 Classification and Model Selection

Prior to classification, all response variables were $\log_{10}$ transformed, centered, and scaled to unit variance. Unless otherwise stated, variables for which more than four patients were missing, or for which two or more patients belonging to the same category were missing, were discarded. Missing values in the remaining 70 response variables were imputed from their conditional means [86]. Specifically, for each missing value, a linear regression model was identified by forward model selection using Akaike's information criterion (AIC). Regressors were chosen from the 32 response variables for which no data was missing, including patient category. Forward selection was terminated when there was no further reduction in the AIC, or when the complexity of the model reached 12 regressors. Imputation by conditional means was chosen because of the relatively high correlation observed between variables [87, 88].

Linear discriminant analysis (LDA) was performed in R using the 'lda' function. Accuracy of the resulting linear discriminant function, or classifier, was then assessed using the 'predict' function in conjunction with leave-one-out cross-validation. To identify the optimal classifier for a given cross-section of the data, LDA was performed using all pairwise combinations of variables

contained in the cross-section. Top-performing pairs, defined as those pairs of variables that trained a classifier with the highest accuracy, were then used to seed model selection. During model selection, a variable was chosen at each step whose inclusion in the classifier resulted in the greatest increase in accuracy, up to a backtracking factor of 0.03 (1 patient). Since a multiplicity of models could satisfy this selection criteria, each selection was performed 20 times. The model ultimately identified by forward selection was taken to be that which yielded the highest classification accuracy while using the fewest number of variables.

5.3 Results

5.3.1 Inflammatory cytokine gene expression is increased in brucellosis relapse patients

To quantify the induction of cytokine gene expression in response to inflammatory stimuli, we first measured the resting, or basal, expression in unstimulated PBMCs. We found that basal expression of IL-1β and GM-CSF was significantly higher in relapse patients than in control patients, while TNF-α was significantly higher in both acute and relapse patients compared to control (Figure 5.1).

Next, PBMCs were stimulated overnight with LPS, heat-killed *B. melitensis* (HKBM) or R848. In response to LPS, relapse patients exhibited higher expression of GM-CSF and IL-10 and significantly higher TNF-α and

IFN-γ than either control or acute patients (Figure 5.2A). This trend was also observed in response to HKBM, except relapse and acute patients exhibited similarly and significantly elevated levels of GM-CSF, TNF-α, and IL-10 (Figure 5.2B). Thus while cytokine gene expression in response to LPS appears to discriminate well between relapse and either acute or control patients, the response to HKBM appears to discriminate between control patients and either acute or relapse patients.

In summary, relapse patients uniquely demonstrated elevated basal IL-1β and GM-CSF expression compared to control donors. In comparison to both acute and control donors, relapse patients exhibit increased IFN-γ expression after HKBM stimulation and increased TNF-α expression after LPS.

5.3.2 Inflammatory cytokine secretion is elevated in brucellosis relapse patients

To test whether the differences observed in cytokine gene expression were also manifest in the synthesis and secretion of cytokine proteins, we used a multiplex bead-based immunoassay to quantify *ex vivo* cytokine secretion in the culture supernatant of unstimulated and stimulated PBMCs. We measured the concentrations of GM-CSF, IFN-γ, IL-1β, IL-2, IL-4, IL-5, IL-6, IL-8, IL-10, and TNF-α. In unstimulated cells we found that the basal secretion of IL-6, IL-8, and TNF-α was elevated in both acute and relapse

patients compared to control patients. IL-8 was higher in relapse patients than in acute patients, while basal IL-2 was increased in relapse patients compared to control patients (Figure 5.3). All differences were significant (p<0.05).

Next we stimulated PMBCs with LPS, heat-killed *B. melitensis* (HKBM) or heat-killed *B. melitensis* vaccine strain Rev1 (Rev1). As observed in our gene expression data, after stimulating with HKBM, Rev1, or LPS, secretion of GM-CSF, IFN-γ, and TNF-α was significantly elevated in relapse patients compared to control patients (Figure 5.4). Additionally, IL-1β and IL-2 secretion was significantly elevated in acute and relapse patients compared to control donors after both HKBM and Rev1, but not LPS, stimulation. Several of the cytokine concentrations measured in response to other stimuli fell out of the observable range of the assay (Figure 5.7).

5.3.3 A robust cytokine signature accurately distinguishes relapsing from non-relapsing patients and controls

To test whether the differences observed in cytokine gene expression and protein secretion were sufficient to accurately discriminate between patients that did and did not experience a relapse in brucellosis, we trained a linear discriminant classifier using different cross-sections of the data and assessed its accuracy by leave-one-out cross validation. Linear discriminant analysis (LDA) is a supervised learning method that maximizes separation in the data -- defined here as the ratio of variances between patient categories to

the variance within -- using a linear recombination of response variables, in this case our observed gene expression or cytokine secretion measurements. Using LDA in conjunction with a model selection strategy allowed us to ask whether a subset of the response variables that we assayed could accurately classify patients as control, acute, or relapse.

First, cross-sections of the cytokine gene expression and protein secretion data were chosen such that all response variables were of the same cytokine or generated using the same stimulus. We refer to these as "cytokine" and "stimulus" cross-sections, respectively. A classifier trained on a cytokine cross-section is said to be trained "across stimuli", and *vice versa*. Response variables for which more than four patients were missing, or for which two or more patients belonging to the same category were missing, were discarded. Missing values in the remaining 70 response variables were imputed from their conditional means [86]. Linear discriminant functions were then identified for each cross-section using a forward model selection strategy with backtracking (see Methods).

On average, we found that higher classification accuracy was achieved by training across stimuli than across cytokines. Training across the four gene expression or eight protein secretion stimuli yielded accuracies of 0.679±0.073 and 0.642±0.119, respectively, compared to 0.598±0.045 and 0.606±0.116 across cytokines (Figures 5.8-5.10). This result is likely due to the higher cross-correlation observed between cytokines in response to a single stimulus,

compared to the cross-correlation observed in a single cytokine in response to multiple stimuli.

Second, we observed that the cytokine secretion assay was superior at discriminating between acute and relapse patients compared to gene expression. With expression, only the IFN-γ cross-section correctly classified more than one relapse patient (Figure 5.8D). Conversely, four cytokine secretion cross-sections (IL-1, IL-6, IL-10, and TNF-α) and two stimulus cross-sections (Pam3CSK4 and R848) correctly classified half or more relapse patients (Figures 5.9-5.10). This result is likely due to better separation in the response variables between acute and relapse patients in the cytokine secretion data compared to gene expression (Figure 5.11).

Indeed, clustering the patients hierarchically by Euclidean distance in their gene expression or cytokine secretion profiles, we found that the gene expression profile for every relapse patient most closely matches that of an acute patient (Figure 5.5A). Similarly, control patient 70005 and acute patient 10288 cross-cluster with acute and control patients, respectively. Consequently, these seven patients are misclassified in over half of the 20 qPCR models identified by forward selection. In contrast, five of the six relapse patients cluster together according to their cytokine secretion profile, resulting in significantly better classification performance (Figure 5.5B). Among the other patients, control patient 70005 and acute patient 10288 were again the

most often misclassified, suggesting that these two may be outliers in their respective patient categories.

Examining the optimal gene expression model identified by forward selection, we found that it classified 28 of 33 patients correctly. Distinguishing between acute and relapse patients was the primary source of misclassification, with 83% relapse sensitivity (one false negative), but 71% precision (two false positives) (Figure 5.6A). In contrast, four cytokine secretion models correctly classified 32 of 33 patients. These models also classified five of six relapse patients correctly, but with perfect precision and fewer variables than gene expression (Figure 5.6B). Interestingly, these models all share the following eight response variables: TNF-α and IL-2 in response to HKBM and LPS, IL-1β in response to Rev1 and LPS, IFN-γ in response to HKBM, and basal IL-6. Pairing these variables with, for example, IL-1β and GM-CSF in response to HKBM, or TNF-α and GM-CSF in response to Rev1, achieves 97% patient classification accuracy. We therefore propose that these variables constitute an innate immune cytokine signature for accurate identification of patients at risk for brucellosis relapse.

5.4 Discussion

Here we present evidence that patients with a history of acute-and-cleared or relapsing brucellosis can be distinguished with a robust inflammatory cytokine signature even months or years after successful

treatment. Currently, under standard treatment, many patients experience relapsing brucellosis, the cause of which remains poorly understood. In this study we stimulated PBMCs from patients with a past history of acute or relapsing brucellosis and measured *ex vivo* innate inflammatory cytokine expression and secretion to determine if at a clinically normal baseline there was a cytokine signature that might be associated with relapsing infection.

Brucella spp. are intracellular pathogens whose effective control and elimination requires a potent cell-mediated Th1 immune response [78, 89, 90]. We found that relapse brucellosis patients demonstrated higher basal IL-1β and GM-CSF gene expression compared to control donors, increased IFN-γ expression after heat-killed *B. melitensis* (HKBM) stimulation and higher TNF-α expression after LPS stimulation compared to both acute brucellosis patients and control donors. Surprisingly, this indicates relapse patients are capable of inducing the expression of cytokines needed to mount a Th1 response. However increased IL-10 gene expression after stimulation with HKBM in both acute and relapse brucellosis patients, but not after LPS stimulation, may suggest a possible *Brucella* spp. specific elevated Th2 response. Th2 cytokines like IL-10 have been shown to downregulate immunity to *Brucella* spp [91, 92].

Additionally, relapse patients produced more TNF-α protein compared to control donors and secrete more GM-CSF compared to both groups. Indeed, previous studies indicate GM-CSF secretion can stimulate IL-1β and

TNF-α secretion by monocytes after *in vitro B. abortus* challenge [93]. Taken together, the *ex vivo* innate immune cytokine expression and secretion of acute or relapse patients indicates a functional and Th1-dominated response. IL-2, TNF-α, and IFN-γ secretion have previously been shown to be increased during brucellosis [94, 95], and recent studies also suggest that adequate levels are required for control of the infection as genetic polymorphisms in these genes may increase susceptibility to, or duration of, disease [75, 96]. In accordance with our findings, others have shown elevated IFN-γ after *ex vivo B. melitensis* antigen stimulation in patients less than one year after diagnosis [97]. Here we confirm that this remains true even several years after the resolution of infection.

Though gene expression of the Th2 cytokine IL-10 was elevated in some brucellosis patients, IL-10 protein secretion was not significantly altered in these patients under any stimulation condition; IL-4, another important Th2 cytokine, was not highly secreted in any condition (Figure 5.7). However, one key limitation of the study was the multiplex approach used to determine cytokine protein levels: several of the cytokines measured in the assay fell above or below the standard range defined in the manufacturer's protocol and some concentration values were extrapolated or not detected. Due to the limited quantity of patient sample and culture supernatant, individual optimization for each cytokine and standard in the 10-cytokine kit was not possible. To address this issue in future studies, multiplex kits with improved

standard ranges could be used or individual conventional ELISA assays might be useful for key cytokines which still fall outside the detection of the multiplex assay.

In summary, this study demonstrates that innate immune cytokine variations can be detected between patients with a history of acute or relapsing brucellosis and control donors using an *ex vivo* assay system. Standard clinical methods for monitoring brucellosis treatment outcomes remain unreliable: antibody titers used for serological diagnosis of brucellosis and circulating *B. melitensis* DNA load used for diagnosis by PCR, have been shown to persist for years after successful treatment [98-102]. In contrast, we show that an *ex vivo* cytokine signature can accurately distinguish between relapse and acute patients, and may provide a novel approach to monitor clinical outcomes. Further work would be required to validate this *ex vivo* assay as a method for predicting or confirming actively relapsing infections.

5.5 Acknowledgements

Figure 5.1 Basal PBMC cytokine gene expression. Relative basal amounts of IL-1β, GM-CSF, TNF-α, IFN-γ, and IL-10 mRNA compared to the housekeeping gene GAPDH (ΔC_T) in unstimulated PBMCs from control donors or acute or relapse brucellosis patients (asterisk indicates p≤0.05).
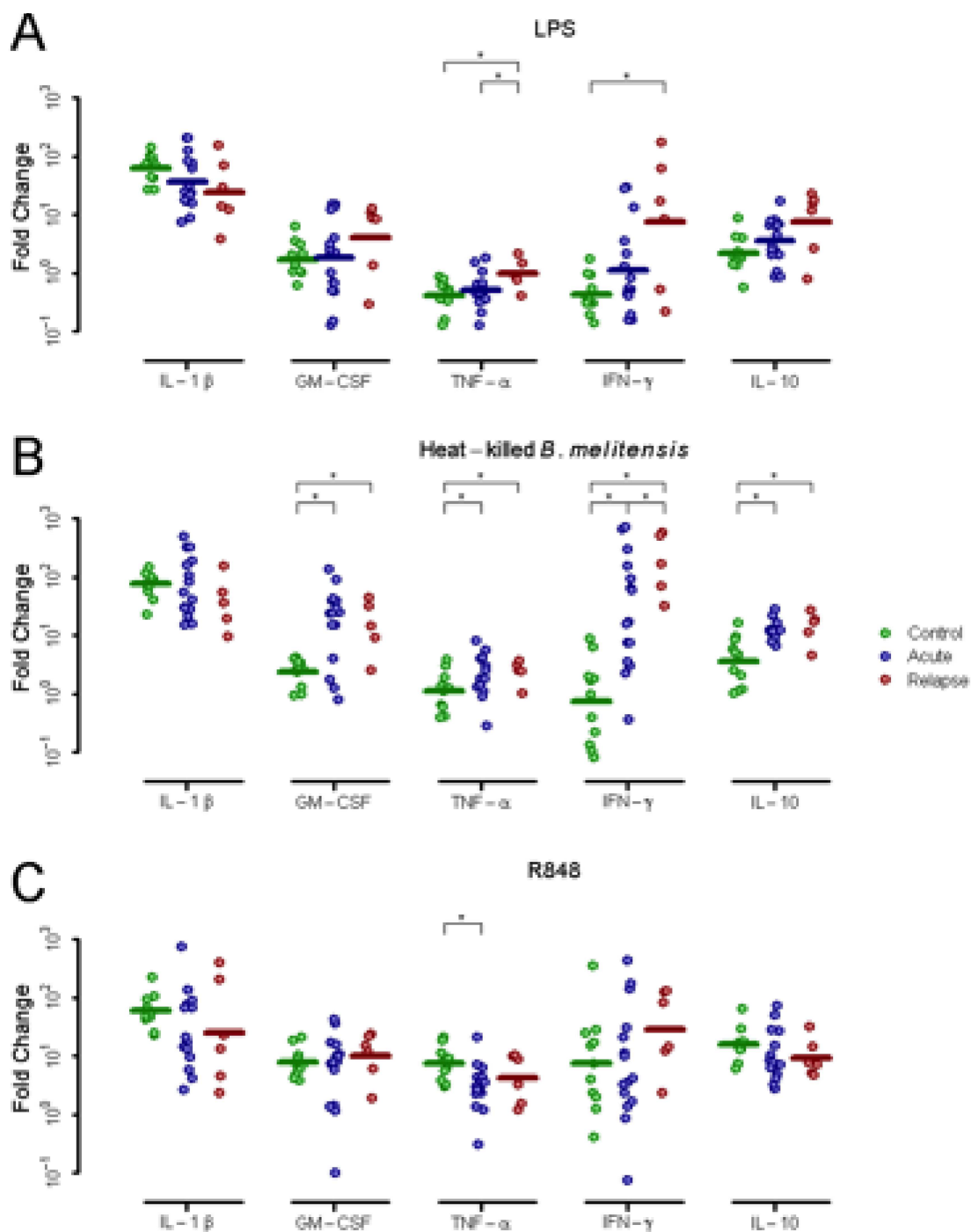
Figure 5.2 PBMC cytokine gene expression after stimulation. Fold change of gene expression for IL-1β, GM-CSF, TNF-α, IFN-γ and IL-10 in PBMCs from control donors or acute or relapse brucellosis patients after stimulation with (A) LPS (B) Heat-killed *B. melitensis* or (C) R848 (asterisk indicates p≤0.05).
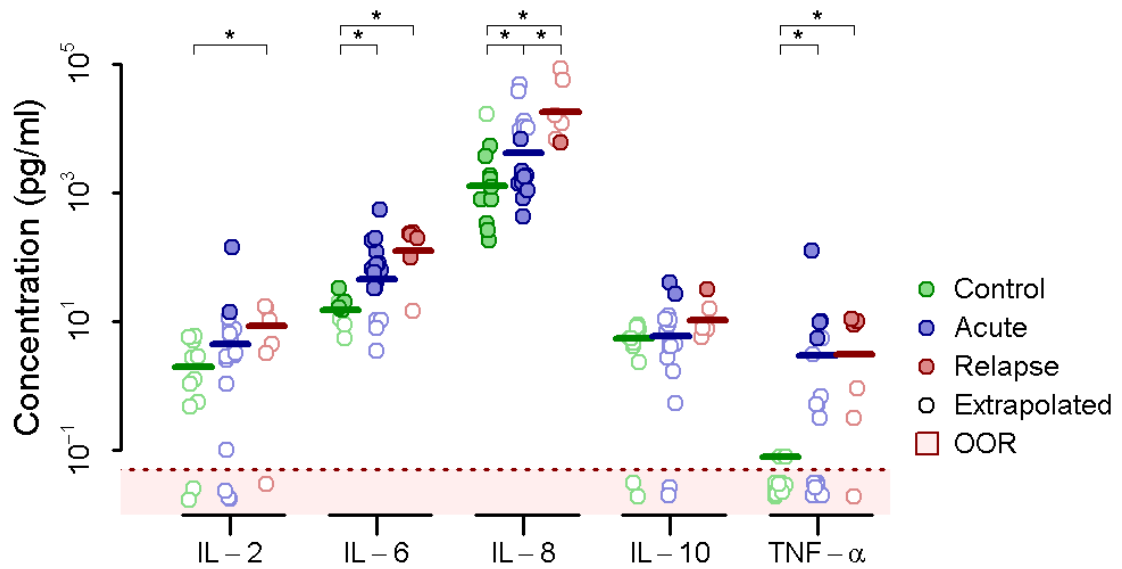
Figure 5.3 Basal PBMC cytokine secretion measured by multiplex immunoassay. IL-2, IL-6, IL-8, IL-10, and TNF-α secretion in unstimulated PBMCs from control donors or acute or relapse brucellosis patients (asterisk indicates p≤0.05). Concentrations indicated by open circles were extrapolated beyond the assay standard curve and values in the red shaded zone fell outside the observable range (OOR).
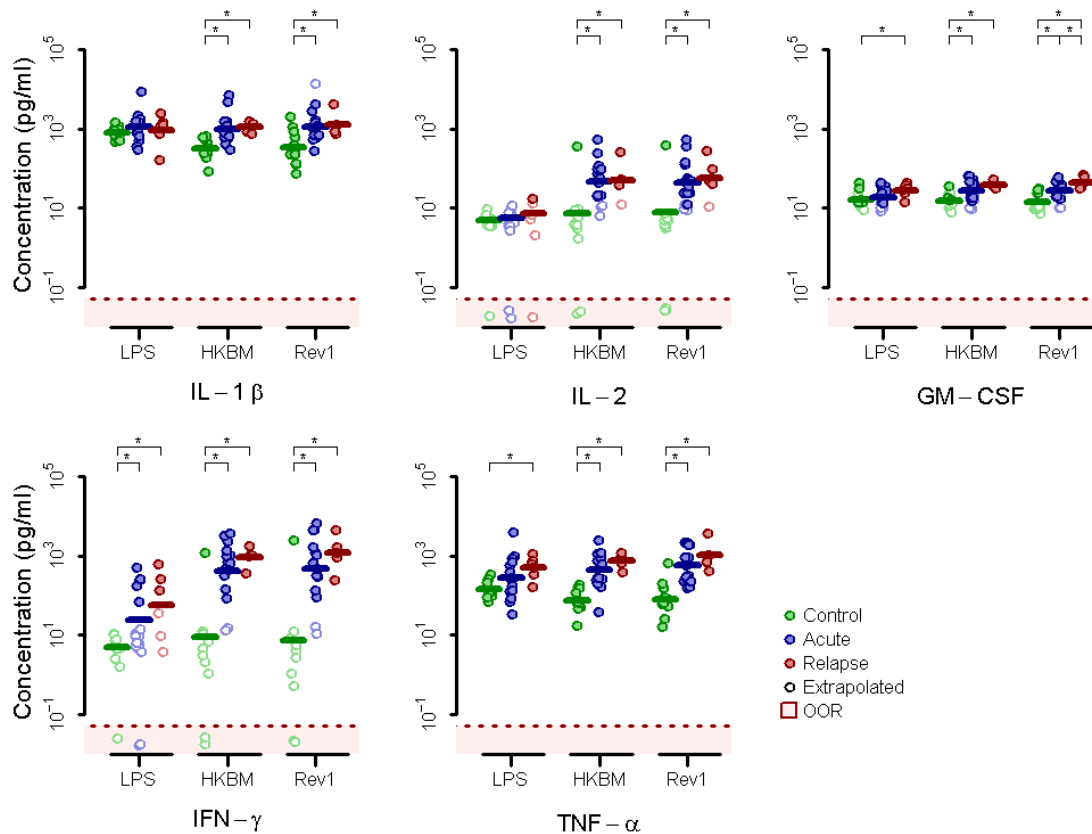
Figure 5.4 PBMC cytokine secretion after stimulation measured by multiplex immunoassay. IL-1β, IL-2, GM-CSF, IFN-γ, and TNF-α protein secretion by from control donors or acute or relapse brucellosis patients after stimulation with LPS, heat-killed B. melitensis (HKBM), or the heat-killed B. melitensis vaccine Rev1, as measured by multiplex immunoassay (asterisk indicates p≤0.05). Concentrations indicated by open circles were extrapolated beyond the assay standard curve and values in the red shaded zone fell outside the observable range (OOR).
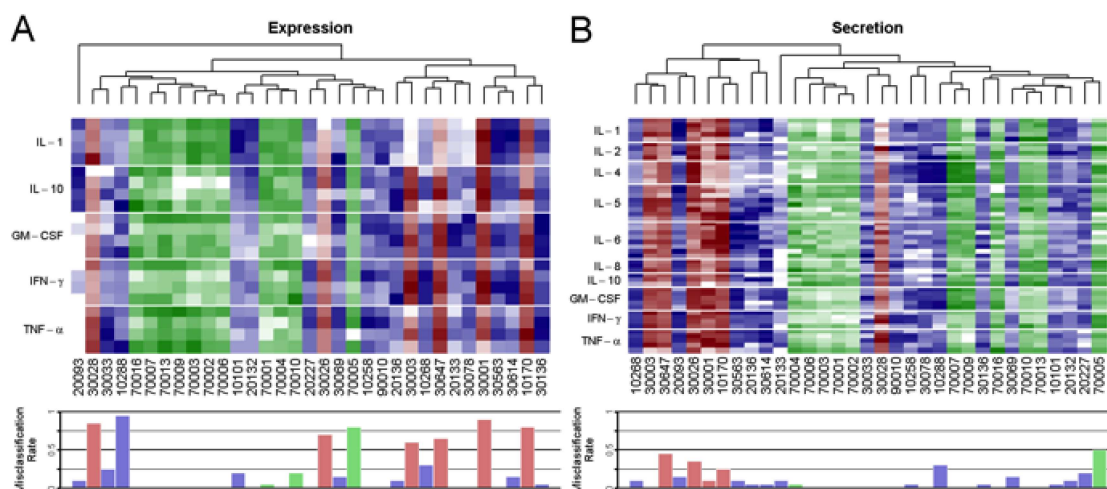
Figure 5.5 Hierarchical clustering of patients by gene expression or cytokine secretion. Control (green), acute (blue), and relapse (red) patients were clustered hierarchically by Euclidean distance in their scaled gene expression (A) or cytokine secretion (B) profiles (see Methods). Response variables are grouped by cytokine, indicated in the left margin, and values are indicated by luminosity. Misclassification rates for each patient after 20 model selection runs are indicated underneath the corresponding patient code (see Table 5.1).
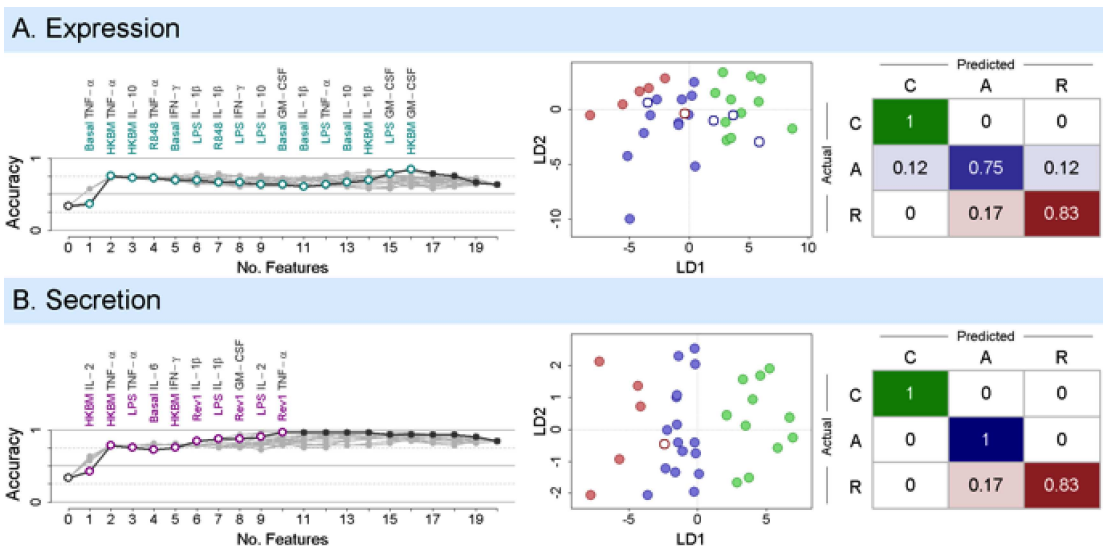
Figure 5.6 Model selection and classification results. Response variables were selected and a linear discriminant classifier was trained using the transformed gene expression (A) or cytokine secretion data (B). The left panels show the results of 20 model selection runs, with the best-performing classifier highlighted in color. The variable included after each step in the forward selection is listed for the optimal model. Zero features is equivalent to random guessing. The center column shows all 33 patients after being mapped by the first (LD1) and second (LD2) linear discriminant functions used by the best-performing classifier. Classification performance is summarized by the confusion matrix on the right. This matrix gives the proportion of (C)ontrol, (A)cute, and (R)elapse patients that were correctly (on-diagonal) and incorrectly classified (off-diagonal).
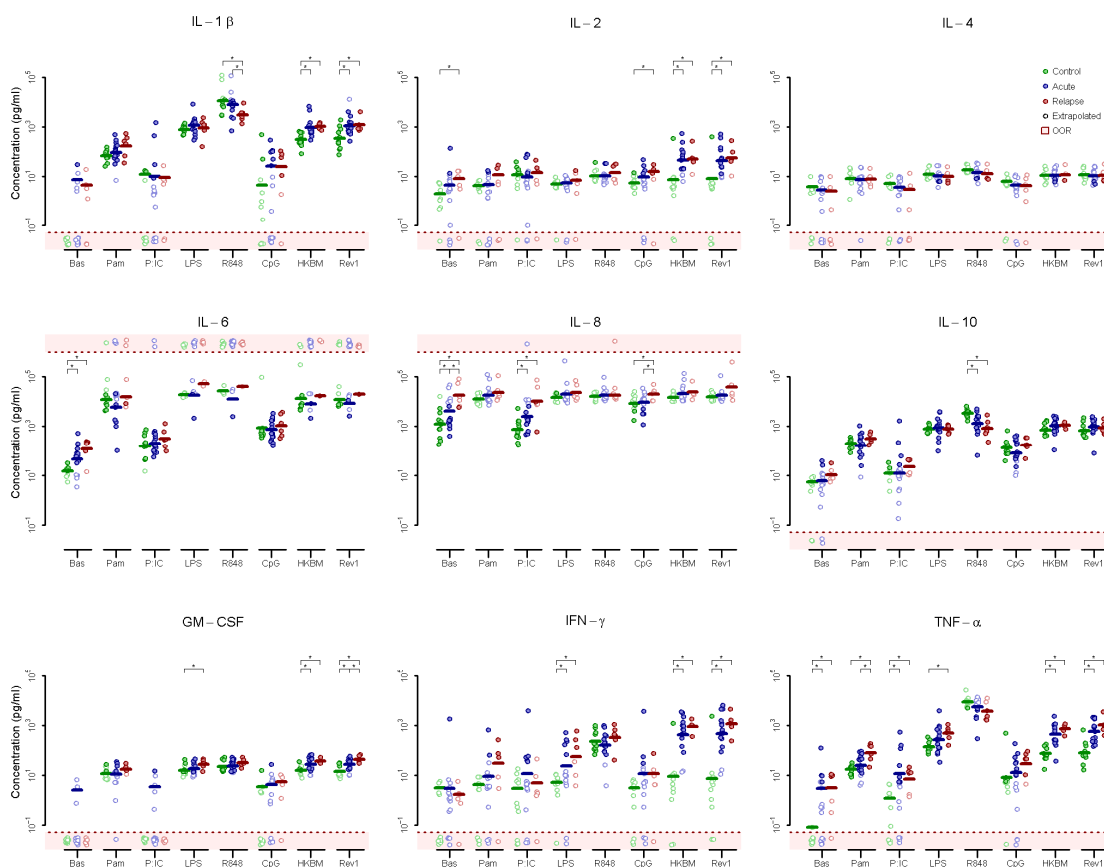
Figure 5.7 PBMC cytokine secretion after stimulation measured by multiplex immunoassay. Secretion of IL-1β, IL-2, IL-4, IL-6, IL-8, IL-10, GM-CSF, IFN-γ, and TNF-α in PBMCs from control donors or acute or relapse brucellosis patients without stimulation (basal) or after stimulation with Pam3CSK4, Poly(I:C), LPS, R848, CpG, HKBM, or Rev1. Concentrations indicated by open circles were extrapolated beyond the assay standard curve and values in the red shaded zone fell outside the observable range (OOR).
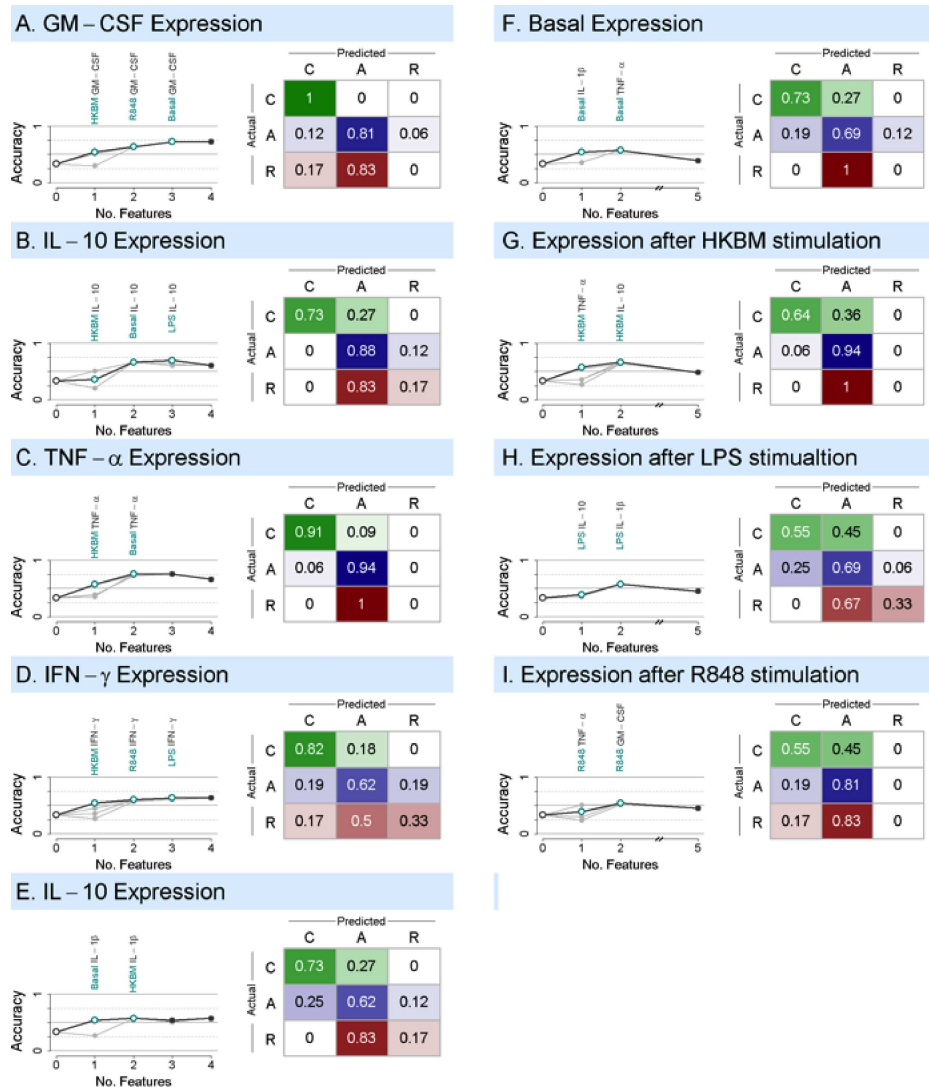
Figure 5.8 Classifiers identified by forward model selection using all cytokine (A-E) and stimulus (F-I) cross-sections in the gene expression data. Each panel illustrates the model selection (left) and resulting classifier performance (right) for cytokines (A) GM-CSF (B) IL-10 (C) TNF- α (D) IFN- γ and (E) IL-10 and stimuli (F) Basal (no stimulus) (G) HKBM (H) LPS and (I) R848. For model selection, the accuracy of the resulting classifier is given as a function of the number of variables incorporated. The results of 20 selections are shown for each cross-section, with the best-performing classifier highlighted in bold. The identity of each variable incorporated into the best-performing classifier is indicated above its corresponding index. Zero features is equivalent to random guessing. For each cross-section, the confusion matrix generated by the best-performing classifier is shown at right. This matrix gives the proportion of the 11 (C)ontrol, 16 (A)cute, and 6 (R)elapse patients that were correctly and incorrectly classified.
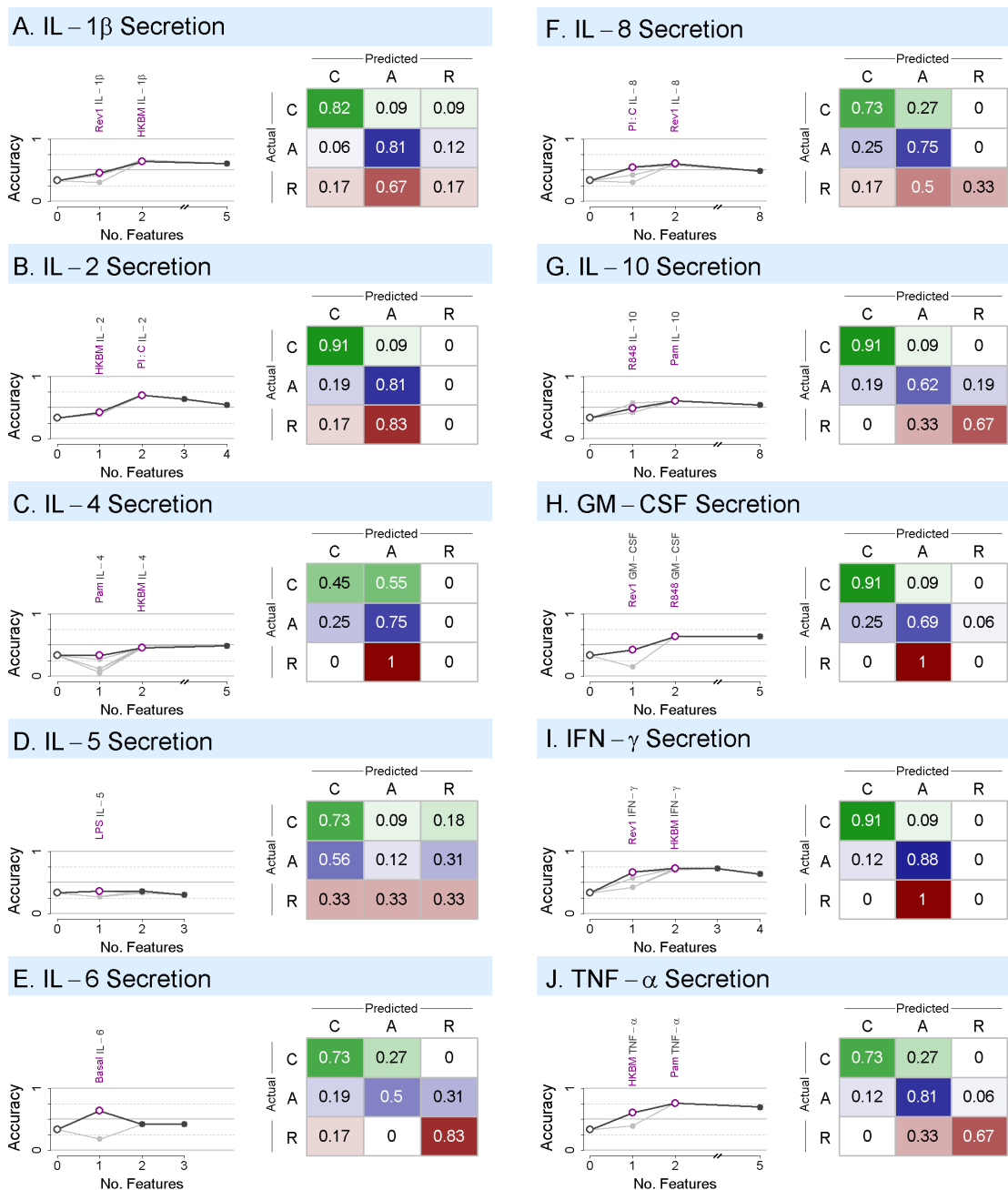
Figure 5.9 Classifiers identified by forward model selection for all cytokine cross-sections in the cytokine secretion data. Each panel illustrates the model selection (left) and resulting classifier performance (right) for cytokines (A) IL-1β (B) IL-2 (C) IL-4 (D) IL-5 (E) IL-6 (F) IL-8 (G) IL-10 (H) GM-CSF (I) IFN- γ and (J) TNF- α. See Figure S2 for details.
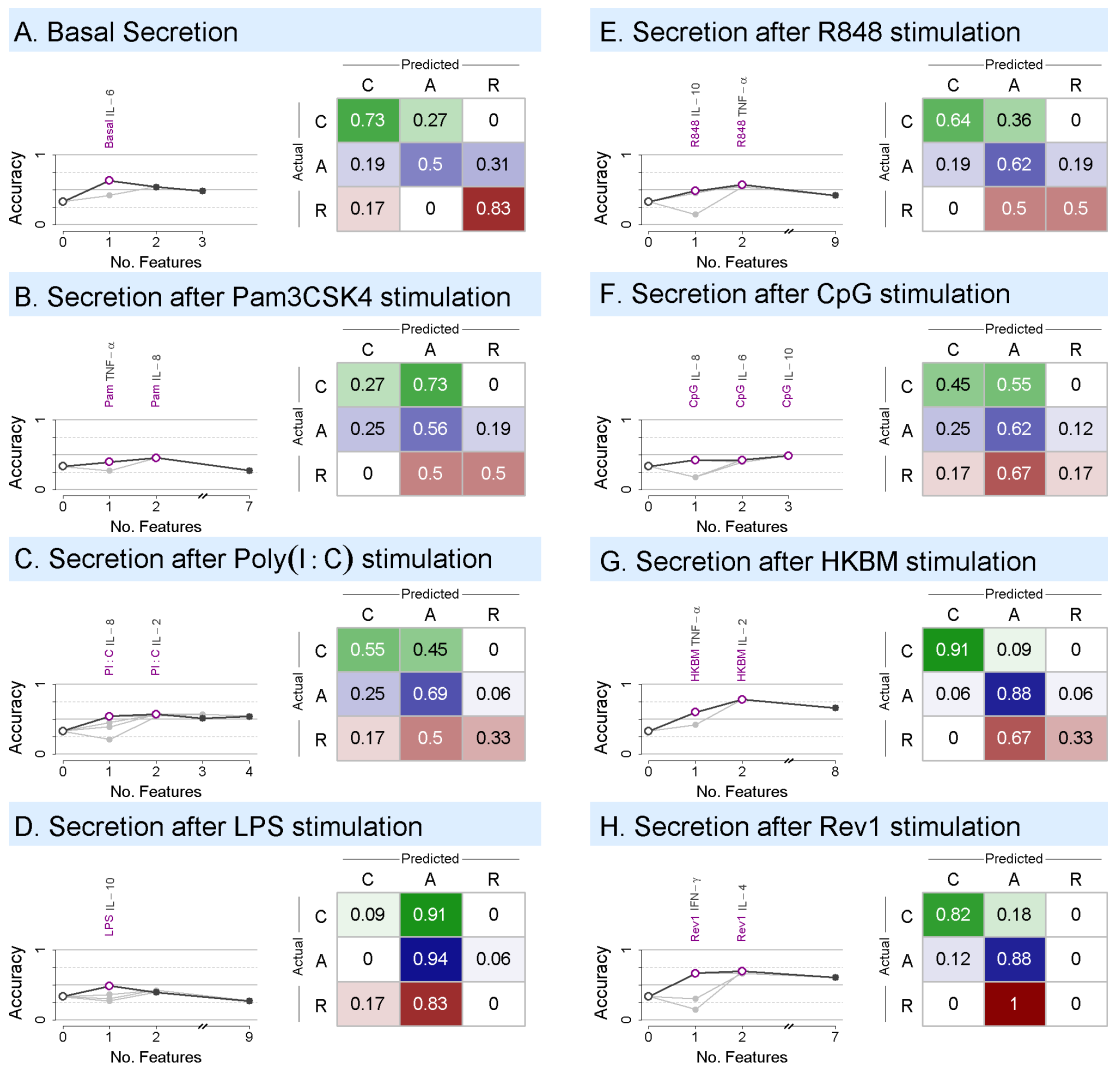
Figure 5.10 Classifiers identified by forward model selection for all stimulus cross-sections in the cytokine secretion data. Each panel illustrates the model selection (left) and resulting classifier performance (right) for stimuli (A) Basal (no stimulus) (B) Pam3CSK4 (C) Poly(I:C) (D) LPS (E) R848 (F) CpG (G) HKBM and (H) Rev1. See Figure S2 for details.
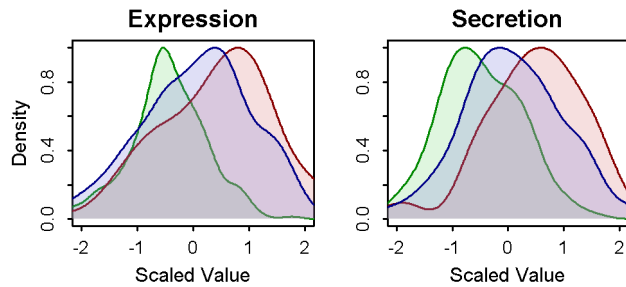
Figure 5.11 Data separation in the gene expression and cytokine secretion data sets. Scaled, $\log_{10}$-transformed response variables were taken from the full gene expression data set (left) and the partial, imputed cytokine secretion data set (right), where no variable was missing more than four values and no patient category was missing more than one value (see Methods). Variables for which relapse patients exhibited a mean value less than that of control patients were inverted (multiplied by -1). The density of the resulting variables was estimated using the 'density' function in R, then overlayed by patient category: control (green), acute (blue) and relapse (red).

Table 5.1 Clinical characteristics of patient population.

Patient Category	Age	Sex	Sample Collection	Date Collected	Patient Code
Acute	43	F	Venous blood	10/21/10	BR10101
Acute	40	M	Venous blood	10/28/10	BR10258
Acute	19	F	Leukapheresis	10/23/10	BR10268
Acute	38	F	Venous blood	11/22/10	BR10288
Acute	40	M	Venous blood	12/4/10	BR20093
Acute	52	M	Leukapheresis	10/30/10	BR20113
Acute	50	F	Venous blood	12/9/10	BR20132
Acute	45	F	Venous blood	11/29/10	BR20227
Acute	23	M	Leukapheresis	11/10/10	BR20316
Acute	46	F	Venous blood	9/23/10	BR30033
Acute	41	M	Venous blood	12/4/10	BR30069
Acute	70	M	Venous blood	11/22/10	BR30078
Acute	48	F	Venous blood	10/23/10	BR30136
Acute	63	F	Leukapheresis	11/20/10	BR30563
Acute	50	F	Leukapheresis	10/22/10	BR30614
Acute	49	F	Venous blood	12/6/10	BR90010
Relapse	53	F	Leukapheresis	12/6/10	BR10170
Relapse	18	M	Leukapheresis	11/8/10	BR30001
Relapse	60	F	Leukapheresis	10/28/10	BR30003
Relapse	32	F	Venous blood	10/13/10	BR30026
Relapse	35	F	Venous blood	9/7/10	BR30028
Relapse	36	F	Leukapheresis	10/6/10	BR30647
Control	29	F	Venous blood	10/12/10	BR70001
Control	30	F	Venous blood	10/12/10	BR70002
Control	37	M	Venous blood	10/19/10	BR70003
Control	20	M	Venous blood	10/19/10	BR70004
Control	35	F	Venous blood	10/20/10	BR70005
Control	46	F	Venous blood	11/24/10	BR70006
Control	36	F	Venous blood	12/3/10	BR70007
Control	29	F	Venous blood	11/29/10	BR70009
Control	27	M	Venous blood	11/29/10	BR70010
Control	23	M	Venous blood	11/26/10	BR70013
Control	27	M	Venous blood	12/9/10	BR70016

Table 5.2 Primers used for quantitative real-time PCR.

Gene	Accession number	Sequence (5' -> 3')	Product
GAPDH	NM_002046.3	F:AATCAAGTGGGGCGATGCTG R:TGCAAATGAGCCCCAGCCTT	87
IL-10	NM_000572.2	F:GACCCAGACATCAAGGCGCA R:GAAATCGATGACAGCGCCGTAG	85
GM-CSF	NM_000758.2	F:AGACACTGCTGCTGAGATGAATGAA R:TCTGTAGGCAGGTCGGCTCC	80
TNF-α	NM_000594.2	F:AGCCCATGTTGTAGCAAACCCT R:TCTCTCAGCTCCACGCCATTG	96
IL-1β	NM_000576.2	F: ATTACAGTGGCAATGAGGATGACT R:ATCCAGAGGGCAGAGGTCCAG	95
IFN-γ	NM_000619.2	F:TTGGAAAGAGGAGAGTGACAGAA R:CCACACTCTTTTGGATGCTCTGG	107

Chapter 6: Concluding Overview

Our findings in Chapter 2 revealed unexpected cross-regulation between two primary transcription factor families that coordinate innate immune responses. Whereas the NF-κB and IRF activators bind to their respective cognate sites (κB and ISRE, respectively), we report that the NF-κB p50-p50 repressor is able to bind to and regulate a previously unrecognized binding site, the ISRE. By using both *in vitro* biochemical assays and unbiased gene expression phenotyping studies, we showed that p50 homodimers are highly induced and can bind to a subset of IFN-inducible genes many of which contain the core IRE binding site in their promoters. One prominent gene which showed hyperexpression in the absence of p50 was IFN-β; as IFN-β has both autocrine and paracrine effects on ISG induction, it was difficult to determine whether many of the IFN-inducible hyperexpressed genes identified were directly controlled by p50 or were hyperexpressed a consequence of increased type I IFN signaling.

To investigate this in Chapter 3, we generated IFNAR/p50ko mice, which lack both the nfkb1 gene and the type I IFN receptor. We observed that BMDMs from these mice do show hyperexpression of a number of inflammatory genes previously identified to be hyperexpressed in p50ko BMDMs. Using genome wide expression analysis, we showed that LPS- and CpG-responsive p50-repressed genes are enriched for ISRE and p65 binding motifs, which suggests that p50-p50 may be competing with these

transcription factors and repressing transcription in WT mice. Furthermore, we show that while a number of these p50-repressed genes are still hyperexpressed in IFNAR/p50ko BMDMs, the vast majority of the expression phenotype is lost in the absence if type I IFN signaling.

To determine if p50 was competing with IRF3, we performed ChIP assays and found that both p50 and IRF3 were binding to several genes simultaneously. Interestingly, IRF3 and p65 occupancy was observed to be higher in the absence of p50 on several genes examined. Taken together, our results and previous studies indicate that p50-p50 is regulating transcription by 3 distinct mechanisms: competition with p65-containing dimers, competition with factors which bind to the ISRE, namely IRF3, and repression of IFN-β expression and subsequent ISG expression (Figure 6.1).

In Chapter 4, we used unbiased next-generation RNA-sequencing to interrogate the transcriptome of BMDMs which were stimulated with an extensive panel of cytokines, PAMPs, or live pathogens. While many stimuli did display a core innate immune gene activation program, stimulus-specific activation clusters were still apparent. Genes which are differentially expressed after live viral or bacterial infection but not PAMP stimulation represent possible pathogen-targeted genes which may be manipulated by the live microbes to enhance infection. Further studies would be necessary to determine if these observed expression effects were directly controlled by the pathogens and what effect they may have on infection outcome.

In Chapter 5 we demonstrated that innate immune cytokine variations can be detected between patients with a history of acute or relapsing brucellosis and control donors using an *ex vivo* assay system. We show that an *ex vivo* cytokine signature can accurately distinguish between relapse and acute patients, and may provide a novel approach to monitor clinical outcomes. Further work would be required to validate this *ex vivo* assay as a method for predicting or confirming actively relapsing infections.

Overall, we demonstrate the innate immune response to pathogens is capable of stimulus-specificity, with NF-κB playing a key role in the transcriptional response of immune cells like the macrophage.
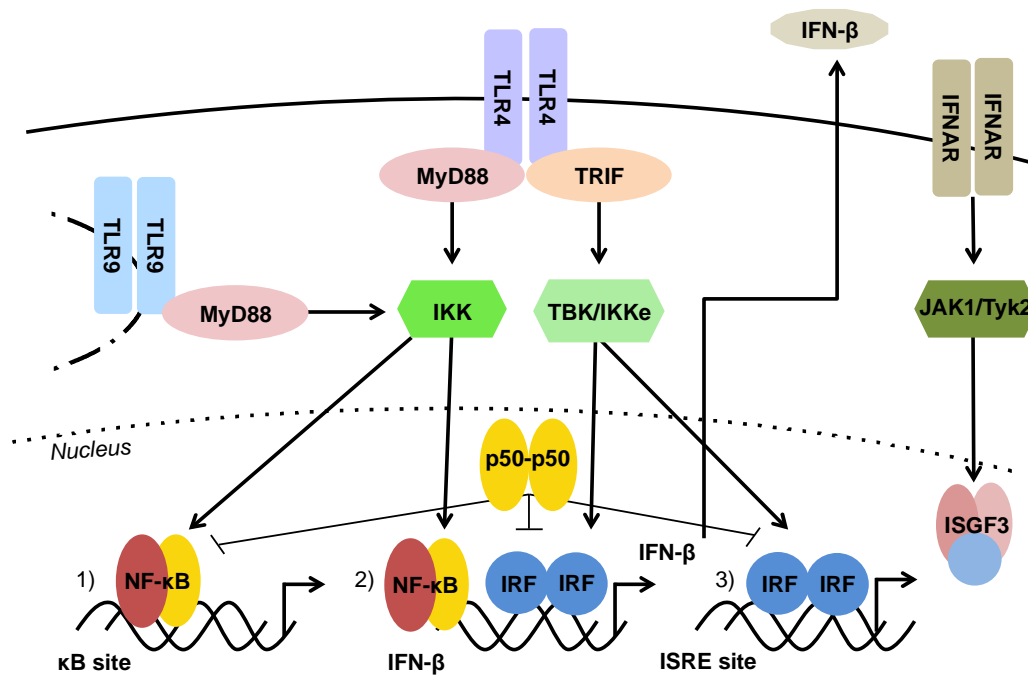
Figure 6.1 NF-κB p50-p50 can control innate immune gene expression through 3 mechanisms. NF-κB p50 homodimers are highly induced and can bind to 1) κB sites and can subsequently block or prevent the access of other activating NF-κB dimers like p65-50 2) the IFN-β promoter which has both autocrine and paracrine effects on ISG induction and 3) a subset of IFN-inducible genes many of which contain the core ISRE binding site in their promoters.

REFERENCES

[1] Hoffmann A, Baltimore D. Circuitry of nuclear factor kappaB signaling. Immunol Rev. 2006 Apr;210:171-86.

[2] Li Q, Verma IM. NF-kappaB regulation in the immune system. Nat Rev Immunol. 2002 Oct;2(10):725-34.

[3] Schreiber J, Jenner RG, Murray HL, Gerber GK, Gifford DK, Young RA. Coordinated binding of NF-kappaB family members in the response of human cells to lipopolysaccharide. Proc Natl Acad Sci U S A. 2006 Apr 11;103(15):5899-904.

[4] Lenardo MJ, Baltimore D. NF-kappa B: A pleiotropic mediator of inducible and tissue-specific gene control. Cell. 1989 Jul 28;58(2):227-9.

[5] Kawai T, Akira S. Signaling to NF-kappaB by toll-like receptors. Trends Mol Med. 2007 Nov;13(11):460-9.

[6] Hayden MS, West AP, Ghosh S. NF-kappaB and the immune response. Oncogene. 2006 Oct 30;25(51):6758-80.

[7] Yamamoto M, Sato S, Hemmi H, Hoshino K, Kaisho T, Sanjo H, et al. Role of adaptor TRIF in the MyD88-independent toll-like receptor signaling pathway. Science. 2003 Aug 1;301(5633):640-3.

[8] O'Neill LA, Bowie AG. The family of five: TIR-domain-containing adaptors in toll-like receptor signalling. Nat Rev Immunol. 2007 May;7(5):353-64.

[9] Hacker H, Redecke V, Blagoev B, Kratchmarova I, Hsu LC, Wang GG, et al. Specificity in toll-like receptor signalling through distinct effector functions of TRAF3 and TRAF6. Nature. 2006 Jan 12;439(7073):204-7.

[10] Sen GC. Viruses and interferons. Annu Rev Microbiol. 2001;55:255-81.

[11] Malmgaard L. Induction and regulation of IFNs during viral infections. J Interferon Cytokine Res. 2004 Aug;24(8):439-54.

[12] Sharma S, tenOever BR, Grandvaux N, Zhou GP, Lin R, Hiscott J. Triggering the interferon antiviral response through an IKK-related pathway. Science. 2003 May 16;300(5622):1148-51.

[13] Taniguchi T, Ogasawara K, Takaoka A, Tanaka N. IRF family of transcription factors as regulators of host defense. Annu Rev Immunol. 2001;19:623-55.

[14] Fujii Y, Shimizu T, Kusumoto M, Kyogoku Y, Taniguchi T, Hakoshima T. Crystal structure of an IRF-DNA complex reveals novel DNA recognition and cooperative binding to a tandem repeat of core sequences. EMBO J. 1999 Sep 15;18(18):5028-41.

[15] Pappas G, Akritidis N, Bosilkovski M, Tsianos E. Brucellosis. N Engl J Med. 2005 Jun 2;352(22):2325-36.

[16] Pappas G, Panagopoulou P, Christou L, Akritidis N. Brucella as a biological weapon. Cell Mol Life Sci. 2006 Oct;63(19-20):2229-36.

[17] Pappas G, Papadimitriou P, Akritidis N, Christou L, Tsianos EV. The new global map of human brucellosis. Lancet Infect Dis. 2006 Feb;6(2):91-9.

[18] Nau GJ, Richmond JF, Schlesinger A, Jennings EG, Lander ES, Young RA. Human macrophage activation programs induced by bacterial pathogens. Proc Natl Acad Sci U S A. 2002 Feb 5;99(3):1503-8.

[19] Doyle S, Vaidya S, O'Connell R, Dadgostar H, Dempsey P, Wu T, et al. IRF3 mediates a TLR3/TLR4-specific antiviral gene program. Immunity. 2002 Sep;17(3):251-63.

[20] Ogawa S, Lozach J, Benner C, Pascual G, Tangirala RK, Westin S, et al. Molecular determinants of crosstalk between nuclear receptors and toll-like receptors. Cell. 2005 Sep 9;122(5):707-21.

[21] Foster SL, Hargreaves DC, Medzhitov R. Gene-specific control of inflammation by TLR-induced chromatin modifications. Nature. 2007 Jun 21;447(7147):972-8.

[22] Marshak-Rothstein A. Toll-like receptors in systemic autoimmune disease. Nat Rev Immunol. 2006 Nov;6(11):823-35.

[23] Nathan C. Points of control in inflammation. Nature. 2002 Dec 19-26;420(6917):846-52.

[24] Decker T, Muller M, Stockinger S. The yin and yang of type I interferon activity in bacterial infection. Nat Rev Immunol. 2005 Sep;5(9):675-87.

[25] Roach JC, Smith KD, Strobe KL, Nissen SM, Haudenschild CD, Zhou D, et al. Transcription factor expression in lipopolysaccharide-activated peripheral-blood-derived mononuclear cells. Proc Natl Acad Sci U S A. 2007 Oct 9;104(41):16245-50.

[26] Ramsey SA, Klemm SL, Zak DE, Kennedy KA, Thorsson V, Li B, et al. Uncovering a macrophage transcriptional program by integrating

evidence from motif scanning and expression dynamics. PLoS Comput Biol. 2008 Mar 21;4(3):e1000021.

[27] Amit I, Garber M, Chevrier N, Leite AP, Donner Y, Eisenhaure T, et al. Unbiased reconstruction of a mammalian transcriptional network mediating pathogen responses. Science. 2009 Oct 9;326(5950):257-63.

[28] Oganesyan G, Saha SK, Guo B, He JQ, Shahangian A, Zarnegar B, et al. Critical role of TRAF3 in the toll-like receptor-dependent and - independent antiviral response. Nature. 2006 Jan 12;439(7073):208-11.

[29] Akira S, Takeda K. Toll-like receptor signalling. Nat Rev Immunol. 2004 Jul;4(7):499-511.

[30] Akira S, Uematsu S, Takeuchi O. Pathogen recognition and innate immunity. Cell. 2006 Feb 24;124(4):783-801.

[31] Medzhitov R. Origin and physiological roles of inflammation. Nature. 2008 Jul 24;454(7203):428-35.

[32] Kawai T, Akira S. The role of pattern-recognition receptors in innate immunity: Update on toll-like receptors. Nat Immunol. 2010 May;11(5):373-84.

[33] Hoffmann A, Natoli G, Ghosh G. Transcriptional regulation via the NF-kappaB signaling module. Oncogene. 2006 Oct 30;25(51):6706-16.

[34] Sanjabi S, Hoffmann A, Liou HC, Baltimore D, Smale ST. Selective requirement for c-rel during IL-12 P40 gene induction in macrophages. Proc Natl Acad Sci U S A. 2000 Nov 7;97(23):12705-10.

[35] Hoffmann A, Leung TH, Baltimore D. Genetic analysis of NF-kappaB/rel transcription factors defines functional specificities. EMBO J. 2003 Oct 15;22(20):5530-9.

[36] Kang SM, Tran AC, Grilli M, Lenardo MJ. NF-kappa B subunit regulation in nontransformed CD4+ T lymphocytes. Science. 1992 Jun 5;256(5062):1452-6.

[37] Ten RM, Paya CV, Israel N, Le Bail O, Mattei MG, Virelizier JL, et al. The characterization of the promoter of the gene encoding the p50 subunit of NF-kappa B indicates that it participates in its own regulation. EMBO J. 1992 Jan;11(1):195-203.

[38] Plaksin D, Baeuerle PA, Eisenbach L. KBF1 (p50 NF-kappa B homodimer) acts as a repressor of H-2Kb gene expression in metastatic tumor cells. J Exp Med. 1993 Jun 1;177(6):1651-62.

[39] Ledebur HC, Parks TP. Transcriptional regulation of the intercellular adhesion molecule-1 gene by inflammatory cytokines in human endothelial cells. essential roles of a variant NF-kappa B site and p65 homodimers. J Biol Chem. 1995 Jan 13;270(2):933-43.

[40] Sha WC, Liou HC, Tuomanen EI, Baltimore D. Targeted disruption of the p50 subunit of NF-kappa B leads to multifocal defects in immune responses. Cell. 1995 Jan 27;80(2):321-30.

[41] Udalova IA, Richardson A, Denys A, Smith C, Ackerman H, Foxwell B, et al. Functional consequences of a polymorphism affecting NF-kappaB p50-p50 binding to the TNF promoter region. Mol Cell Biol. 2000 Dec;20(24):9113-9.

[42] Bohuslav J, Kravchenko VV, Parry GC, Erlich JH, Gerondakis S, Mackman N, et al. Regulation of an essential innate immune response by the p50 subunit of NF-kappaB. J Clin Invest. 1998 Nov 1;102(9):1645-52.

[43] Weischenfeldt J, Porse B. Bone marrow-derived macrophages (BMM): Isolation and applications. CSH Protoc. 2008 Dec 1;2008:pdb.prot5080.

[44] Schmittgen TD, Livak KJ. Analyzing real-time PCR data by the comparative C(T) method. Nat Protoc. 2008;3(6):1101-8.

[45] Hoffmann A, Levchenko A, Scott ML, Baltimore D. The IkappaB-NF-kappaB signaling module: Temporal control and selective gene activation. Science. 2002 Nov 8;298(5596):1241-5.

[46] Shih VF, Davis-Turak J, Macal M, Huang JQ, Ponomarenko J, Kearns JD, et al. Control of RelB during dendritic cell activation integrates canonical and noncanonical NF-kappaB pathways. Nat Immunol. 2012 Dec;13(12):1162-70.

[47] Mathys S, Schroeder T, Ellwart J, Koszinowski UH, Messerle M, Just U. Dendritic cells under influence of mouse cytomegalovirus have a physiologic dual role: To initiate and to restrict T cell activation. J Infect Dis. 2003 Mar 15;187(6):988-99.

[48] Wei L, Sandbulte MR, Thomas PG, Webby RJ, Homayouni R, Pfeffer LM. NFkappaB negatively regulates interferon-induced gene expression and anti-influenza activity. J Biol Chem. 2006 Apr 28;281(17):11678-84.

[49] Cheng CS, Feldman KE, Lee J, Verma S, Huang DB, Huynh K, et al. The specificity of innate immune responses is enforced by repression of interferon response elements by NF-kappaB p50. Sci Signal. 2011 Feb 22;4(161):ra11.

[50] Ziegler-Heitbrock L. The p50-homodimer mechanism in tolerance to LPS. J Endotoxin Res. 2001;7(3):219-22.

[51] Kastenbauer S, Ziegler-Heitbrock HW. NF-kappaB1 (p50) is upregulated in lipopolysaccharide tolerance and can block tumor necrosis factor gene expression. Infect Immun. 1999 Apr;67(4):1553-9.

[52] Tong X, Yin L, Washington R, Rosenberg DW, Giardina C. The p50-p50 NF-kappaB complex as a stimulus-specific repressor of gene activation. Mol Cell Biochem. 2004 Oct;265(1-2):171-83.

[53] Elsharkawy AM, Oakley F, Lin F, Packham G, Mann DA, Mann J. The NF-kappaB p50:p50:HDAC-1 repressor complex orchestrates transcriptional inhibition of multiple pro-inflammatory genes. J Hepatol. 2010 Sep;53(3):519-27.

[54] Ea CK, Hao S, Yeo KS, Baltimore D. EHMT1 protein binds to nuclear factor-kappaB p50 and represses gene expression. J Biol Chem. 2012 Sep 7;287(37):31207-17.

[55] Schwarz EM, Badorff C, Hiura TS, Wessely R, Badorff A, Verma IM, et al. NF-kappaB-mediated inhibition of apoptosis is required for encephalomyocarditis virus virulence: A mechanism of resistance in p50 knockout mice. J Virol. 1998 Jul;72(7):5654-60.

[56] Pfeffer LM, Kim JG, Pfeffer SR, Carrigan DJ, Baker DP, Wei L, et al. Role of nuclear factor-kappaB in the antiviral action of interferon and interferon-regulated gene expression. J Biol Chem. 2004 Jul 23;279(30):31304-11.

[57] Heinz S, Benner C, Spann N, Bertolino E, Lin YC, Laslo P, et al. Simple combinations of lineage-determining transcription factors prime cis-regulatory elements required for macrophage and B cell identities. Mol Cell. 2010 May 28;38(4):576-89.

[58] Nordmann A, Wixler L, Boergeling Y, Wixler V, Ludwig S. A new splice variant of the human guanylate-binding protein 3 mediates anti-influenza activity through inhibition of viral transcription and replication. FASEB J. 2012 Mar;26(3):1290-300.

[59] Shenoy AR, Wellington DA, Kumar P, Kassa H, Booth CJ, Cresswell P, et al. GBP5 promotes NLRP3 inflammasome assembly and immunity in mammals. Science. 2012 Apr 27;336(6080):481-5.

[60] Fensterl V, Wetzel JL, Ramachandran S, Ogino T, Stohlman SA, Bergmann CC, et al. Interferon-induced Ifit2/ISG54 protects mice from lethal VSV neuropathogenesis. PLoS Pathog. 2012;8(5):e1002712.

[61] Eskildsen S, Justesen J, Schierup MH, Hartmann R. Characterization of the 2'-5'-oligoadenylate synthetase ubiquitin-like family. Nucleic Acids Res. 2003 Jun 15;31(12):3166-73.

[62] Seo JY, Yaneva R, Cresswell P. Viperin: A multifunctional, interferon-inducible protein that regulates virus replication. Cell Host Microbe. 2011 Dec 15;10(6):534-9.

[63] Geissmann F, Manz MG, Jung S, Sieweke MH, Merad M, Ley K. Development of monocytes, macrophages, and dendritic cells. Science. 2010 Feb 5;327(5966):656-61.

[64] Nau GJ, Schlesinger A, Richmond JF, Young RA. Cumulative toll-like receptor activation in human macrophages treated with whole bacteria. J Immunol. 2003 May 15;170(10):5203-9.

[65] Ozsolak F, Milos PM. RNA sequencing: Advances, challenges and opportunities. Nat Rev Genet. 2011 Feb;12(2):87-98.

[66] Wang Z, Gerstein M, Snyder M. RNA-seq: A revolutionary tool for transcriptomics. Nat Rev Genet. 2009 Jan;10(1):57-63.

[67] Marioni JC, Mason CE, Mane SM, Stephens M, Gilad Y. RNA-seq: An assessment of technical reproducibility and comparison with gene expression arrays. Genome Res. 2008 Sep;18(9):1509-17.

[68] Trapnell C, Williams BA, Pertea G, Mortazavi A, Kwan G, van Baren MJ, et al. Transcript assembly and quantification by RNA-seq reveals unannotated transcripts and isoform switching during cell differentiation. Nat Biotechnol. 2010 May;28(5):511-5.

[69] Anders S, Huber W. Differential expression analysis for sequence count data. Genome Biol. 2010;11(10):R106,2010-11-10-r106. Epub 2010 Oct 27.

[70] Pollier J, Rombauts S, Goossens A. Analysis of RNA-seq data with TopHat and cufflinks for genome-wide expression analysis of jasmonate-treated plants and plant cultures. Methods Mol Biol. 2013;1011:305-15.

[71] Pappas G, Panagopoulou P, Christou L, Akritidis N. Brucella as a biological weapon. Cell Mol Life Sci. 2006 Oct;63(19-20):2229-36.

[72] Pappas G, Papadimitriou P, Akritidis N, Christou L, Tsianos EV. The new global map of human brucellosis. Lancet Infect Dis. 2006 Feb;6(2):91-9.

[73] Yagupsky P, Baron EJ. Laboratory exposures to brucellae and implications for bioterrorism. Emerg Infect Dis. 2005 Aug;11(8):1180-5.

[74] Solera J, Martinez-Alfaro E, Espinosa A, Castillejos ML, Geijo P, Rodriguez-Zapata M. Multivariate model for predicting relapse in human brucellosis. J Infect. 1998 Jan;36(1):85-92.

[75] Davoudi S, Amirzargar AA, Hajiabdolbaghi M, Rasoolinejad M, Soodbakhsh A, Jafari S, et al. Th-1 cytokines gene polymorphism in human brucellosis. Int J Immunogenet. 2006 Oct;33(5):355-9.

[76] Skendros P, Pappas G, Boura P. Cell-mediated immunity in human brucellosis. Microbes Infect. 2011 Feb;13(2):134-42.

[77] Celli J. Surviving inside a macrophage: The many ways of brucella. Res Microbiol. 2006 Mar;157(2):93-8.

[78] Giambartolomei GH, Delpino MV, Cahanovich ME, Wallach JC, Baldi PC, Velikovsky CA, et al. Diminished production of T helper 1 cytokines correlates with T cell unresponsiveness to brucella cytoplasmic proteins in chronic human brucellosis. J Infect Dis. 2002 Jul 15;186(2):252-9.

[79] Rodriguez-Zapata M, Salmeron I, Manzano L, Salmeron OJ, Prieto A, Alvarez-Mon M. Defective interferon-gamma production by T-lymphocytes from patients with acute brucellosis. Eur J Clin Invest. 1996 Feb;26(2):136-40.

[80] Caballero A, Bravo MJ, Nieto A, Colmenero JD, Alonso A, Martin J. TNFA promoter polymorphism and susceptibility to brucellosis. Clin Exp Immunol. 2000 Sep;121(3):480-3.

[81] Zhan Y, Liu Z, Cheers C. Tumor necrosis factor alpha and interleukin-12 contribute to resistance to the intracellular bacterium brucella abortus by different mechanisms. Infect Immun. 1996 Jul;64(7):2782-6.

[82] Yingst S, Hoover DL. T cell immunity to brucellosis. Crit Rev Microbiol. 2003;29(4):313-31.

[83] D'Andrea A, Aste-Amezaga M, Valiante NM, Ma X, Kubin M, Trinchieri G. Interleukin 10 (IL-10) inhibits human lymphocyte interferon gamma-

production by suppressing natural killer cell stimulatory factor/IL-12 synthesis in accessory cells. J Exp Med. 1993 Sep 1;178(3):1041-8.

[84] Makis AC, Galanakis E, Hatzimichael EC, Papadopoulou ZL, Siamopoulou A, Bourantas KL. Serum levels of soluble interleukin-2 receptor alpha (sIL-2Ralpha) as a predictor of outcome in brucellosis. J Infect. 2005 Oct;51(3):206-10.

[85] Fuss IJ, Kanof ME, Smith PD, Zola H. Isolation of whole mononuclear cells from peripheral blood and cord blood. Curr Protoc Immunol. 2009 Apr;Chapter 7:Unit7.1.

[86] Buck SF. A method of estimation of missing values in multivariate data suitable for use with an electronic computer. Journal of the Royal Statistical Society.Series B (Methodological). 1960;22(2):pp. 302-306.

[87] Gleason TC, Staelin R. A proposal for handling missing data. Psychometrika. 1975 jun;40(2):229-52.

[88] Timm NH. The estimation of variance-covariance and correlation matrices from incomplete data. Psychometrika. 1970 dec;35(4):417-37.

[89] Scharf O, Agranovich I, Lee K, Eller NL, Levy L, Inman J, et al. Ontogeny of Th1 memory responses against a brucella abortus conjugate. Infect Immun. 2001 Sep;69(9):5417-22.

[90] Ahmed K, Al-Matrouk KA, Martinez G, Oishi K, Rotimi VO, Nagatake T. Increased serum levels of interferon-gamma and interleukin-12 during human brucellosis. Am J Trop Med Hyg. 1999 Sep;61(3):425-7.

[91] Fernandes DM, Baldwin CL. Interleukin-10 downregulates protective immunity to brucella abortus. Infect Immun. 1995 Mar;63(3):1130-3.

[92] Rafiei A, Ardestani SK, Kariminia A, Keyhani A, Mohraz M, Amirkhani A. Dominant Th1 cytokine production in early onset of human brucellosis followed by switching towards Th2 along prolongation of disease. J Infect. 2006 Nov;53(5):315-24.

[93] Scian R, Barrionuevo P, Giambartolomei GH, Fossati CA, Baldi PC, Delpino MV. Granulocyte-macrophage colony-stimulating factor- and tumor necrosis factor alpha-mediated matrix metalloproteinase production by human osteoblasts and monocytes after infection with brucella abortus. Infect Immun. 2011 Jan;79(1):192-202.

[94] Demirdag K, Ozden M, Kalkan A, Godekmerdan A, Sirri Kilic S. Serum cytokine levels in patients with acute brucellosis and their relation to the

traditional inflammatory markers. FEMS Immunol Med Microbiol. 2003 Nov 28;39(2):149-53.

[95] Rodriguez-Zapata M, Matias MJ, Prieto A, Jonde MA, Monserrat J, Sanchez L, et al. Human brucellosis is characterized by an intense Th1 profile associated with a defective monocyte function. Infect Immun. 2010 Jul;78(7):3272-9.

[96] Karaoglan I, Pehlivan S, Namiduru M, Pehlivan M, Kilincarslan C, Balkan Y, et al. TNF-alpha, TGF-beta, IL-10, IL-6 and IFN-gamma gene polymorphisms as risk factors for brucellosis. New Microbiol. 2009 Apr;32(2):173-8.

[97] Akhvlediani T, Chitadze N, Laws TR, Makharadze M, Chubinidze M, Tsanava S, et al. Comparison of total antibody and interferon-gamma T-cell responses in patients following infection with brucellosis in georgia. J Infect Public Health. 2012 Oct;5(5):321-31.

[98] Ariza J, Pellicer T, Pallares R, Foz A, Gudiol F. Specific antibody profile in human brucellosis. Clin Infect Dis. 1992 Jan;14(1):131-40.

[99] Casanova A, Ariza J, Rubio M, Masuet C, Diaz R. BrucellaCapt versus classical tests in the serological diagnosis and management of human brucellosis. Clin Vaccine Immunol. 2009 Jun;16(6):844-51.

[100] Maas KS, Mendez M, Zavaleta M, Manrique J, Franco MP, Mulder M, et al. Evaluation of brucellosis by PCR and persistence after treatment in patients returning to the hospital for follow-up. Am J Trop Med Hyg. 2007 Apr;76(4):698-702.

[101] Vrioni G, Pappas G, Priavali E, Gartzonika C, Levidiotou S. An eternal microbe: Brucella DNA load persists for years after clinical cure. Clin Infect Dis. 2008 Jun 15;46(12):e131-6.

[102] Navarro E, Segura JC, Castano MJ, Solera J. Use of real-time quantitative polymerase chain reaction to monitor the evolution of brucella melitensis DNA load during therapy and post-therapy follow-up in patients with brucellosis. Clin Infect Dis. 2006 May 1;42(9):1266-73.